

This is a repository copy of *Streptomyces coelicolor* strains lacking polyprenol phosphate mannose synthase and protein O-mannosyl transferase are hyper-susceptible to multiple antibiotics.

White Rose Research Online URL for this paper:

<https://eprints.whiterose.ac.uk/128020/>

Version: Accepted Version

Article:

Howlett, Robert, Read, Nicholas, Varghese, Anpu S. et al. (3 more authors) (2018) *Streptomyces coelicolor* strains lacking polyprenol phosphate mannose synthase and protein O-mannosyl transferase are hyper-susceptible to multiple antibiotics. *Microbiology*. pp. 369-382. ISSN 1465-2080

<https://doi.org/10.1099/mic.0.000605>

Reuse

Items deposited in White Rose Research Online are protected by copyright, with all rights reserved unless indicated otherwise. They may be downloaded and/or printed for private study, or other acts as permitted by national copyright laws. The publisher or other rights holders may allow further reproduction and re-use of the full text version. This is indicated by the licence information on the White Rose Research Online record for the item.

Takedown

If you consider content in White Rose Research Online to be in breach of UK law, please notify us by emailing eprints@whiterose.ac.uk including the URL of the record and the reason for the withdrawal request.

Microbiology

Streptomyces coelicolor strains lacking polyprenol phosphate mannose synthase and protein O-mannosyl transferase are hyper-susceptible to multiple antibiotics --Manuscript Draft--

Manuscript Number:	MIC-D-17-00343R1
Full Title:	Streptomyces coelicolor strains lacking polyprenol phosphate mannose synthase and protein O-mannosyl transferase are hyper-susceptible to multiple antibiotics
Article Type:	Research Article
Section/Category:	Physiology and metabolism
Corresponding Author:	Margaret CM Smith, PhD University of Leeds Leeds, West Yorkshire UNITED KINGDOM
First Author:	Robert Howlett
Order of Authors:	Robert Howlett Nicholas Read Anpu Varghese Charles Kershaw Yvette Hancock Margaret CM Smith, PhD
Abstract:	<p>Polyprenol phosphate mannose (PPM) is a lipid linked sugar donor used by extra-cytoplasmic glycosyl transferases in bacteria. PPM is synthesised by polyprenol phosphate mannose synthase, Ppm1, and in most Actinobacteria is used as the sugar donor for protein O-mannosyl transferase, Pmt, in protein glycosylation. Ppm1 and Pmt have homologues in yeasts and humans, where they are required for protein O-mannosylation. Actinobacteria also use PPM for lipoglycan biosynthesis. Here we show that ppm1 mutants of Streptomyces coelicolor have increased susceptibility to a number of antibiotics that target cell wall biosynthesis. The pmt mutants also have mildly increased antibiotic susceptibilities, in particular to β-lactams and vancomycin. Despite normal induction of the vancomycin gene cluster, vanSRJKHAX, the pmt and ppm1 mutants remained highly vancomycin sensitive indicating that the mechanism of resistance is blocked post-transcriptionally. Differential RNA expression analysis indicated that catabolic pathways were downregulated and anabolic ones upregulated in the ppm1 mutant compared to the parent or complemented strains. Of note was the increase in expression of fatty acid biosynthetic genes in the ppm1- mutant. A change in lipid composition was confirmed using Raman spectroscopy, which showed that the ppm1- mutant had a greater relative proportion of unsaturated fatty acids compared to the parent or the complemented mutant. Taken together these data suggest that an inability to synthesise PPM (ppm1-) and loss of the glycoproteome (pmt- mutant) can detrimentally affect membrane or cell envelope functions leading to loss of intrinsic and, in the case of vancomycin, acquired antibiotic resistance.</p>

1 ***Streptomyces coelicolor* strains lacking polyprenol phosphate mannose**
2 **synthase and protein O-mannosyl transferase are hyper-susceptible to multiple**
3 **antibiotics**

4 Robert Howlett^{a,¶}, Nicholas Read^{a,¶}, Anpu Varghese^b, Charles Kershaw^c, Y.
5 Hancock^{c,d} and Margaret C. M. Smith^{a,b, #}

6
7 ¶ Joint first authors.

8
9 ^a Department of Biology, University of York, York, United Kingdom;

10 ^b Institute of Medical Sciences, University of Aberdeen, Aberdeen, United Kingdom;

11 ^c Department of Physics, University of York, York, United Kingdom;

12 ^d York Centre for Complex Systems Analysis, University of York, York, United
13 Kingdom^d

14
15 Running Title: Antibiotic hypersensitive mutants of *S. coelicolor*

16 Abbreviations; PPM; polyprenol phosphate mannose, Ppm1; polyprenol phosphate
17 mannose synthase, Pmt; protein mannosyl transferase, TUFA; total unsaturated fatty
18 acids, TFA; total fatty acids.

19
20
21
22 #Address correspondence to Margaret C.M. Smith, Maggie.smith@york.ac.uk

23 RH and NR contributed equally to this work.

24

25

26 **Abstract**

27 Polyprenol phosphate mannose (PPM) is a lipid linked sugar donor used by extra-
28 cytoplasmic glycosyl transferases in bacteria. PPM is synthesised by polyprenol
29 phosphate mannose synthase, Ppm1, and in most Actinobacteria is used as the
30 sugar donor for protein O-mannosyl transferase, Pmt, in protein glycosylation. Ppm1
31 and Pmt have homologues in yeasts and humans, where they are required for
32 protein O-mannosylation. Actinobacteria also use PPM for lipoglycan biosynthesis.
33 Here we show that *ppm1* mutants of *Streptomyces coelicolor* have increased
34 susceptibility to a number of antibiotics that target cell wall biosynthesis. The *pmt*
35 mutants also have mildly increased antibiotic susceptibilities, in particular to β -
36 lactams and vancomycin. Despite normal induction of the vancomycin gene cluster,
37 *vanSRJKHAX*, the *pmt* and *ppm1* mutants remained highly vancomycin sensitive
38 indicating that the mechanism of resistance is blocked post-transcriptionally.
39 Differential RNA expression analysis indicated that catabolic pathways were
40 downregulated and anabolic ones upregulated in the *ppm1* mutant compared to the
41 parent or complemented strains. Of note was the increase in expression of fatty acid
42 biosynthetic genes in the *ppm1*⁻ mutant. A change in lipid composition was confirmed
43 using Raman spectroscopy, which showed that the *ppm1*⁻ mutant had a greater
44 relative proportion of unsaturated fatty acids compared to the parent or the
45 complemented mutant. Taken together these data suggest that an inability to
46 synthesise PPM (*ppm1*⁻) and loss of the glycoproteome (*pmt* mutant) can
47 detrimentally affect membrane or cell envelope functions leading to loss of intrinsic
48 and, in the case of vancomycin, acquired antibiotic resistance.

49

50

51 **Introduction**

52

53 In the Actinobacteria, mannose is an important component of extracellular
54 glycoconjugates including lipoglycans and glycoproteins [1, 2]. Lipomannan (LM)
55 and lipoarabinomannan (LAM) are essential constituents of the cell envelope in
56 mycobacteria [3] and mutants of corynebacteria that lack these molecules grow
57 poorly [4]. Membrane and secreted proteins are also modified by mannose residues
58 in the Actinobacteria and species of *Mycobacterium*, *Corynebacterium* and
59 *Streptomyces* have been shown to contain glycoproteins [5-9]. Extra-cytoplasmic
60 glycosyl transferases require a lipid linked sugar donor, which for the transfer of
61 mannose is polyprenol phosphate mannose (PPM). The enzyme polyprenol
62 phosphate mannose synthase, Ppm1, synthesises PPM by catalysing the transfer of
63 mannose from GDP-mannose to polyprenol phosphate on the cytoplasmic face of the
64 plasma membrane and PPM is then flipped in the membrane, transporting the
65 mannose moiety to the periplasm [10] (Fig.1). In mycobacteria, Ppm1, is an essential
66 enzyme, as it is required for lipomannan biosynthesis [11] and *Corynebacterium*
67 *ppm1* mutants have a reduced growth rate [12].

68

69 We are interested in the role of protein O-glycosylation in bacteria and ultimately we
70 aim to understand how the glycans affect protein function. The protein O-
71 glycosylation pathway in the Actinobacteria is highly reminiscent of the O-
72 mannosylation pathway in yeast and humans [2, 9, 13]. In fungi, mutations that
73 inactivate PMTs lead to loss of fitness and/or avirulent phenotypes [14-19]. In
74 humans loss of PoMT leads to a developmental phenotype [20]. Overall the evidence

75 suggests that protein O-mannosylation is a fundamentally important protein
76 modification in prokaryotes and eukaryotes.

77

78 *S. coelicolor* is a convenient model to study the protein O-glycosylation pathway in
79 bacteria as the *pmt* and *ppm1* genes are not essential [21, 22] and *Streptomyces*
80 *spp.* are not known to generate the heavily glycosylated lipomannans and
81 lipoarabinomannans that depend on the activity of Ppm1. In previous work we
82 showed that *S. coelicolor* Ppm1 (SCO1423) catalyses the transfer of mannose from
83 GDP-mannose to polyprenol phosphate to generate PPM and Pmt (SCO3154) was
84 shown to transfer mannose from PPM to target peptides [9] (Fig.1). Ppm1 and Pmt
85 activities are confined to the membrane fractions. The periplasmic phosphate binding
86 protein, PstS, part of a high affinity phosphate uptake system, was shown to be O-
87 glycosylated with a trihexose [9]. The enzymes Pmt and Ppm1 were first identified as
88 being required for phage ϕ C31 infection, suggesting the phage receptor is a
89 glycoprotein(s) [21, 22].

90

91 Here we report on the global phenotypes of mutations that lead to an inability to
92 synthesise PPM and the glycoproteome in *S. coelicolor*. Mutations in *pmt* and *ppm1*
93 confer pleiotropic phenotypes including increased susceptibilities to multiple
94 antibiotics, most of which act at different stages of cell wall biogenesis. Global
95 transcriptional analysis in the *ppm1*⁻ mutant compared to the parent (*ppm1*⁺) strain
96 showed that this mutation conferred a general switch from catabolism to anabolism
97 and a major change in fatty acid metabolism. Changes in lipid composition in the
98 *ppm1*⁻ mutant were confirmed using Raman spectroscopy. We propose that these

99 global effects on the cell envelope affects periplasmic and membrane protein function
100 leading to antibiotic susceptibility.

101

102 **Methods**

103 **Bacterial strains**

104 *Streptomyces coelicolor* strains with mutations in *ppm1* (DT3017; *ppm1E218V*,
105 DT1020; *ppm1H116D* and DT1029; *ppm1S163L*) and *pmt* (DT1025; frameshift from
106 A121, and DT2008; mutation uncharacterised) were obtained previously [21, 22]. *E.*
107 *coli* strain DH5 α was used for propagation of plasmids pDT10 and pDT16, also
108 published previously [21, 22]. The DNA methylation deficient strain of *E. coli*,
109 ET12567 (pUZ8002) was used as the donor host for plasmid conjugation to
110 *Streptomyces* species as described previously [23, 24]. *Streptomyces* strains were
111 routinely maintained on Soya Mannitol (SM) agar at 30°C [24] and spore stocks
112 maintained at -38 °C.

113

114 **Disc diffusion assays**

115 Difco nutrient (DN) agar plates were evenly spread with approximately 1×10^7
116 *Streptomyces* spores. Sterile filter discs (5 mm width) were placed on the surface of
117 the inoculated agar plates and 10 μ l of an antibiotic stock solution was allowed to
118 absorb to the disc. Plates were incubated at 30 °C for 2 days and the zones of
119 inhibition were measured. At least three biological replicates and at least two
120 technical replicates were used for each strain.

121

122 **Quantitative mRNA analysis and culture conditions**

123 Samples were prepared for quantitative reverse transcriptase - polymerase chain
124 reaction (qRT-PCR) analysis by inoculation of 500 ml DN broth in a 2 L baffled flask
125 to a starting OD₄₅₀ of 0.05 with heat shocked pre-germinated spores. Pre-
126 germination was performed according to Kieser et al, [24]; approximately 10⁹ CFU *S.*
127 *coelicolor* spores were germinated for 10 hrs in 100 ml germination medium in 1 L
128 baffled flasks at 30 °C. Cultures were then grown at 30 °C for 6 hours at 250 rpm
129 before the addition of vancomycin to a final concentration of 0.1 µg/ml. 43 ml of
130 culture was sampled and added to 7 ml stop solution (5% phenol in ethanol, stored at
131 – 20 °C) at time-points 0, 30, 60 and 90 minutes. RNA was extracted from samples
132 as described below and cDNA was created using SuperScript[®] III reverse
133 transcriptase (Life technologies) using manufacturers instructions with the following
134 altered temperature cycle: 25 °C, 10 min; 42 °C, 120 min; 50 °C, 30 min; 55 °C, 30
135 min; 85 °C, 5 min. Primers used for qRT-PCR were designed using Primer3 software
136 ⁵⁶. Reactions were carried out on a StepOne PCR machine (Applied Biosystems)
137 with each 20 µl qRT-PCR reaction containing 10 µl Fast SYBR[®] Green Mast Mix
138 (Applied Biosystems) 25 ng cDNA and optimized primer and DMSO concentrations.
139 Optimised conditions were as follows: primers RH111 and RH112 300 nM no DMSO;
140 RH107 and RH108 500 nM with 4.8 % DMSO; RH109 and RH110 200 nM with 4.8 %
141 DMSO (Table S1). The principal sigma factor of *S. coelicolor* (*hrdB*) was used as a
142 representative constitutively expressed, housekeeping gene.

143

144 **Fermentor cultivation conditions**

145 Cultivations for RNAseq analysis were performed in 7 litre fermentors (Applikon)
146 containing 2.5 litres of DN broth and 2 ml antifoam C emulsion (Sigma-Aldrich) with a
147 starting pH adjusted to 7 with NaOH. Temperature was maintained at 30 °C and pH

148 maintained at 7 through the automatic addition of 2 M HCl. Dissolved oxygen was
149 maintained at a minimum of 30 % by automatic adjustment of the agitation speed,
150 with a minimum and maximum rate of 300 and 1000 respectively, and a constant
151 aeration pressure of 2.5 - 3.5 bar. For the inoculum approximately 10^9 CFU *S.*
152 *coelicolor* spores were germinated for 10 hrs in 100 ml germination medium in 1 L
153 baffled flasks at 30 °C following heat shock as described in Kieser *et al.* (2000) [24]
154 before being used to inoculate equilibrated fermentor culture medium to an OD₄₅₀ of
155 0.05. Growth was measured using dry weight while dissolved oxygen, pH, agitation
156 speed and temperature were logged online throughout.

157

158 **Isolation of RNA and transcriptome analysis**

159 RNA for RNAseq analysis was isolated from fermentor-grown cultures as described
160 above. The equivalent of 40 OD₆₀₀ units were sampled and immediately added to
161 1/8th volume stop solution (5% phenol in ethanol, stored at – 20 °C). Cultures were
162 spun down at 12,000 rpm, 4 °C for 5 minutes before pellets were flash frozen in liquid
163 nitrogen and stored at -80 °C for future processing. RNA isolation was performed
164 using a modified version of the Kirby mix protocol as follows [24]: 14 g of glass beads
165 were added to defrosted pellets along with 5 ml of 30 °C modified Kirby mix before
166 being vigorously vortexed for 2 minutes. Acid phenol: chloroform 1:1 was then used
167 to isolate nucleic acids before being precipitated with 4 M acetate and 100 %
168 isopropanol. Nucleic acids were subject to an ethanol wash before final resuspension
169 in water. Nucleic acids were repeatedly treated with DNase I using conditions
170 described by the vendor (Roche) until DNA could no longer be amplified using
171 polymerase chain reaction (PCR). RNA was then enriched for mRNA using
172 *MICROBExpress*TM Bacteria beads, as described by the manufacturer (Ambion).

173

174 The use of stop solution to prevent artefacts due to variations in harvesting of
175 samples was validated as follows: Two samples were collected from the fermentor
176 (containing J1929, time point 24 hours) and stop solution was added to both. RNA
177 was prepared immediately for one sample whereas the other was incubated on ice
178 for 1 hour prior to preparation of RNA. The RNA sequences of both samples was
179 analysed for significant changes that might have resulted from RNA degradation.
180 Subsequence linear regression analysis gave an R^2 of 0.959 indicating that the use
181 of the stop solution was a valid procedure for sample preparation (Supplementary
182 information; Figure S2).

183

184 Generation of cDNA and production of Illumina HiSeq data was performed by Vertis
185 Biotechnologie AG (Germany). In brief mRNAs were fragmented with ultrasound
186 before antarctic phosphatase treatment and re-phosphorylation with polynucleotide
187 kinase. RNA fragments were then poly(A)-tailed using poly(A) polymerase and an
188 RNA adapter was ligated to mRNA 5' phosphate. First strand cDNA synthesis was
189 performed using an oligo(dT)-adapter primer and M-MLV reverse transcriptase
190 before PCR amplification. The cDNA samples were pooled and size fractionated in
191 the range of 250-500 bp and run on an Illumina HiSeq 2000 system with a 100 bp
192 read length.

193 Sequences were trimmed using Sickle and aligned to the *S. coelicolor* genome
194 (NCBI, accession number NC_003888) using BWA MEM ([http://bio-](http://bio-bwa.sourceforge.net)
195 [bwa.sourceforge.net](http://bio-bwa.sourceforge.net)). Normalized counts and differential gene expression analysis
196 was performed with DESeq2 in R/Bioconductor [25]. Gene ontology analysis was
197 performed using GOEAST [26] and read counts were visualized using the Integrated

198 Genomics Viewer [27, 28]. RNA sequencing data is available at the GEO database
199 accession number GSE107982.

200

201 **Raman spectroscopy sample preparation**

202 *S. coelicolor* strains J1929, DT3017 (*ppm1*⁻ mutant) and DT3017:pDT16
203 (complemented mutant) were prepared for Raman spectroscopy by subjecting
204 spores (approximately 10⁹ CFU in 10 mL TES 0.5 M, pH8) to heat shock (50°C, 10
205 mins) and then adding to 10 mL double strength germination medium in a 250 mL
206 baffled conical flask [24]. After incubation (37°C, 180rpm for 8 to 9 hours) and
207 centrifugation to pellet cells, the pellet was resuspended in 40 mL DN broth to an
208 OD₄₅₀ of 0.05 and incubation continued for a further 12 to 13 hours. 10 mL was
209 removed for dry weight measurement and the remaining culture was centrifuged, the
210 cell pellet washed once in 30 mL high-purity deionised water and then plated via
211 pipette-deposit directly onto small CaF₂ disks (13mm diameter and 1mm thick). The
212 bacteria were then gently spread over the disk surface with excess water removed by
213 pipette aspiration and then air-dried in a fume cupboard in preparation for Raman
214 spectroscopy.

215

216 **Raman spectroscopy experiments and analyses**

217 Raman spectroscopy point spectra were collected from randomly selected cell
218 populations of *S. coelicolor* J1929 (parent), DT3017 (*ppm1*⁻ mutant) and
219 DT3017:pDT16 (complemented mutant) using an HORIBA XploRA micro-Raman
220 instrument with 532 nm laser, x100 objective (0.9 NA) and 2400 lines/mm spectral
221 grating. Measurements were made in confocal mode using a laser spot size of ~1
222 μm, with 3.5 mW laser power and 1 cm⁻¹ spectral resolution.

223

224 Spectra were collected using the HORIBA LabSpec 6 software in the 600–1800 cm^{-1}
225 cell-fingerprint and 2750–3110 cm^{-1} high-wavenumber ranges. Each spectrum was
226 obtained using 90s acquisition time averaged over two spectral repetitions with 40 to
227 55 spectra randomly collected across each cell line over three experimental repeats.
228 The total number of spectra were averaged to obtain a single representative
229 spectrum for each strain.

230 The averaged spectra were baseline-corrected from the first to the last spectral point
231 in the fingerprint and high-wavenumber ranges using the '*Raman tool set*' package
232 [29]. Peak regions in the acquired spectral ranges were then linear baseline-
233 corrected and Gaussian peak-fitted using IGOR Pro 6.35 to obtain the peak
234 properties (peak positions, peak intensities, *etc.*). Biomolecular peak assignments
235 were made by correlating the fitted peak positions to literature references [30, 31].
236 The total unsaturated fatty acid (TUFA)/total fatty acid (TFA) peak intensity ratio for
237 each cell line was determined with uncertainties calculated from the propagated
238 standard error of the mean in the measured TUFA and TFA peak intensity values.
239 The percentage standard error of the mean for the TUFA/TFA ratio was converged
240 as a function of the number of spectra in each spectral average ensuring that
241 sufficient spectra were collected for accurate representation of each sample
242 population.

243

244 **Results**

245 *Mutations in ppm1 and pmt in S. coelicolor confer hypersensitivity to cell wall acting*
246 *antibiotics.*

247 *S. coelicolor* A3(2) J1929 strains with mutations in *ppm1* (DT3017, DT1020, DT1029)
248 and *pmt* (DT2008, DT1025) were isolated previously [21, 22] (see also Material and
249 Methods). The *ppm1* and *pmt* mutants display a small colony phenotype when
250 growing on Difco nutrient agar or soya mannitol agar that could be complemented by
251 plasmids pDT16 or pDT10, encoding the wild type *ppm1* or *pmt*, respectively (Fig
252 S1). Microscopic techniques revealed no obvious morphological differences in the
253 mutant strains so, to probe the underlying physiological changes, the *ppm1* and *pmt*
254 mutants were subjected to antibiotic stress. Increased sensitivities to a number of
255 antibiotics, measured using disc diffusion assays, were detected in multiple
256 independently isolated *ppm1*⁻ and *pmt* mutant strains (Fig. 2; Dataset S1).
257 Whilst both *ppm1* and *pmt* mutants had increased susceptibilities to ampicillin,
258 imipenem, meropenem, rifampicin and vancomycin compared to the parent strain,
259 the *ppm1* mutants also had greater sensitivities to daptomycin, tunicamycin,
260 bacitracin, nisin and ramoplanin. Complementation of the *ppm1*⁻ and the *pmt*
261 mutations with their corresponding wild type alleles alleviated the antibiotic
262 susceptible phenotypes (Fig. 2). The *ppm1* and *pmt* mutant strains showed no
263 change in susceptibilities to D-cycloserine, polymyxin, monensin, tetracycline,
264 kanamycin, thiostrepton, chloramphenicol, ciprofloxacin and moenomycin, arguing
265 against a general increase in permeability underlying the antibiotic susceptible
266 phenotype. Overall, with the exception of rifampicin, which targets RNA polymerase,
267 the antibiotics with increased efficacy on the *ppm1*⁻ and *pmt* mutants act at different
268 stages of cell wall biosynthesis (Fig. 2).
269
270 *The vancomycin resistance cluster is induced by vancomycin in the ppm1 and pmt*
271 *mutants*

272 *S. coelicolor* encodes a well-characterized vancomycin resistance mechanism
273 conferring a MIC of approximately 80 µg/ml [32, 33]. This mechanism of resistance is
274 shared with the pathogenic bacteria *Enterococcus faecium* and involves
275 reprogramming of cell wall biosynthesis so that the vancomycin target of the
276 peptidoglycan pentapeptide, the terminal D-Ala-D-Ala, is replaced by D-Ala-D-Lac
277 [34-36]. The *S. coelicolor* resistance cluster consists of seven genes split into four
278 operons; *vanRS*, a two component signal transduction system, *vanHAX*, encoding
279 enzymes required for the production of D-Lac, ligation of D-Ala to D-Lac and
280 breakdown of D-Ala-D-Ala respectively; *vanK*, encoding a Fem protein, a non-
281 ribosomal peptidyltransferases that adds the cross-bridge amino acids to the stem
282 pentapeptide ending in D-Ala-D-Lac, and *vanJ*, required for resistance to the
283 structurally related antibiotic teicoplanin [32, 33, 37]. Addition of vancomycin, but not
284 teicoplanin, induces expression of the *van* cluster genes. To test whether the *van*
285 cluster is being induced in the *ppm1* and *pmt* mutants, we measured the level of
286 *vanH* mRNA (Fig 3; Supplementary information, Dataset S2). As the *ppm1* and *pmt*
287 mutant strains are highly sensitive to vancomycin, we used a very low concentration
288 of drug to induce (0.1 µg/ml vancomycin). Even at this low concentration the *van*
289 cluster in the parent strain and in DT2008 is induced between 10 to 100 fold. The
290 *ppm1* mutant strain also showed induction of *vanH* but the extent varied widely from
291 experiment to experiment leading to a large standard error. This observation and the
292 low levels of induction in the complemented *pmt* strain are most likely due to the use
293 of a vancomycin concentration for induction which is at the lower limit. We conclude
294 that failure to transcribe the *van* cluster in the *ppm1* or the *pmt* mutants is not the
295 reason why these strains are highly sensitive to vancomycin and that delivery of
296 resistance in these strains is blocked post-transcriptionally.

297

298 *Loss of Ppm1 activity leads to a global switch from catabolism to anabolism,*
299 *including a change in fatty acid metabolism*

300 In order to further our understanding of the underlying processes that led to a loss of
301 intrinsic antibiotic resistance, global transcriptional profiling using RNAseq was
302 performed in the *ppm1* mutant, DT3017, the original isogenic parent, J1929, and the
303 complemented strain, DT3017:pDT16. A *ppm1*⁻ mutant was chosen for RNAseq
304 analysis because of the more extreme phenotype of the *ppm1*⁻ mutants. Samples
305 were collected during growth in controlled fermentation conditions where DT3017
306 showed only a modest growth defect (Fig S2). Deseq analysis revealed that
307 expression of 658 genes had changed with a $p < 0.05$ level of significance between
308 DT3017 and J1929 (461 with a >2-fold difference), 574 of these changes showed at
309 least some restoration towards J1929 levels in DT3017:pDT16 and were used for
310 further gene ontology analysis (Dataset S3). The majority (69%) of the 574 genes
311 used for gene ontology analysis were down-regulated in the *ppm1* mutant compared
312 to the parent, J1929.

313

314 Gene ontology analysis showed that membrane and periplasmic functions have been
315 severely affected in the *ppm1* mutant. The most prevalent downregulated genes are
316 associated with the GO terms transport and catabolic processes and in particular
317 organic acid, carbohydrate and amino acid transport, and carboxylic acid, fatty acid
318 and lipid catabolism are significantly down regulated (Dataset S4; Table 1). The GO
319 terms that describe the upregulated genes are broadly biosynthetic processes; these
320 are notably involving carboxylic acids (31 genes), which includes fatty acid (9 genes)
321 and amino acid biosynthesis (19 genes). 66 genes reached the Benjamini-Hochberg

322 level of significance and were at least partially restored through complementation
323 (Table S2). Almost half of the genes in the Benjamini-Hochberg set for which a
324 function is predicted have a putative role in lipid metabolism.

325

326 Closer inspection of fatty acid metabolism revealed an upregulation of all the
327 components of the *S. coelicolor* ACCase and FAS II complex (Fig. 4) and a general
328 down regulation of a variety of genes predicted to perform β -oxidation and fatty acid
329 degradation. These results suggest upregulation of fatty acid production in DT3017,
330 and hence possible alterations to membrane composition. Alterations to membrane
331 fluidity, topology and composition are all known to effect stability and sensitivity to
332 stress agents such as antibiotics [38-41].

333 The enriched gene set was searched for genes that might be involved in cell wall
334 biosynthesis, and/or antibiotic targets. Genes that were upregulated and might be
335 directly involved in peptidoglycan biosynthesis encode an FtsI like PBP (*sco3771*), a
336 putative muramoyl-pentapeptide carboxypeptidase (*sco5467*) and a putative
337 deacetylase (*sco2962*). Genes that were downregulated encode a putative PG
338 deacetylase (*sco6178*), a putative AmpC β -lactamase/D-alanyl-D-alanine
339 carboxypeptidase (*sco5660*), a putative D-alanyl-D-alanine dipeptidase (*sco1396*)
340 and a putative murein DD-endopeptidase (*sco0543*). Enriched GO terms did not
341 include cell envelope biogenesis and the expression of the putative major PG
342 biogenesis operon in *S. coelicolor* (*sco2077-sco2092*) was unchanged in DT3017.
343 Amongst the downregulated gene set, there were no obvious candidates that might
344 contribute to enhanced antibiotic susceptibilities. On the contrary, genes that are
345 predicted to encode efflux systems were upregulated (*sco5950*, *sco5516*, *sco3206*,
346 *sco1742* and *sco0756*) as well as a gene, *sco4049*, encoding a putative penicillin

347 amidase/syclase. Two upregulated genes have been linked with vancomycin
348 resistance; *sco6183* (*cwgE*), a GT1 putative heptosyl transferase that is part of the
349 vancomycin induced putative cell wall glycan operon (*cwg*) [42] and *sco2472* a
350 homologue of an uncharacterised protein, SanA, that affects membrane permeability
351 to vancomycin [43].

352

353 The gene, *sco3736*, encoding an ECF sigma factor and the two upstream genes
354 *sco3737* and *sco3738*, encoding a putative lipoprotein/sortase (homology to SrtE
355 family – cd05829; $E = 3e^{-51}$) and membrane protein respectively are the most
356 significantly upregulated genes in the *ppm1*⁻ strain, DT3017 (13, 37 and 32 fold
357 respectively) (Fig 5). The ECF sigma factor *sco3450* is also 1.9 fold upregulated and
358 there is a strong down regulation (15 fold) of ECF sigma factor gene, *sco4938*. It is
359 worth emphasizing that the expression of *sco3356* encoding the known cell wall
360 stress ECF sigma factor, SigE, [44] did not change (Dataset S3).

361

362 *The Ppm1-defective strain contains a higher relative proportion of unsaturated fatty*
363 *acids*

364 Raman spectroscopy was used to investigate changes in the fatty acid profile in the
365 *ppm1* mutant by means of quantitative lipid phenotyping. The Raman spectroscopy
366 approach involves the inelastic scattering of light to produce high-discriminatory,
367 molecular-scale cell characterisation (i.e. fingerprinting). Raman fingerprinting
368 provides detailed information on the cellular components including proteins, nucleic
369 acids, lipids and carbohydrates [30, 45] and has been used to characterise microbial
370 species and subspecies, and phenotypic changes [31, 46-48].

371

372 Raman spectroscopy was previously applied to lipid profiling in several studies. Wu
373 *et al* correlated the relative intensities of the 1650 cm⁻¹ C=C and 1440 cm⁻¹ CH₂
374 Raman bands (I_{1650}/I_{1440} ratio) to the degree of lipid unsaturation in extracted lipids
375 from algae cells [49]. Potcoava *et al.* used the degree of unsaturation (I_{1655}/I_{1440} and
376 I_{1655}/I_{1294}), lipid chain length (I_{2930}/I_{2959}), and total unsaturated fatty acid (TUFA) to
377 total fatty acid (TFA) (I_{3015}/I_{2851}) ratios to characterise lipid droplets in treated and
378 untreated breast and prostate cancer cells, noting that the TUFA/TFA ratio correlates
379 to the number of C=C to CH₂ species in pure fatty acids [50]. The TUFA/TFA ratio
380 has also been used by Nieva *et al* to stratify the degree of malignancy in breast
381 cancer cells and is regarded as a key Raman bio-marker for lipid phenotyping [51].
382 Whereas peak intensity ratios for the degree of lipid unsaturation and chain length
383 also relate to proteins, the TUFA/TFA ratio comprises lipid molecule vibrations only
384 [30] and is therefore a reliable biomarker to interrogate the fatty acids in intact cells.
385 In this work, the TUFA/TFA ratio was used to determine changes in the lipid content
386 of the parent *S. coelicolor strain* J1929, the *ppm1* mutant derivative, DT3017 and the
387 complemented mutant, DT3017:pDT16.

388

389 Averaged Raman spectra and peak assignments obtained for J1929, DT3017
390 DT3017:pDT16 (Fig. 6, Fig. S3, Table S3) agree with previously published spectra
391 for *Streptomyces* cells [31] and other published works on bacteria [47]. The
392 TUFA/TFA peak intensity ratios determined from these spectra showed the parent
393 strain, J1929, and the complemented mutant DT3017:pDT16 have similar lipid
394 compositions (Fig. 6C)). For the DT3017 *ppm1* strain, the TUFA/TFA value was
395 outside of the J1929 and DT3017:pDT16 ranges confirming it has a larger relative
396 unsaturated fatty acid component, hence different lipid composition. The converged

397 percentage standard error of the mean for the TUF_A/TFA values as a function of the
398 number of randomly selected individual spectra in the spectral averages indicated
399 that sufficient data were collected (N=40–55 spectra/strain) to establish reliable
400 statistics for these measurements (Fig. S3).

401

402 **Discussion**

403 Previous work has shown that mutations in the genes encoding Ppm1 and Pmt
404 required for synthesis of polyprenol phosphate mannose (PPM; *ppm1*) and O-
405 glycoproteins (*pmt* and *ppm1*) in *Streptomyces coelicolor* lead to phage resistance [9,
406 21, 22]. Here we show that *pmt* and *ppm1*⁻ mutations also lead to an increase in
407 susceptibility to antibiotics, particularly those that target cell wall biogenesis. We
408 propose that in *ppm1*⁻ strains, the extremely antibiotic susceptible phenotype is due
409 to global changes in lipid, membrane and periplasmic protein functions. The *pmt*
410 mutants have a similar but less extreme phenotype to the *ppm1* mutants, suggesting
411 that loss of membrane and periplasmic glycoproteins contribute to antibiotic hyper-
412 susceptibility.

413

414 The *ppm1* mutants show greater sensitivity to vancomycin and β-lactams, and higher
415 susceptibility to a greater range of antibiotics that target membrane or periplasmic
416 enzymes than *pmt* mutant strains (Fig. 2). *ppm1* mutants fail to generate the lipid
417 linked mannose donor, polyprenol phosphate mannose, PPM, whereas *pmt* strains
418 are able to generate PPM but fail to use PPM in protein O-glycosylation [9].
419 *Streptomyces* spp. have been shown to produce phosphatidylinositolmannosides
420 (PIMs) whose synthesis could also require PPM, depending on the degree of
421 mannosylation [52, 53]. In mycobacteria myo-inositol is sequentially mannosylated

422 generating PIM₁ to PIM₆ with PPM acting as the sugar donor for the later steps in the
423 pathway [54]. *S. coelicolor* contains close homologues of the *M. tuberculosis* genes
424 required for PIM biosynthesis; PimA (Rv2610c, SCO1525; E=3e-122) and PimB
425 (Rv2188c, SCO2132; E=9e-127) that synthesise *myo*-inositol with one (PIM₁) or two
426 (PIM₂) mannose residues attached, respectively. Both PimA and PimB act on the
427 inner face of the cytoplasmic membrane and use GDP-mannose as the sugar donor.
428 PimE in *M. tuberculosis* uses PPM to transfer mannose to the growing mannose
429 chain i.e. PIM₄ to PIM₅. SCO2335 is a distant (E = 4e-15) homologue of *M.*
430 *tuberculosis* PimE (Rv1159) and could be involved in the polymerisation of the
431 mannoside chain using PPM as the sugar donor. Another candidate protein from *S.*
432 *coelicolor* that could utilise PPM is SCO4023, which is annotated as a dolichyl-
433 phosphate-mannose protein mannosyltransferase (PMT_2, Pfam13231). The gene
434 *sco4023* is located adjacent to *sco4022*, which is a homologue of *ppm1*. In
435 preliminary work we have knocked out both of these genes and mutation in neither
436 gene confers resistance to ϕ C31 (Dr Anpu Varghese, unpublished work). According
437 to the Carbohydrate Active Enzymes (CAZY) database (cazy.org), the *S. coelicolor*
438 genome encodes 29 and 17 GT2 and GT4 family glycosyl transferases, respectively;
439 members of both families can use polyprenol-containing glycoconjugates as
440 substrates. Loss of PPM from the *S. coelicolor* membrane is therefore expected to
441 affect synthesis of periplasmic O-glycoproteins, periplasmic mannosylation of PIMs
442 and, possibly, a variety of as yet uncharacterised cell envelope macromolecules.
443 While disruption of the O-glycosylation pathway by mutation of *pmt* leads to mild
444 antibiotic hypersusceptibility, the extreme antibiotic hyper-susceptibility when PPM is
445 depleted indicates that multiple pathways depend on PPM as a sugar donor.
446

447 RNAseq was used to provide insight into the global changes in the *ppm1⁻* mutant
448 strain compared to its parent. The *ppm1⁻* strain has undergone a major shift from a
449 largely catabolic metabolism to an anabolic one. Genes coding for membrane and
450 periplasmic proteins, particularly transport proteins, were down-regulated in the *ppm1⁻*
451 mutant, DT3017, whereas genes for biosynthetic cytoplasmic functions were up-
452 regulated. This response might be expected after transfer of a bacterial culture to a
453 minimal medium where biosynthetic functions would be up-regulated. However the
454 growth of all the strains for RNAseq was performed in rich medium (Difco nutrient
455 broth). The logical interpretation of the switch from the parental catabolic metabolism
456 to the *ppm1⁻* mutant anabolic metabolism is that some systems for sensing nutrients
457 and their uptake are defective. At this stage we cannot, however, propose a direct
458 mechanism through which loss of PPM might lead to the observed metabolic switch
459 other than multiple effects caused by a lack of mannose containing glycoconjugates
460 in the cell envelope and/or an accumulation of polyprenol phosphate.

461
462 Differential gene expression showed a switch in fatty acid metabolism in the *ppm1⁻*-
463 strain with genes coding for β -oxidation enzymes downregulated and those for
464 synthesis upregulated (Table 1; Fig 4) [55, 56]. The upregulation of the ACC complex
465 might have increased the proportion of straight chain fatty acids as ACC, but not the
466 PCC complex, can use acetyl-CoA as a primer for FA biosynthesis [55]. To study the
467 lipids in the *Streptomyces* strains, we used Raman Spectroscopy of whole cells. The
468 *ppm1⁻* mutant was shown to have a small but significant increase in the ratio of TUFA
469 acids to total fatty acids TFA compared to the TUFA/TFA ratios in the parent strain or
470 the complemented mutant. The only enzyme in *Streptomyces* known to introduce the
471 C=C double bond in FA biosynthesis is FabA (SCO4636 and SCO4637), a

472 hydroxyacyl-ACP dehydratase [57] and the corresponding genes are upregulated in
473 the *ppm1* mutant. Upregulation of *fabA* in *E. coli* is known to lead to a higher
474 proportion of unsaturated FAs [56, 58, 59]. However it is not clear whether
475 upregulation of the *fabA* genes in the *S. coelicolor ppm1*⁻ mutant has led directly to
476 the observed higher TUFA/TFA ratio or whether the upregulation is simply in line with
477 the overall upregulation of the FA biosynthesis pathway. The net result however is a
478 change in lipid composition in the *ppm1*⁻ strain DT3017 compared to its parent.

479

480 Changes in lipid composition can have profound effects on the activities of
481 membrane proteins, perhaps providing a mechanism for the proposed defects in
482 periplasmic nutrient sensing and transport protein function. Membrane composition
483 is important in maintaining topology of membrane proteins. Although the 'positive
484 inside rule' is believed to be the major proponent of determining membrane protein
485 topology, head group charge, fatty acid chain length and fatty acid unsaturation have
486 also been shown to be important [60]. Pertinent to our work is that changes in
487 membrane composition are also correlated with changes in sensitivity to antibiotics
488 and/or detergents. For example a *B. subtilis* strain lacking three extracytoplasmic
489 function, ECF, sigma factors (σ_M , σ_W and σ_X) is significantly more sensitive to cell
490 wall acting antibiotics than either the double mutants or the parents [61]. Expression
491 of σ_W was shown to lead to a decrease in membrane fluidity with concomitant
492 increase in resistance to detergents [41]. The *S. coelicolor ppm1* mutants are highly
493 susceptible to daptomycin, an antibiotic that targets the cytoplasmic membrane,
494 possibly causing depolarisation, and in *Enterococcus faecalis* inhibits cell division by
495 concentrating at the septum [62]. Changes in membrane fluidity have been
496 associated with daptomycin resistance in *S. aureus*; *in vitro* derived daptomycin

497 resistant strains have increased membrane fluidity although highly fluid membranes
498 also display increased resistance to cationic peptides including daptomycin,
499 supporting the view that membrane fluidity is only one component of the cell
500 envelope that mediates susceptibility to this antibiotic [38, 62, 63]. A decrease in the
501 supply of undecaprenol phosphate (*uppS* mutant) in *B. subtilis* can lead to increased
502 vancomycin resistance and this was shown to be due to elevated σ^M expression.
503 Mutation in a teichoic acid biosynthesis gene (TagF) can also increase sensitivity to
504 vancomycin and lysozyme in *Streptomyces* [64].

505

506 Gene regulation by ECF sigma factors is important in *B. subtilis* in sensing and
507 reacting to cell wall stresses [65]. The RNAseq data on the *S. coelicolor ppm1*⁻
508 mutant showed significant changes in expression of regulators, but not where
509 expected. For example genes for sigma factors such as SigE (*sco3356*, linked to cell
510 wall stress; [44]), SCO0600 (*sigB*; osmotic stress; [66]), SCO2954 (linked to
511 increased expression of extracellular proteases; [67]), SCO4005 (upregulated by
512 ppGpp; [68]), and SCO4938 were downregulated in the *ppm1*⁻ strain DT3017. Three
513 of four of the most significantly upregulated genes in DT3017 were the consecutive
514 genes *sco3736-sco3738*, probably co-transcribed and encoding a putative ECF
515 sigma factor, a lipoprotein with putative sortase E function, and integral membrane
516 protein, respectively (Fig .5). Sortases are transpeptidases that attach proteins to the
517 cell wall [69]. The major 'housekeeping' sortase, normally recognises a conserved
518 pentapeptide sorting sequence in a variety of substrates that in *S. coelicolor* is
519 predicted to be LAXTG [70]. Sortase E homologues are thought to have a more
520 specific range of substrates and two of these SCO3849 and SCO3850 have been
521 shown to be required for normal development in *S. coelicolor* [71]. SCO3737 belongs

522 to a more diverged group of putative sortases and it has been proposed that genes
523 for this group are cotranscribed with their substrates, in the case of *sco3737* this
524 would be *sco3738* encoding a putative membrane protein [69, 71]. A gene encoding
525 a second putative ECF sigma factor, *sco3450* (SigR2 transcribed by SigR, which
526 mediates the major thiol-oxidative stress response) [72, 73]), is also upregulated.
527 Both upregulated sigma factors are expressed early in the life cycle of *Streptomyces*;
528 *sco3736* and *sco3450* were identified in a study examining regulatory networks
529 during germination [73].

530

531 The changes in the complement of sigma factors in DT3017 might be responsible
532 directly for the global phenotypic response to growth without the ability to synthesise
533 PPM. Changes in sigma factors might also explain why *ppm1* and *pmt* mutants are
534 more sensitive to rifampicin, an antibiotic inhibiting transcription initiation by binding
535 within the DNA/RNA channel of the β -subunit of RNA polymerase [74]. Although
536 rifampicin is considered a general inhibitor of RNA polymerase there are examples of
537 altered promoter responses to rifampicin for differing holoenzymes. These include;
538 the *tdc* operon is insensitive to rifampicin [75] and there is increased sensitivity to
539 rifampicin *in vivo* and *in vitro* for σ^{70} -RNAPol over σ^{32} -RNAPol in *E. coli* [76]. In *B.*
540 *subtilis* SigB dependent transcription is less sensitive to rifampicin [77] and
541 transcription of a *sigR* dependent promoter is more resistant to rifampicin than
542 transcription of a *hrdB* dependent promoter (*rrn*) [78].

543

544 The *pmt* mutants are, like the *ppm1* mutants, considerably more sensitive to
545 vancomycin and β -lactams (including ampicillin and imipenem) than the parent strain
546 (Fig 2). Our hypothesis, which is consistent with the mechanism of protein mannosyl

547 transferases in yeasts and in another actinobacterium *M. smegmatis*, is that secreted
548 and membrane proteins are targets for O-glycosylation [2, 9, 13] and that the
549 modification affects protein function. It has been established by others that protein
550 glycosylation can have an impact on protein function [79, 80] and it has recently been
551 shown to have a role in regulating the function of a peptidoglycan hydrolase [81]. The
552 relative activities of transpeptidase and carboxypeptidase cell wall biosynthesis
553 enzymes are known to play a role in providing intrinsic vancomycin resistance in *S.*
554 *coelicolor* suggesting that subtle changes to protein activities could have a large
555 effect on antibiotic sensitivities [82]. Our observations are reminiscent of the
556 phenotypes of PMT mutants of fungi where the most common phenotype is
557 increased susceptibility to cell wall acting inhibitors [2]. The consistency across
558 kingdoms in the phenotypes of *pmt* mutants implies that the O-glycosylation has
559 similar roles in protein function in fungi and bacteria.

560

561 Both *pmt* and *ppm1* mutants are highly susceptible to vancomycin despite the
562 presence in in *S. coelicolor* of *vanRSJHAX* gene cluster conferring resistance [32,
563 33]. The cluster is induced by vancomycin, which binds the VanS sensor protein and,
564 through phosphorylation of VanR, switches on the *van* promoters. We showed that
565 the *van* genes are induced normally by vancomycin in the *ppm1* and *pmt* mutants
566 and yet the strains are still very sensitive to the antibiotic. There are two possible
567 explanations for the persistent sensitivity to vancomycin; either the substrates for the
568 resistance enzymes to generate the D-ala-D-lac pentapeptides are in limited supply
569 or resistance could be masked epistatically by membrane associated steps such as
570 flipping of lipid II, or the lipid II polymerization steps transglycosylation and
571 transpeptidation. In the *ppm1* mutant changes in membrane physiology are predicted

572 by RNAseq analysis and observed through Raman spectroscopy, arguing that
573 perturbation of membrane associated steps in peptidoglycan biosynthesis might be
574 responsible for preventing the normal ability of the *van* gene products to deliver
575 resistance to vancomycin.

576

577 In summary we have provided insights into the complex phenotypes of mutants in *S.*
578 *coelicolor* that lack the ability to synthesise PPM and O-glycoproteins. We have
579 presented evidence for a remodelling of the plasma membrane in terms of the protein
580 and fatty acid components possibly mediated by changes in ECF sigma factors in the
581 *ppm1⁻* mutant. The result of these adaptations is a loss of intrinsic resistance to
582 antibiotics that target cell wall biogenesis, particularly those that act outside the
583 plasma membrane, and to rifampicin. As the *pmt* mutant strains have also lost some
584 intrinsic resistance to a similar subset of antibiotics (particularly vancomycin,
585 imipenem and rifampicin) as the *ppm1⁻* strain, we conclude that loss of protein O-
586 glycosylation contributes in part to the phenotype of the *ppm1⁻* strains.

587

588 **Acknowledgements**

589 We are grateful to Drs Toby Hodge and Katherine Newling from the York Bioscience
590 Technology Facility for discussions and help with bioinformatics.

591

592 **Funding Information**

593 This work was funded by project grants_BB/J016691 and BBS/B/05990 from the
594 Biotechnology and Biological Sciences Research Council, UK.

595

596 **Conflicts of Interest and Ethics**

597 None

598

599

600 References

- 601 1. **Mishra AK, Driessen NN, Appelmek BJ, Besra GS.** Lipoarabinomannan and
602 related glycoconjugates: structure, biogenesis and role in Mycobacterium tuberculosis
603 physiology and host-pathogen interaction. *FEMS Microbiol Rev* 2011;35(6):1126-1157.
- 604 2. **Lommel M, Strahl S.** Protein O-mannosylation: conserved from bacteria to
605 humans. *Glycobiology* 2009;19(8):816-828.
- 606 3. **Fukuda T, Matsumura T, Ato M, Hamasaki M, Nishiuchi Y et al.** Critical roles
607 for lipomannan and lipoarabinomannan in cell wall integrity of mycobacteria and
608 pathogenesis of tuberculosis. *mBio* 2013;4(1):e00472-00412.
- 609 4. **Mishra AK, Alderwick LJ, Rittmann D, Wang C, Bhatt A et al.** Identification of a
610 novel alpha(1-->6) mannosyltransferase MptB from Corynebacterium
611 glutamicum by deletion of a conserved gene, NCgl1505, affords a lipomannan- and
612 lipoarabinomannan-deficient mutant. *Mol Microbiol* 2008;68(6):1595-1613.
- 613 5. **Dobos KM, Khoo KH, Swiderek KM, Brennan PJ, Belisle JT.** Definition of the
614 full extent of glycosylation of the 45-kilodalton glycoprotein of Mycobacterium
615 tuberculosis. *J Bacteriol* 1996;178(9):2498-2506.
- 616 6. **Michell SL, Whelan AO, Wheeler PR, Panico M, Easton RL et al.** The MPB83
617 antigen from Mycobacterium bovis contains O-linked mannose and (1-->3)-mannobiose
618 moieties. *J Biol Chem* 2003;278(18):16423-16432.
- 619 7. **Espitia C, Servin-Gonzalez L, Mancilla R.** New insights into protein O-
620 mannosylation in actinomycetes. *Mol Biosyst* 2010;6(5):775-781.
- 621 8. **Mahne M, Tauch A, Puhler A, Kalinowski J.** The Corynebacterium glutamicum
622 gene pmt encoding a glycosyltransferase related to eukaryotic protein-O-
623 mannosyltransferases is essential for glycosylation of the resuscitation promoting factor
624 (Rpf2) and other secreted proteins. *FEMS Microbiol Lett* 2006;259(2):226-233.
- 625 9. **Wehmeier S, Varghese AS, Gurcha SS, Tissot B, Panico M et al.** Glycosylation
626 of the phosphate binding protein, PstS, in Streptomyces coelicolor by a pathway that
627 resembles protein O-mannosylation in eukaryotes. *Mol Microbiol* 2009;71(2):421-433.
- 628 10. **Gurcha SS, Baulard AR, Kremer L, Locht C, Moody DB et al.** Ppm1, a novel
629 polyprenol monophosphomannose synthase from Mycobacterium tuberculosis. *Biochem*
630 *J* 2002;365(Pt 2):441-450.
- 631 11. **Rana AK, Singh A, Gurcha SS, Cox LR, Bhatt A et al.** Ppm1-encoded polyprenyl
632 monophosphomannose synthase activity is essential for lipoglycan synthesis and
633 survival in mycobacteria. *PloS one* 2012;7(10):e48211.
- 634 12. **Gibson KJ, Eggeling L, Maughan WN, Krumbach K, Gurcha SS et al.** Disruption
635 of Cg-Ppm1, a polyprenyl monophosphomannose synthase, and the generation of
636 lipoglycan-less mutants in Corynebacterium glutamicum. *J Biol Chem*
637 2003;278(42):40842-40850.
- 638 13. **VanderVen BC, Harder JD, Crick DC, Belisle JT.** Export-mediated assembly of
639 mycobacterial glycoproteins parallels eukaryotic pathways. *Science*
640 2005;309(5736):941-943.
- 641 14. **Fernandez-Alvarez A, Marin-Menguiano M, Lanver D, Jimenez-Martin A,**
642 **Elias-Villalobos A et al.** Identification of O-mannosylated virulence factors in Ustilago
643 maydis. *Plos Pathog* 2012;8(3):e1002563.

- 644 15. **Gentzsch M, Tanner W.** The PMT gene family: protein O-glycosylation in
645 *Saccharomyces cerevisiae* is vital. *EMBO J* 1996;15(21):5752-5759.
- 646 16. **Mouyna I, Kniemeyer O, Jank T, Loussert C, Mellado E et al.** Members of
647 protein O-mannosyltransferase family in *Aspergillus fumigatus* differentially affect
648 growth, morphogenesis and viability. *Mol Microbiol* 2010;76(5):1205-1221.
- 649 17. **Olson GM, Fox DS, Wang P, Alspaugh JA, Buchanan KL.** Role of protein O-
650 mannosyltransferase *Pmt4* in the morphogenesis and virulence of *Cryptococcus*
651 *neoformans*. *Eukaryotic cell* 2007;6(2):222-234.
- 652 18. **Prill SK, Klinkert B, Timpel C, Gale CA, Schroppel K et al.** PMT family of
653 *Candida albicans*: five protein mannosyltransferase isoforms affect growth,
654 morphogenesis and antifungal resistance. *Mol Microbiol* 2005;55(2):546-560.
- 655 19. **Willer T, Brandl M, Sipiczki M, Strahl S.** Protein O-mannosylation is crucial for
656 cell wall integrity, septation and viability in fission yeast. *Mol Microbiol* 2005;57(1):156-
657 170.
- 658 20. **Willer T, Prados B, Falcon-Perez JM, Renner-Muller I, Przemeck GK et al.**
659 Targeted disruption of the Walker-Warburg syndrome gene *Pomt1* in mouse results in
660 embryonic lethality. *Proc Natl Acad Sci U S A* 2004;101(39):14126-14131.
- 661 21. **Cowlshaw DA, Smith MC.** Glycosylation of a *Streptomyces coelicolor* A3(2) cell
662 envelope protein is required for infection by bacteriophage phi C31. *Mol Microbiol*
663 2001;41(3):601-610.
- 664 22. **Cowlshaw DA, Smith MC.** A gene encoding a homologue of dolichol phosphate-
665 b-D mannose synthase is required for infection of *Streptomyces coelicolor* A3(2) by
666 phage fC31. *J Bacteriol* 2002;184(21):6081-6083.
- 667 23. **MacNeil DJ.** Characterization of a unique methyl-specific restriction system in
668 *Streptomyces avermitilis*. *J Bacteriol* 1988;170(12):5607-5612.
- 669 24. **Kieser T, Bibb MJ, Buttner MJ, Chater KF, Hopwood DA.** *Practical Streptomyces*
670 *Genetics*. Norwich: The John Innes Foundation; 2000.
- 671 25. **Love MI, Huber W, Anders S.** Moderated estimation of fold change and
672 dispersion for RNA-seq data with DESeq2. *Genome Biol* 2014;15(12):550.
- 673 26. **Zheng Q, Wang XJ.** GOEAST: a web-based software toolkit for Gene Ontology
674 enrichment analysis. *Nucleic Acids Res* 2008;36(Web Server issue):W358-363.
- 675 27. **Robinson JT, Thorvaldsdottir H, Winckler W, Guttman M, Lander ES et al.**
676 Integrative genomics viewer. *Nat Biotechnol* 2011;29(1):24-26.
- 677 28. **Thorvaldsdottir H, Robinson JT, Mesirov JP.** Integrative Genomics Viewer
678 (IGV): high-performance genomics data visualization and exploration. *Brief Bioinform*
679 2013;14(2):178-192.
- 680 29. **Candeloro P, Grande E, Raimondo R, Di Mascolo D, Gentile F et al.** Raman
681 database of amino acids solutions: a critical study of extended multiplicative signal
682 correction. *Analyst* 2013;138(24):7331-7340.
- 683 30. **Movasaghi Z, Rehman S, Rehman IU.** Raman Spectroscopy of Biological Tissues.
684 *Applied Spectroscopy Reviews* 2007;42:493-541.
- 685 31. **Walter A, Schumacher W, Bocklitz T, Reinicke M, Rosch P et al.** From bulk to
686 single-cell classification of the filamentous growing *Streptomyces* bacteria by means of
687 Raman spectroscopy. *Appl Spectrosc* 2011;65(10):1116-1125.
- 688 32. **Hong HJ, Hutchings MI, Buttner MJ, Biotechnology, Biological Sciences**
689 **Research Council UK.** Vancomycin resistance VanS/VanR two-component systems. *Adv*
690 *Exp Med Biol* 2008;631:200-213.

- 691 33. **Hong HJ, Hutchings MI, Neu JM, Wright GD, Paget MS et al.** Characterization of
692 an inducible vancomycin resistance system in *Streptomyces coelicolor* reveals a novel
693 gene (vanK) required for drug resistance. *Mol Microbiol* 2004;52(4):1107-1121.
- 694 34. **Arthur M, Molinas C, Depardieu F, Courvalin P.** Characterization of Tn1546, a
695 Tn3-related transposon conferring glycopeptide resistance by synthesis of depsipeptide
696 peptidoglycan precursors in *Enterococcus faecium* BM4147. *J Bacteriol*
697 1993;175(1):117-127.
- 698 35. **Bugg TD, Wright GD, Dutka-Malen S, Arthur M, Courvalin P et al.** Molecular
699 basis for vancomycin resistance in *Enterococcus faecium* BM4147: biosynthesis of a
700 depsipeptide peptidoglycan precursor by vancomycin resistance proteins VanH and
701 VanA. *Biochemistry* 1991;30(43):10408-10415.
- 702 36. **Healy VL, Lessard IA, Roper DI, Knox JR, Walsh CT.** Vancomycin resistance in
703 enterococci: reprogramming of the D-ala-D-Ala ligases in bacterial peptidoglycan
704 biosynthesis. *Chem Biol* 2000;7(5):R109-119.
- 705 37. **Hong HJ, Hutchings MI, Hill LM, Buttner MJ.** The role of the novel Fem protein
706 VanK in vancomycin resistance in *Streptomyces coelicolor*. *J Biol Chem*
707 2005;280(13):13055-13061.
- 708 38. **Bayer AS, Schneider T, Sahl HG.** Mechanisms of daptomycin resistance in
709 *Staphylococcus aureus*: role of the cell membrane and cell wall. *Ann N Y Acad Sci*
710 2013;1277:139-158.
- 711 39. **Mascher T, Margulis NG, Wang T, Ye RW, Helmann JD.** Cell wall stress
712 responses in *Bacillus subtilis*: the regulatory network of the bacitracin stimulon. *Mol*
713 *Microbiol* 2003;50(5):1591-1604.
- 714 40. **Boechat AL, Kaihama GH, Politi MJ, Lepine F, Baldini RL.** A novel role for an
715 ECF sigma factor in fatty acid biosynthesis and membrane fluidity in *Pseudomonas*
716 *aeruginosa*. *PloS one* 2013;8(12):e84775.
- 717 41. **Kingston AW, Subramanian C, Rock CO, Helmann JD.** A sigmaW-dependent
718 stress response in *Bacillus subtilis* that reduces membrane fluidity. *Mol Microbiol*
719 2011;81(1):69-79.
- 720 42. **Hong HJ, Paget MS, Buttner MJ.** A signal transduction system in *Streptomyces*
721 *coelicolor* that activates the expression of a putative cell wall glycan operon in response
722 to vancomycin and other cell wall-specific antibiotics. *Mol Microbiol* 2002;44(5):1199-
723 1211.
- 724 43. **Rida S, Caillet J, Alix JH.** Amplification of a novel gene, sanA, abolishes a
725 vancomycin-sensitive defect in *Escherichia coli*. *J Bacteriol* 1996;178(1):94-102.
- 726 44. **Paget MSB, Chamberlin L, Atrih A, Foster SJ, Buttner MJ.** Evidence that the
727 extracytoplasmic function sigma factor sigmaE is required for normal cell wall structure
728 in *Streptomyces coelicolor* A3(2). *Journal of Bacteriology* 1999;181(1):204-211.
- 729 45. **Ashton L, Lau K, Winder CL, Goodacre R.** Raman spectroscopy: lighting up the
730 future of microbial identification. *Future microbiology* 2011;6(9):991-997.
- 731 46. **Walter A, Reinicke M, Bocklitz T, Schumacher W, Rosch P et al.** Raman
732 spectroscopic detection of physiology changes in plasmid-bearing *Escherichia coli* with
733 and without antibiotic treatment. *Anal Bioanal Chem* 2011;400(9):2763-2773.
- 734 47. **Stöckel S, Kirchhoff J, Neugebauer U, Rösch P, Popp J.** The application of
735 Raman spectroscopy for the detection and identification of microorganisms. *Journal of*
736 *Raman Spectroscopy* 2016;47(1):89-109.
- 737 48. **Munchberg U, Rosch P, Bauer M, Popp J.** Raman spectroscopic identification of
738 single bacterial cells under antibiotic influence. *Anal Bioanal Chem* 2014;406(13):3041-
739 3050.

- 740 49. **Wu H, Volponi JV, Oliver AE, Parikh AN, Simmons BA et al.** In vivo lipidomics
741 using single-cell Raman spectroscopy. *Proc Natl Acad Sci U S A* 2011;108(9):3809-3814.
- 742 50. **Potcoava MC, Futia GL, Aughenbaugh J, Schlaepfer IR, Gibson EA.** Raman and
743 coherent anti-Stokes Raman scattering microscopy studies of changes in lipid content
744 and composition in hormone-treated breast and prostate cancer cells. *J Biomed Opt*
745 2014;19(11):111605.
- 746 51. **Nieva C, Marro M, Santana-Codina N, Rao S, Petrov D et al.** The lipid
747 phenotype of breast cancer cells characterized by Raman microspectroscopy: towards a
748 stratification of malignancy. *PLoS one* 2012;7(10):e46456.
- 749 52. **Hoischen C, Gura K, Luge C, Gumpert J.** Lipid and fatty acid composition of
750 cytoplasmic membranes from *Streptomyces hygroscopicus* and its stable protoplast-
751 type L form. *J Bacteriol* 1997;179(11):3430-3436.
- 752 53. **Sandoval-Calderon M, Geiger O, Guan Z, Barona-Gomez F, Sohlenkamp C.** A
753 eukaryote-like cardiolipin synthase is present in *Streptomyces coelicolor* and in most
754 actinobacteria. *J Biol Chem* 2009;284(26):17383-17390.
- 755 54. **Guerin ME, Kordulakova J, Alzari PM, Brennan PJ, Jackson M.** Molecular basis
756 of phosphatidyl-myo-inositol mannoside biosynthesis and regulation in mycobacteria. *J*
757 *Biol Chem* 2010;285(44):33577-33583.
- 758 55. **Gago G, Diacovich L, Arabolaza A, Tsai SC, Gramajo H.** Fatty acid biosynthesis
759 in actinomycetes. *FEMS Microbiol Rev* 2011;35(3):475-497.
- 760 56. **Zhang YM, Rock CO.** Membrane lipid homeostasis in bacteria. *Nature reviews*
761 2008;6(3):222-233.
- 762 57. **Singh R, Reynolds KA.** Identification and Characterization of FabA from the Type
763 II Fatty Acid Synthase of *Streptomyces coelicolor*. *J Nat Prod* 2016;79(1):240-243.
- 764 58. **Feng Y, Cronan JE.** Escherichia coli unsaturated fatty acid synthesis: complex
765 transcription of the fabA gene and in vivo identification of the essential reaction
766 catalyzed by FabB. *J Biol Chem* 2009;284(43):29526-29535.
- 767 59. **Xiao X, Yu X, Khosla C.** Metabolic flux between unsaturated and saturated fatty
768 acids is controlled by the FabA:FabB ratio in the fully reconstituted fatty acid
769 biosynthetic pathway of *Escherichia coli*. *Biochemistry* 2013;52(46):8304-8312.
- 770 60. **Bogdanov M, Dowhan W, Vitrac H.** Lipids and topological rules governing
771 membrane protein assembly. *Biochim Biophys Acta* 2014;1843(8):1475-1488.
- 772 61. **Mascher T, Hachmann AB, Helmann JD.** Regulatory overlap and functional
773 redundancy among *Bacillus subtilis* extracytoplasmic function sigma factors. *J Bacteriol*
774 2007;189(19):6919-6927.
- 775 62. **Tran TT, Panesso D, Mishra NN, Mileykovskaya E, Guan Z et al.** Daptomycin-
776 resistant *Enterococcus faecalis* diverts the antibiotic molecule from the division septum
777 and remodels cell membrane phospholipids. *mBio* 2013;4(4).
- 778 63. **Mishra NN, Bayer AS, Tran TT, Shamoo Y, Mileykovskaya E et al.** Daptomycin
779 resistance in enterococci is associated with distinct alterations of cell membrane
780 phospholipid content. *PLoS one* 2012;7(8):e43958.
- 781 64. **Kleinschnitz EM, Latus A, Sigle S, Maldener I, Wohlleben W et al.** Genetic
782 analysis of SCO2997, encoding a TagF homologue, indicates a role for wall teichoic acids
783 in sporulation of *Streptomyces coelicolor* A3(2). *J Bacteriol* 2011;193(21):6080-6085.
- 784 65. **Helmann JD.** *Bacillus subtilis* extracytoplasmic function (ECF) sigma factors and
785 defense of the cell envelope. *Curr Opin Microbiol* 2016;30:122-132.
- 786 66. **Fernandez Martinez L, Bishop A, Parkes L, Del Sol R, Salerno P et al.**
787 Osmoregulation in *Streptomyces coelicolor*: modulation of SigB activity by OsaC. *Mol*
788 *Microbiol* 2009;71(5):1250-1262.

- 789 67. **Gordon ND, Ottaviano GL, Connell SE, Tobkin GV, Son CH et al.** Secreted-
790 protein response to sigmaU activity in *Streptomyces coelicolor*. *J Bacteriol*
791 2008;190(3):894-904.
- 792 68. **Hesketh A, Hill C, Mokhtar J, Novotna G, Tran N et al.** Genome-wide dynamics
793 of a bacterial response to antibiotics that target the cell envelope. *BMC genomics*
794 2011;12:226.
- 795 69. **Spirig T, Weiner EM, Clubb RT.** Sortase enzymes in Gram-positive bacteria. *Mol*
796 *Microbiol* 2011;82(5):1044-1059.
- 797 70. **Pallen MJ, Lam AC, Antonio M, Dunbar K.** An embarrassment of sortases - a
798 richness of substrates? *Trends Microbiol* 2001;9(3):97-102.
- 799 71. **Duong A, Capstick DS, Di Berardo C, Findlay KC, Hesketh A et al.** Aerial
800 development in *Streptomyces coelicolor* requires sortase activity. *Mol Microbiol*
801 2012;83(5):992-1005.
- 802 72. **Kim MS, Dufour YS, Yoo JS, Cho YB, Park JH et al.** Conservation of thiol-
803 oxidative stress responses regulated by SigR orthologues in actinomycetes. *Mol*
804 *Microbiol* 2012;85(2):326-344.
- 805 73. **Strakova E, Zikova A, Vohradsky J.** Inference of sigma factor controlled
806 networks by using numerical modeling applied to microarray time series data of the
807 germinating prokaryote. *Nucleic Acids Res* 2014;42(2):748-763.
- 808 74. **Campbell EA, Korzheva N, Mustaev A, Murakami K, Nair S et al.** Structural
809 mechanism for rifampicin inhibition of bacterial rna polymerase. *Cell* 2001;104(6):901-
810 912.
- 811 75. **Selinger DW, Saxena RM, Cheung KJ, Church GM, Rosenow C.** Global RNA half-
812 life analysis in *Escherichia coli* reveals positional patterns of transcript degradation.
813 *Genome Res* 2003;13(2):216-223.
- 814 76. **Wegrzyn A, Szalewska-Palasz A, Blaszczak A, Liberek K, Wegrzyn G.**
815 Differential inhibition of transcription from sigma70- and sigma32-dependent
816 promoters by rifampicin. *FEBS Lett* 1998;440(1-2):172-174.
- 817 77. **Bandow JE, Brotz H, Hecker M.** *Bacillus subtilis* tolerance of moderate
818 concentrations of rifampin involves the sigma(B)-dependent general and multiple stress
819 response. *J Bacteriol* 2002;184(2):459-467.
- 820 78. **Newell KV, Thomas DP, Brekasis D, Paget MS.** The RNA polymerase-binding
821 protein RbpA confers basal levels of rifampicin resistance on *Streptomyces coelicolor*.
822 *Mol Microbiol* 2006;60(3):687-696.
- 823 79. **Lithgow KV, Scott NE, Iwashkiw JA, Thomson EL, Foster LJ et al.** A general
824 protein O-glycosylation system within the Burkholderia cepacia complex is involved in
825 motility and virulence. *Mol Microbiol* 2014;92(1):116-137.
- 826 80. **Zebian N, Merckx-Jacques A, Pittock PP, Houle S, Dozois CM et al.**
827 Comprehensive analysis of flagellin glycosylation in *Campylobacter jejuni* NCTC 11168
828 reveals incorporation of legionaminic acid and its importance for host colonization.
829 *Glycobiology* 2016;26(4):386-397.
- 830 81. **Rolain T, Bernard E, Beaussart A, Degand H, Courtin P et al.** O-Glycosylation
831 as a Novel Control Mechanism of Peptidoglycan Hydrolase Activity. *Journal of Biological*
832 *Chemistry* 2013;288(31):22233-22247.
- 833 82. **Hugonnet JE, Haddache N, Veckerle C, Dubost L, Marie A et al.** Peptidoglycan
834 cross-linking in glycopeptide-resistant Actinomycetales. *Antimicrob Agents Chemother*
835 2014;58(3):1749-1756.

836 83. **Li Y, Florova G, Reynolds KA.** Alteration of the fatty acid profile of *Streptomyces*
837 *coelicolor* by replacement of the initiation enzyme 3-ketoacyl acyl carrier protein
838 synthase III (FabH). *J Bacteriol* 2005;187(11):3795-3799.

839

840

841 **Table 1. Enriched GO terms**

Up-regulated enriched GO terms	Count of genes associated with the listed GOID in the dataset	Count of genes associated with the listed GOID in the full gene list	P value
organic acid biosynthetic process	31	276	0.000
Cytoplasm (cellular component)	42	984	0.004
fatty acid synthase activity (molecular-function)	5	25	0.034
nickel cation binding (molecular-function)	4	13	0.029
carboxylic acid biosynthetic process	31	268	0.000
nucleoside catabolic process	3	7	0.053
nucleoside phosphate biosynthetic process	9	109	0.078
cellular amino acid biosynthetic process	19	179	0.000
monocarboxylic acid biosynthetic process	12	82	0.000
nucleoside monophosphate biosynthetic process	6	43	0.053
glutamine family amino acid biosynthetic process	10	35	0.000
alpha-amino acid biosynthetic process	18	150	0.000
fatty acid biosynthetic process	9	64	0.003
branched-chain amino acid biosynthetic process	5	19	0.010
ribonucleoside monophosphate biosynthetic process	6	39	0.034
biotin biosynthetic process	3	7	0.053
arginine biosynthetic process	7	15	0.000
leucine biosynthetic process	3	7	0.053
'de novo' UMP biosynthetic process	3	7	0.053
Down-regulated enriched GO terms			
periplasmic space (cellular-component)	17	83	0.002
transport	57	693	0.054
single-organism catabolic process	19	151	0.069
organic substance transport	31	261	0.008
organic acid transport	13	69	0.020
carbohydrate transport	13	80	0.062
anion transport	16	97	0.018
monocarboxylic acid catabolic process	14	63	0.003
carboxylic acid transport	13	69	0.020
fatty acid metabolic process	16	108	0.053
fatty acid catabolic process	10	27	0.002
amino acid transport	13	61	0.008

842

843

844

845

846
847
848
849
850
851
852
853
854
855
856
857
858
859
860
861

Supplementary material

Figure S1. Small colony phenotype of the *pmt* and *ppm1* mutants

Figure S2 Growth curve for DT3017, J1929 and DT3017pDT16 in the fermentor;

Validation of the use of the stop solution for RNA preparation.

Figure S3 Statistics for Raman spectroscopy data

Table S1 Oligos

Table S2 Benjamini Hockberg enriched genes.

Table S3 Peak positions for identification of cellular components

Dataset S1 Antibiotic disc diffusion data

Dataset S2 Raw data for RTqPCR *vanH* , *sigE* and *hrdB*

Dataset S3 Genes for GO analysis

Dataset S4 GO analysis

862 **Figure legends**

863 **Figure 1. The protein O-glycosylation pathway in *S. coelicolor*.** A. Two enzyme
864 activities, Ppm1 and Pmt (encoded by *sco1423* and *sco3154*, respectively), required
865 for glycosylation of the periplasmic phosphate binding protein, PstS are membrane
866 bound [9]. *In vitro* Ppm1 transfers mannose from GDP-mannose to a nonaprenol to
867 generate polyprenol phosphate mannose, which then acts as the sugar carrier for
868 Pmt to glycosylate peptides containing a glycosylation site [9]. In *Mycobacterium*
869 *tuberculosis* protein O-glycosylation was associated with the secretion apparatus
870 [13].

871 **Figure 2. *Streptomyces coelicolor* strains defective in protein glycosylation**
872 **genes are hypersensitive to multiple antibiotics.** Shown are diameters of growth
873 inhibition zones from disc diffusion assays for the *ppm1*⁻ mutants, DT1020, DT1029
874 and DT3017 against the parent strain J1929 and the complemented strains
875 DT2010:pDT16, DT1029:pDT16 and DT3017:pDT16 (A), and the *pmt* mutants,
876 DT1025 and DT2008, the parent strain J1929 and the complemented strains
877 DT1025:pDT10 and DT2008:pDT10 (B). Shown are the averages of 4 replicates with
878 SEM. □□ Indicates a p<0.05 that the observed difference between the mutant strains
879 versus J1929 has occurred by chance. The concentration of antibiotic used is shown
880 in brackets; the full set of antibiotic concentrations used is in Dataset S1. (C)
881 Diagrammatic summary of antibiotic targets in cell wall biosynthesis.

882

883 **Figure 3 Transcription of *vanH* in response to vancomycin induction.** qRT-PCR
884 was performed to measure relative levels of *vanH* mRNA following addition of 0.1
885 µg/ml vancomycin in (A) DT3017 (blue; *ppm1*⁻) and (B) DT2008 (red;*pmt*) strains
886 alongside the parent strain (black;J1929) and their respective complemented strains

887 (grey; panel A; DT3017:pDT16 and panel B; DT2008:pDT10). In each instance *hrdB*
888 was used as the reference gene and J1929 time-point 0 as the reference sample.

889

890 **Figure 4. Expression of genes involved in fatty acid metabolism in the *ppm1***
891 **strain DT3017, the parent strain, J1929 and the complemented strain**
892 **DT3017:pDT16.** (A) Pathway for the synthesis of fatty acids in *S. coelicolor*. The
893 thick line feeding into reaction 3 reflects the preference by *S. coelicolor* FabH for
894 branched chain acyl-CoA precursors [83] (B) Deseq normalized expression levels for
895 fatty acid metabolism genes of *S. coelicolor* for strains J1929 (black), DT3017 (red)
896 and DT3017 pDT16 (grey). Red numbering above refers to steps in the pathway
897 indicated in (A) above. Shown values are the average of three replicates. Above
898 DT3017 one star equals $p < 0.05$ and two stars equal Benjamini-Hockberg corrected
899 $p < 0.05$ significance levels against J1929.

900

901 **Figure 5. RNAseq mapped read depth across SCO3736-SCO3738, the most**
902 **significantly changed genes in DT3017.** Deseq analysis of differential gene
903 expression between J1929 and DT3017 revealed the top three most significant
904 changes occurred in one operon, SCO3736-SCO3738, encoding a putative
905 extracytoplasmic sigma factor, lipoprotein and integral membrane protein
906 respectively. Shown are the mapped read depths across this region alongside
907 downstream SCO3735, a putative secreted protein, as visualised by the Integrated
908 Genomics Viewer. Replicate one is shown as representative of all replicates.

909 **Figure 6. Raman spectroscopy analysis of *S. coelicolor* strains.** Averaged
910 Raman spectra obtained in the (A) high wave-number region and (B) the fingerprint
911 region ($600\text{--}1800\text{cm}^{-1}$) for the *S. coelicolor* parent strain J1929 (red; N=42), the

912 *ppm1⁻* mutant strain DT3017 (*blue*; N=55) and the complemented mutant,
913 DT3017:pDT16 (red; N=40). N refers to the total number of individual spectra in each
914 spectral average. Key peak assignments are shown (Table S3) with the spectra
915 vertically shifted to aid visualisation. Panel C; TUFA/TFA (I_{3008}/I_{2850}) peak intensity
916 ratios derived from the averaged spectra in panels A and B.

917

918

919

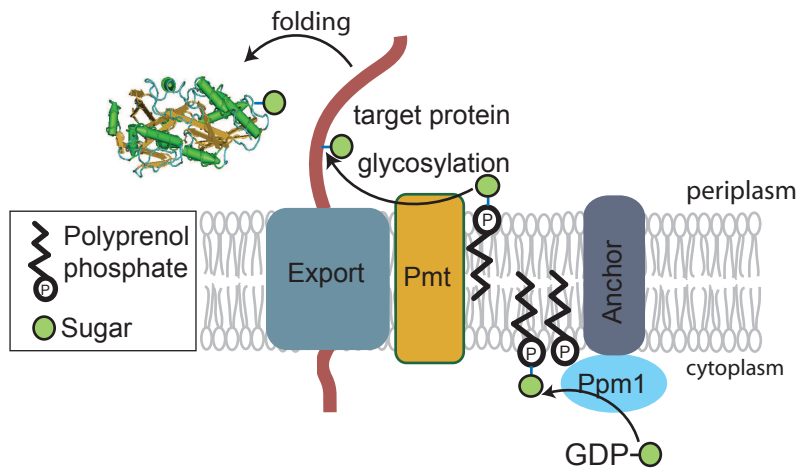


Figure 1

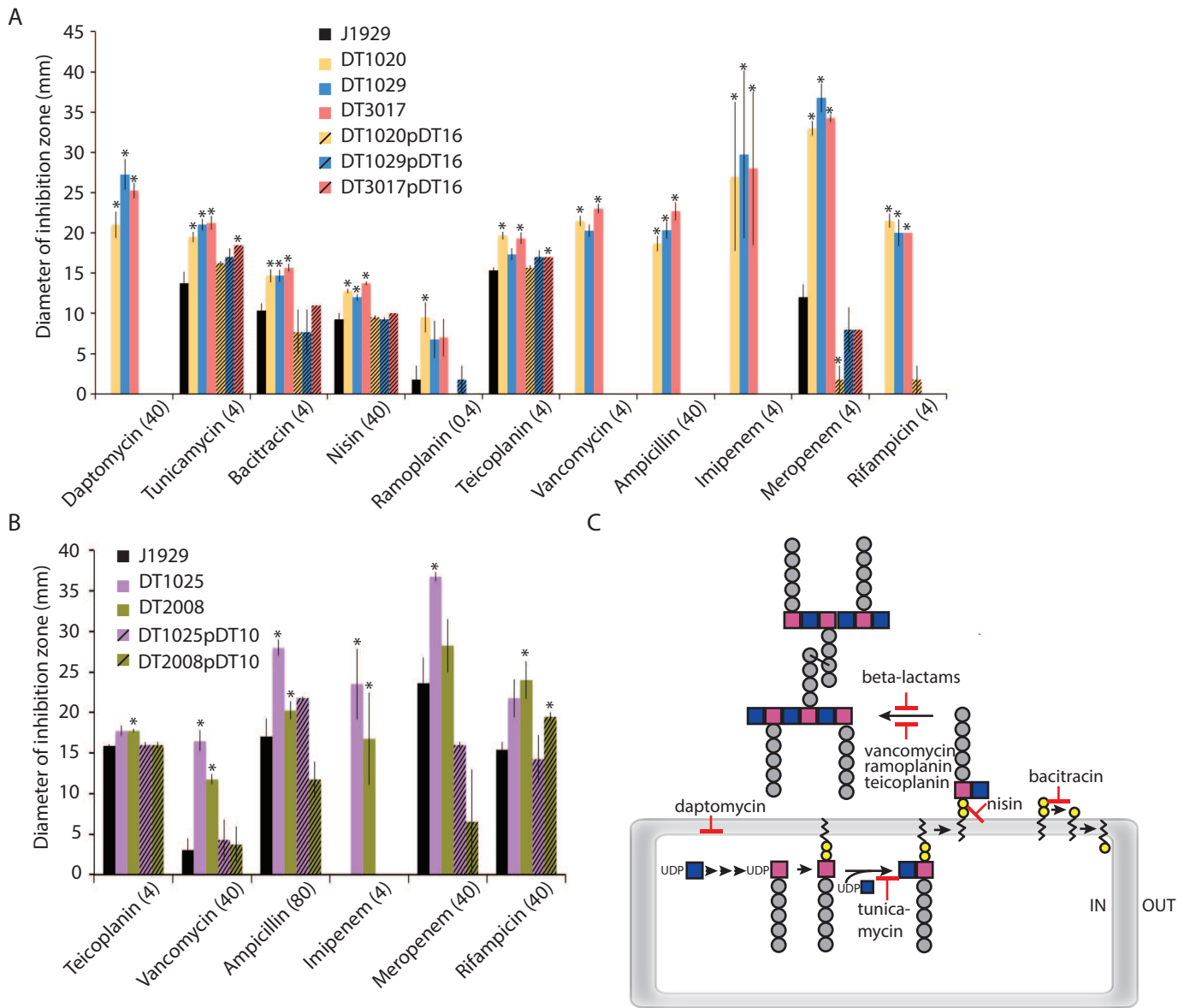


Figure 2

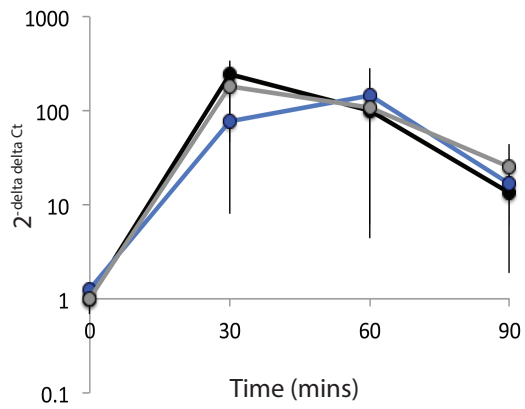
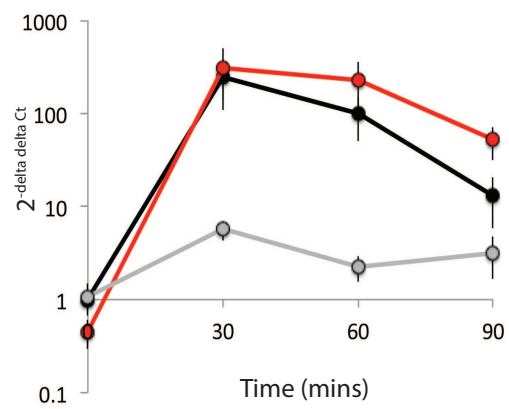
A. Induced *vanH* expression in a *ppm1* strainB. Induced *vanH* expression in a *pmt* strain

Figure 3

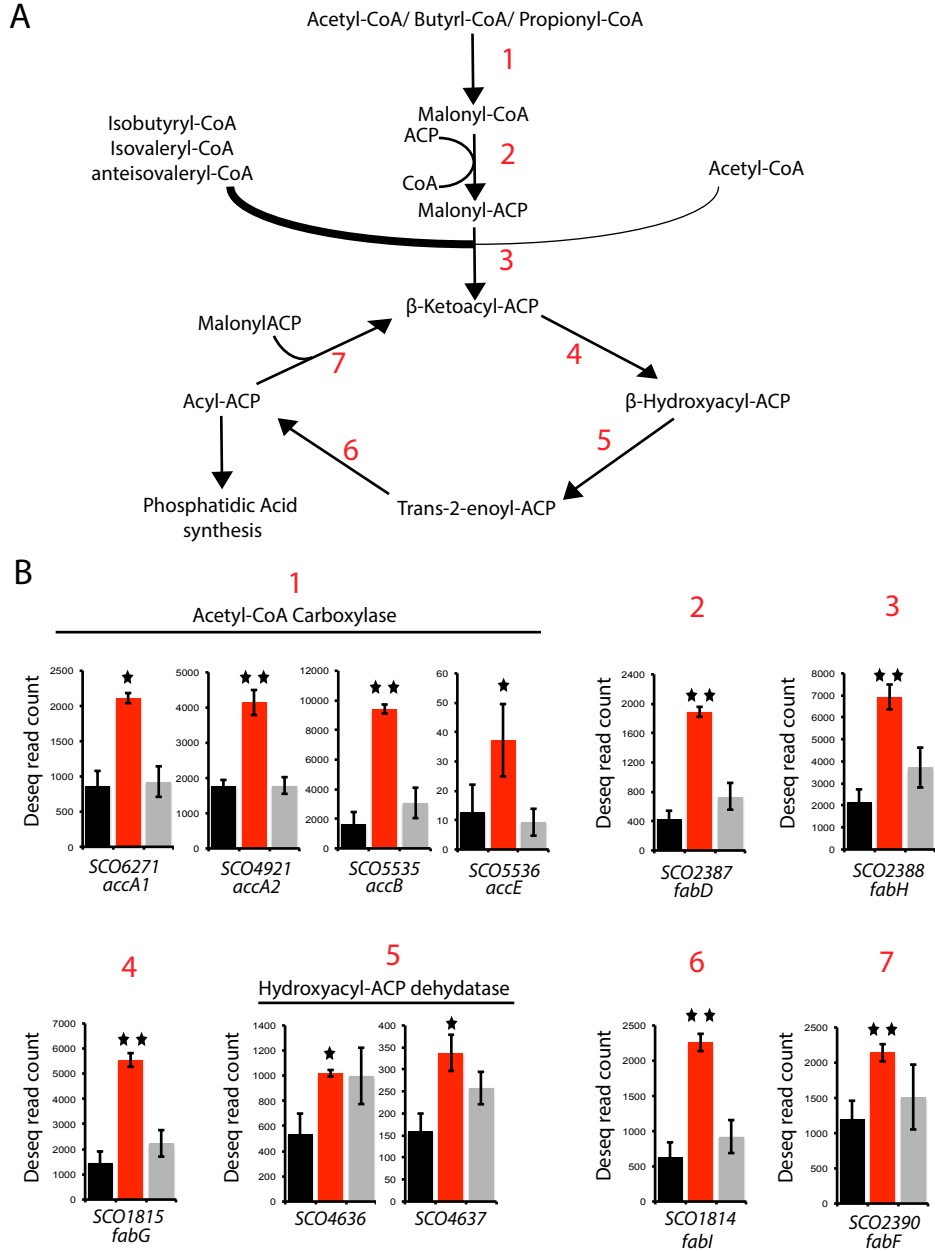


Figure 4

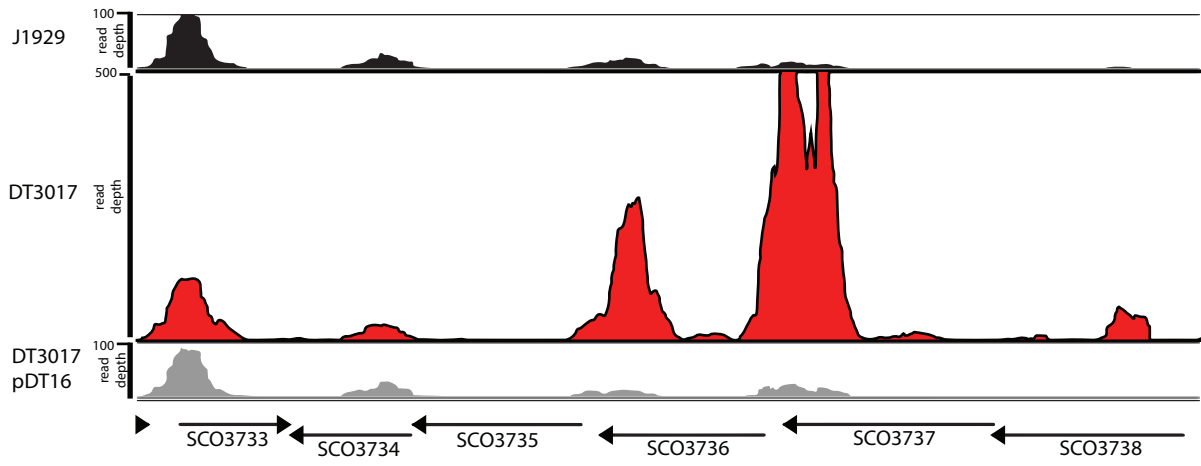


Figure 5

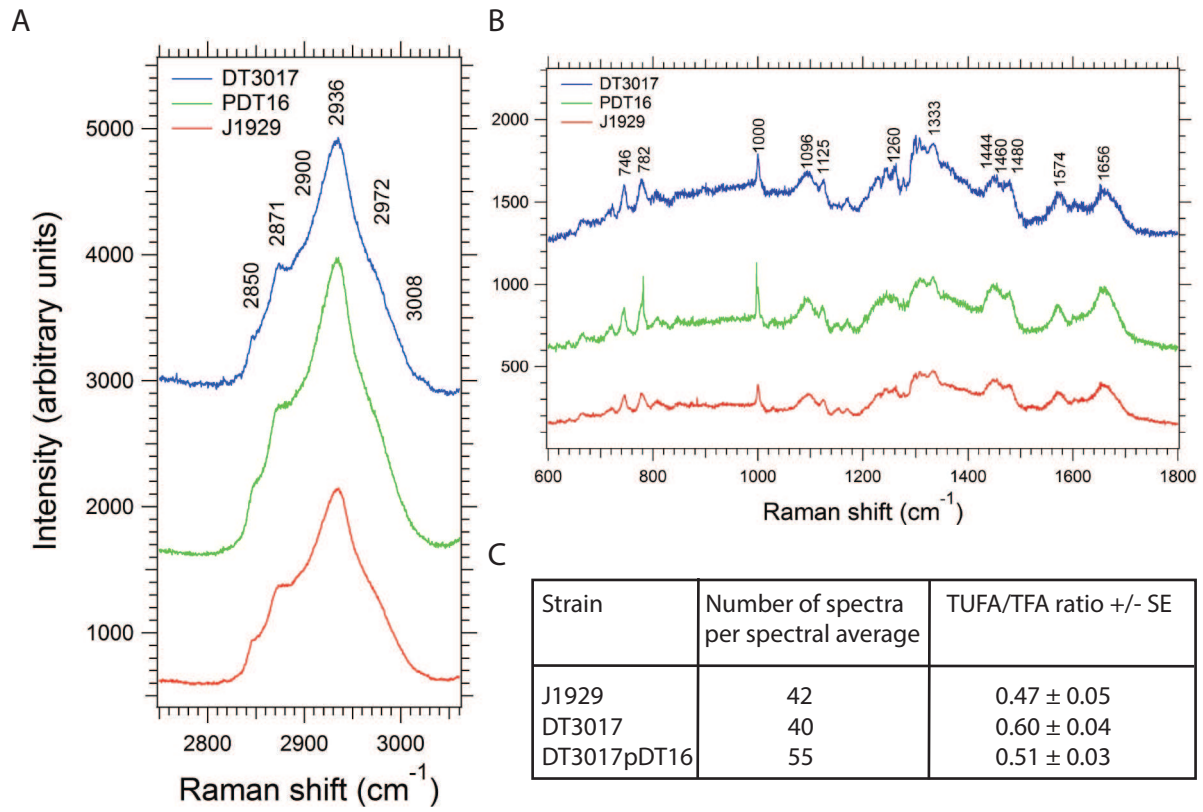


Figure 6

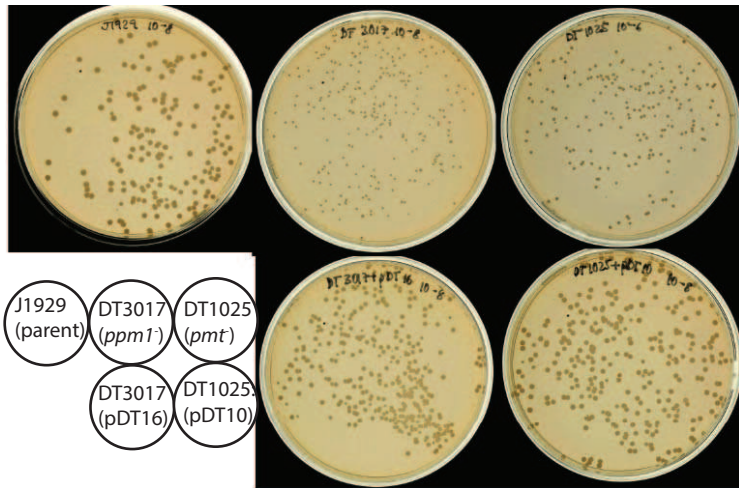


Figure S1

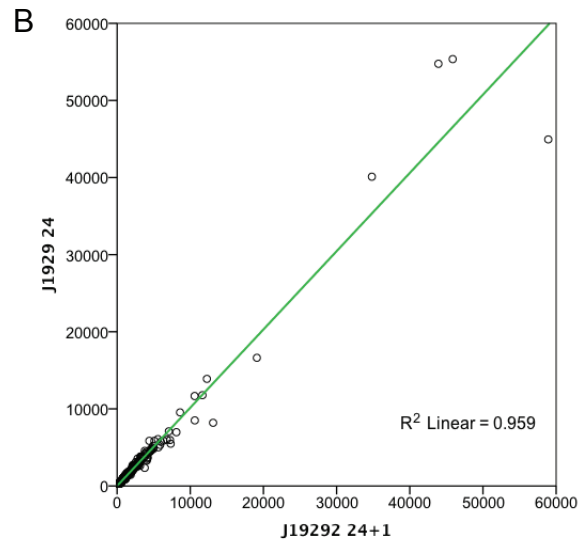
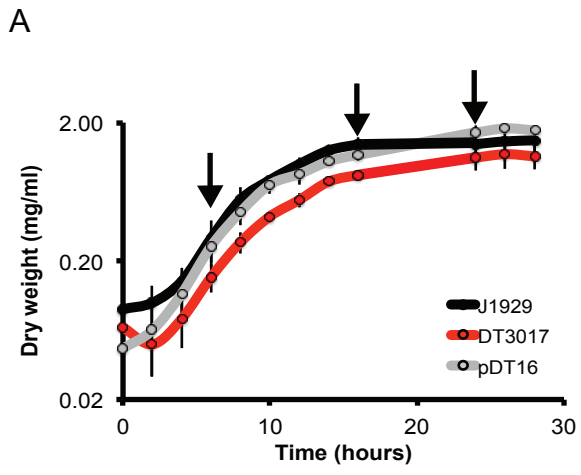


Figure S2

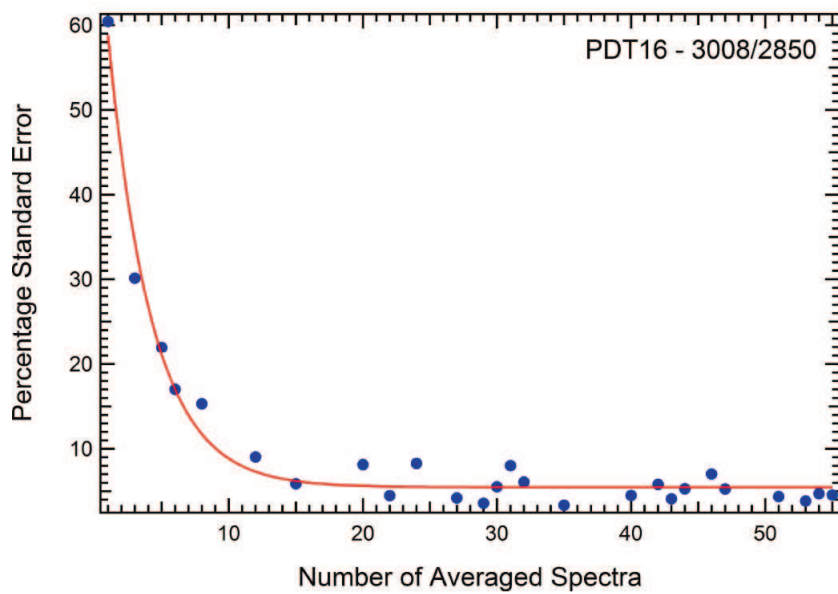
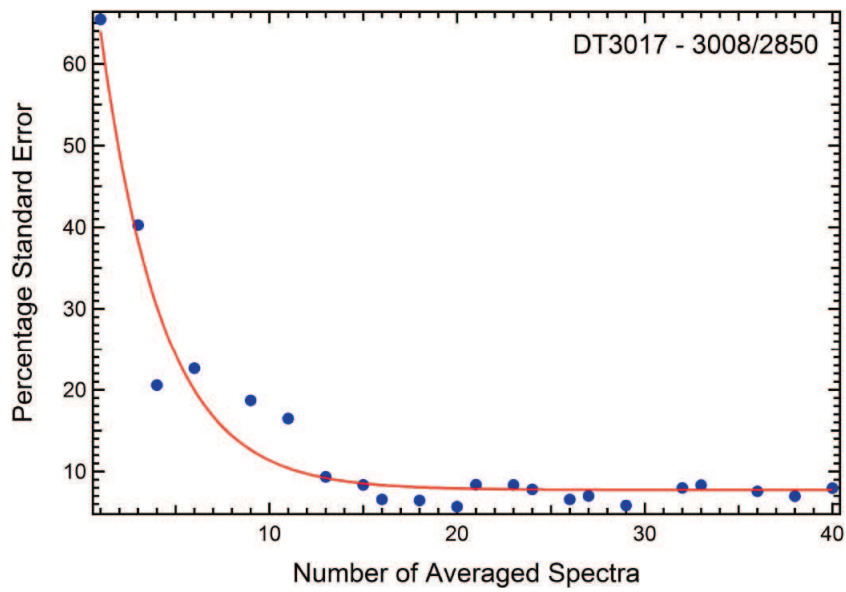
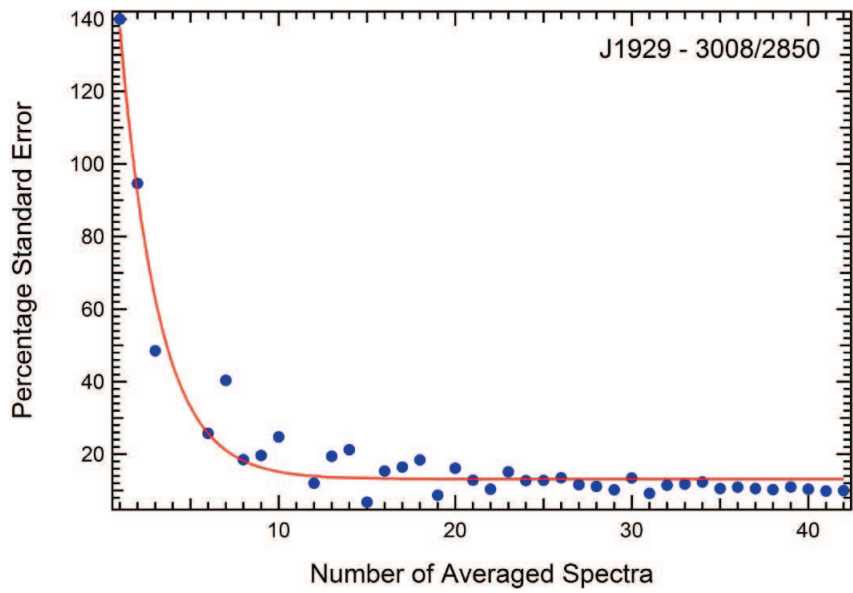


Figure S3

Supplementary Figure legends (Howlett, Read *et al*)

Figure S1. Small colony phenotype in the *pmt*⁻ and *ppm1*⁻ mutants. *S. coelicolor pmt*⁻ (DT1025) and *ppm1*⁻ (DT3017) mutants are derived from J1929 (*pglY*) [1-3]. Plasmids pDT10 and pDT16 used to complement *pmt*⁻ and *ppm1*⁻ mutants, respectively, are derivatives from vector pSET152 and encode wild type *pmt* and *ppm1*, respectively [2, 3]. Strains were grown on Difco nutrient agar and were incubated at 30 °C for 48 hours. Key to strains is bottom left.

Figure S2. Sampling of the transcriptome from *S. coelicolor* J1929, DT3017 and DT3017 pDT16 strains for RNAseq analysis. (A) *S. coelicolor* strains were cultured in controlled fermentor growth conditions in Difco nutrient broth where DT3017 (red) showed a modest growth defect compared to its parent and complement strains J1929 (black) and DT3017 pDT16 (grey) respectively. Samples were collected from all samples at time-point 6 for comparative transcriptome analysis and J1929 replicate 1 at time-point 24 to confirm transcriptome quenching (indicated by black arrows). Shown are averages of three biological repeats with error bars. (B) Validation of the sampling protocol for RNASeq. Two samples were collected from J1929 replicate 1 at time-point 24, one of which was left on ice for one hr following the addition of a stop solution; RNA from both samples was prepared and analyzed by RNAseq to look for significant changes that might have resulted from RNA degradation. Subsequent linear regression analysis was performed, giving an R² value of 0.959 indicating that the use of the stop solution was a valid procedure for sample preparation.

Figure S3. Convergence of the percentage standard error of the mean(SE) for the TUFA/TFA peak intensity ratio I_{3008}/I_{2850} as a function of the number of randomly chosen spectra comprising the spectral average for the parent strain (J1929, top panel), the *ppm1*⁻ mutant (DT3017, middle panel) and the complemented mutant (DT3017:pDT16, bottom panel). In total 42, 55 and 40 spectra were averaged for J1929, DT3017 and DT3017:pDT16, respectively.

References

1. **Bedford, D.J., C. Laity, and M.J. Buttner**, 1995. Two genes involved in the phase-variable fC31 resistance mechanism of *Streptomyces coelicolor* A3(2). *J Bacteriol*, **177**(16): p. 4681-9.
2. **Cowlshaw, D.A. and M.C.M Smith**, 2001. Glycosylation of a *Streptomyces coelicolor* A3(2) cell envelope protein is required for infection by bacteriophage fC31. *Mol Microbiol*, **41**(3): p. 601-10.
3. **Cowlshaw, D.A. and M.C.M Smith**, 2002. A gene encoding a homologue of dolichol phosphate-b-D mannose synthase is required for infection of *Streptomyces coelicolor* A3(2) by phage fC31. *J Bacteriol*, **184**(21): p. 6081-6083.

Table S1 Oligonucleotides used for qRT-PCR

Oligonucleotide	Sequence	Use
RH107	5' CTGATGGACGTCCTGAAGGT	<i>sigE</i> forward
RH108	5' GTCTCCTCCGTCGACATCTG	<i>sigE</i> reverse
RH109	5' ACGAGAATCACGGTTTACGG	<i>vanH</i> forward
RH110	5' CTTGTGGTCAATGCTGATGC	<i>vanH</i> reverse
RH111	5' CCGAGTCCGTCTCTGTCATG	<i>hrdB</i> forward
RH112	5' CGGAATCTGGTCAGCTTCGA	<i>hrdB</i> reverse

Table S2 Benjamin-Hockberg list

Gene	log2 fold change DT3017 Vs		Function
	J1929	DT3017 pDT16	
SCO3737	5.23	4.92	lipoprotein
SCO3736	3.76	3.35	RNA polymerase ECF sigma factor
SCO3738	5.02	4.81	hypothetical protein
SCO2774	-2.07	-0.91	acyl-CoA dehydrogenase
SCO3051	-1.88	-0.92	acyl-CoA dehydrogenase
SCO1182	1.66	0.13	hypothetical protein
SCO3706	2.24	1.71	ABC transporter ATP-binding protein
SCO1346	-1.67	-0.61	3-oxoacyl-ACP reductase
SCO2387	2.16	1.36	ACP S-malonyltransferase
SCO2776	-3.84	-2.13	acetyl/propionyl CoA carboxylase subunit beta
SCO1454	-2.61	-0.90	amino oxidase
SCO3707	2.03	2.35	lipoprotein
SCO3079	-1.81	-0.65	acetyl-CoA acetyltransferase
SCO0107	-2.17	-1.45	aminoglycoside nucleotidyltransferase
SCO1345	-1.89	-0.46	3-ketoacyl-ACP reductase
SCO5515	1.76	1.10	D-3-phosphoglycerate dehydrogenase
SCO4980	-2.01	-1.43	hypothetical protein
SCO6009	-1.61	-0.54	solute-binding protein
SCO2014	1.21	0.52	pyruvate kinase
SCO2779	-3.25	-1.54	acyl-CoA dehydrogenase
SCO5535	2.50	1.61	carboxyl transferase
SCO1459	-3.01	-1.01	amino acid transporter
SCO0215	-4.17	-3.84	hypothetical protein
SCO0174	-4.11	-4.53	DNA-binding protein
SCO2587	-1.35	-1.10	gamma-glutamyl kinase
SCO2773	-2.26	-0.27	acyl CoA thioesterase II
SCO1815	1.92	1.30	3-oxacyl-ACP reductase
SCO0165	-2.72	-2.50	hypothetical protein
SCO6010	-1.48	-0.37	ABC transporter ATP-binding protein
SCO2388	1.67	0.89	3-oxoacyl-ACP synthase
SCO0923	-3.69	-3.82	succinate dehydrogenase flavoprotein subunit
SCO1082	-1.35	-1.00	electron transfer flavoprotein subunit beta
SCO6011	-1.43	-0.27	ABC transporter
SCO4921	1.22	1.22	acyl-CoA carboxylase complex A subunit
SCO7036	1.69	0.75	argininosuccinate synthase
SCO0167	-3.29	-3.78	hypothetical protein
SCO1814	1.84	1.29	enoyl-ACP reductase
SCO4690	-3.41	-2.82	hypothetical protein
SCO0543	-1.85	-1.50	peptidase
SCO1081	-1.57	-1.04	electron transfer flavoprotein subunit alpha
SCO5676	-2.28	-0.44	4-aminobutyrate aminotransferase
SCO5516	1.51	0.92	integral membrane efflux protein
SCO1453	-1.83	-0.41	hypothetical protein

SCO0166	-2.86	-3.17	regulator
SCO6502	-2.74	-3.10	gas vesicle synthesis protein
SCO6564	1.57	1.34	3-oxoacyl-ACP synthase
SCO0168	-3.60	-4.13	regulator protein
SCO3607	-2.02	-1.37	hypothetical protein
SCO4107	1.22	0.89	hypothetical protein
SCO3656	1.68	0.35	hypothetical protein
SCO0211	-4.01	-4.22	hypothetical protein
SCO1225	-1.84	-0.99	osmoprotectant transporter
SCO3286	-2.62	-0.95	hypothetical protein
SCO4255	-1.64	-1.26	hypothetical protein
SCO2492	-4.03	-1.84	hypothetical protein
SCO2391	1.39	0.79	hypothetical protein
SCO2561	-1.03	-0.42	long-chain fatty-acid CoA ligase
SCO1455	-2.31	-0.79	hydrolase
SCO7469	-3.47	-1.25	phenylacetate-CoA ligase
SCO1222	-3.07	-1.14	hypothetical protein
SCO0426	-2.57	-1.74	hypothetical protein
SCO1342	1.55	0.01	hypothetical protein
SCO1457	-2.16	-0.36	transporter
SCO6731	-1.28	-0.07	acetyl-CoA acetyltransferase
SCO0596	-2.02	-2.97	DNA-binding protein
SCO3287	-2.59	-1.40	serine/arginine rich protein

Table S3: Peak positions averaged across the *Streptomyces coelicolor* J1929 (wild-type parent strain), the DT3017 (*ppm1*⁻ mutant strain) and DT3017:pDT16 (the complemented mutant strain) with a maximum uncertainty of $\pm 3\text{cm}^{-1}$ obtained from the average. The TFA band (2850cm^{-1}) and TUFA band (3008cm^{-1}) are highlighted.

Peak position (cm^{-1})	Assignment
746	DNA/RNA*
782	DNA/RNA*
1000	Phenylalanine*
1096	DNA/RNA & nucleic acids*
1125	Lipids*
1260	Amide III*
1333	DNA/RNA*
1444	Lipids (CH_2 deformation)*, proteins*
1460	Lipids*, proteins*, DNA*
1480	Amide II*, DNA§
1574	DNA*§
1656	Lipids ($\text{C}=\text{C}$)*, proteins*
2850	Lipids (CH_2) TFA band
2871	Lipids (CH_2)*, proteins*
2900	Lipids (CH stretch), proteins*
2934	Lipids (CH_2 asymmetric stretch)*, proteins*
2970	Lipids (CH_3)*
3008	=CH stretch lipids* TUFA band

* Movasaghi *et al.*, 2007.

§ Walter *et al.*, 2012.

Dataset S2; RT-PCR raw data

		Ct					
		hrdB			sigE		
Strain	Timepoint	A	B	C	A	B	C
J1929	0	18.799630	20.650000	21.454816	21.586304	24.590130	24.186640
J1929	30	19.581444	23.660000	20.810285	22.035706	27.638845	23.175257
J1929	60	19.978937	19.110000	20.519775	22.709986	22.212990	23.320545
J1929	90	20.026252	18.590000	21.138070	21.947371	21.624706	23.812683
DT3017	0	19.865672	20.277826	20.366220	23.448399	23.262208	23.075092
DT3017	30	21.201283	20.630247	20.216869	24.763846	23.714276	22.807042
DT3017	60	20.747127	21.744322	21.703077	23.967405	25.427483	25.351522
DT3017	90	21.062787	21.567923	20.694414	24.580005	25.288694	23.855792
DT3017pDT16	0	20.527110	22.274062	20.908951	24.340387	25.227647	24.092606
DT3017pDT16	30	20.731414	23.753307	21.081755	24.288817	26.961072	24.056971
DT3017pDT16	60	21.233016	21.756851	20.932545	24.536002	24.266238	23.999046
DT3017pDT16	90	21.658429	20.026058	20.660345	24.698671	22.467578	23.170101
DT2008	0	21.553286	20.571101	19.820496	26.340847	26.255304	25.973239
DT2008	30	20.809232	19.534068	19.895908	26.176449	24.638397	25.580193
DT2008	60	21.621939	21.673930	20.498451	24.718257	25.050780	26.486415
DT2008	90	20.848227	21.170345	20.352083	25.562053	23.913292	26.416597
DT2008pDT10	0	20.604540	22.577943	20.941118	26.006975	24.979057	24.884230
DT2008pDT10	30	21.918685	19.754117	20.233721	23.995457	23.747550	24.766716
DT2008pDT10	60	20.382804	20.032450	21.274306	25.829701	26.071708	24.279032
DT2008pDT10	90	20.897380	18.734000	21.068324	24.963149	24.430338	24.189709

			delta Ct						delta Ct	
vanH			sigE			vanH			sigE	
A	B	C	A	B	C	A	B	C	AVERAGE	SEM
30.002860	31.654559	32.280459	2.786674	3.940130	2.731825	11.203229	11.004559	10.825644	3.152876	0.393945
22.645180	29.102357	23.006241	2.454262	3.978845	2.364972	3.063736	5.442357	2.195956	2.932693	0.523710
23.616922	25.818885	24.868385	2.731049	3.102990	2.800770	3.637986	6.708885	4.348610	2.878270	0.114149
26.429050	26.584279	30.017014	1.921118	3.034706	2.674613	6.402798	7.994279	8.878943	2.543479	0.328083
31.197264	30.991518	30.474890	3.582727	2.984381	2.708872	11.331591	10.713692	10.108669	3.091993	0.257935
24.671139	29.624201	27.444438	3.562563	3.084029	2.590172	3.469856	8.993954	7.227568	3.078921	0.280717
23.249606	31.000706	29.374309	3.220278	3.683160	3.648445	2.502479	9.256384	7.671232	3.517294	0.148846
26.725033	32.216434	30.198291	3.517218	3.720771	3.161378	5.662246	10.648511	9.503878	3.466456	0.163465
31.073481	33.990208	32.113710	3.813277	2.953584	3.183655	10.546370	11.716145	11.204759	3.316839	0.256951
23.102547	30.039613	25.842295	3.557404	3.207766	2.975216	2.371134	6.286306	4.760540	3.246795	0.169192
24.130721	31.840541	28.976849	3.302986	2.509387	3.066500	2.897706	10.083689	8.044303	2.959624	0.235242
26.894819	27.536483	30.405720	3.040242	2.441521	2.509755	5.236390	7.510426	9.745375	2.663839	0.189229
34.868998	33.004412	31.097172	4.787561	5.684203	6.152743	13.315713	12.433311	11.276676	5.541503	0.400501
22.589537	24.661365	23.365168	5.367217	5.104329	5.684285	1.780305	5.127297	3.469261	5.385277	0.167662
23.948778	28.534428	23.711927	3.096317	3.376850	5.987964	2.326839	6.860498	3.213476	4.153710	0.920695
25.956992	28.649881	24.925369	4.713826	2.742947	6.064514	5.108766	7.479537	4.573286	4.507096	0.964409
33.495525	32.853308	31.452630	5.402435	2.401114	3.943112	12.890985	10.275365	10.511512	3.915554	0.866517
31.483201	28.127752	28.104384	2.076772	3.993434	4.532995	9.564516	8.373635	7.870663	3.534400	0.745272
31.703098	29.328746	30.740419	5.446898	6.039258	3.004726	11.320295	9.296295	9.466113	4.830294	0.928663
31.610954	27.096535	30.927499	4.065769	5.696338	3.121385	10.713573	8.362535	9.859175	4.294497	0.752071

average		delta delta Ct						2-de		
vanH		sigE			vanH			sigE		
AVERAGE	SEM	A	B	C	A	B	C	A	B	C
11.011144	0.109049	0.000000	0.000000	0.000000	0.000000	0.000000	0.000000	1.000000	1.000000	1.000000
3.567350	0.970395	-0.332411	0.038715	-0.366852	-8.139493	-5.562202	-8.629688	1.259116	0.973522	1.289536
4.898493	0.928149	-0.055625	-0.837139	0.068945	-7.565243	-4.295675	-6.477034	1.039309	1.786504	0.953335
7.758674	0.724444	-0.865555	-0.905424	-0.057212	-4.800431	-3.010280	-1.946700	1.822041	1.873095	1.040453
10.717984	0.353034	0.796053	-0.955748	-0.022953	0.128362	-0.290868	-0.716974	0.575923	1.939586	1.016037
6.563793	1.628841	0.775889	-0.856101	-0.141652	-7.733374	-2.010605	-3.598075	0.584029	1.810140	1.103168
6.476698	2.039117	0.433604	-0.256970	0.916620	-8.700750	-1.748176	-3.154411	0.740410	1.194966	0.529749
8.604878	1.507963	0.730544	-0.219359	0.429553	-5.540983	-0.356049	-1.321766	0.602676	1.164216	0.742492
11.155758	0.338573	1.026603	-0.986546	0.451831	-0.656859	0.711586	0.379115	0.490865	1.981435	0.731115
4.472660	1.139342	0.770730	-0.732364	0.243391	-8.832095	-4.718253	-6.065104	0.586121	1.661359	0.844757
7.008566	2.138080	0.516312	-1.430743	0.334675	-8.305524	-0.920870	-2.781340	0.699157	2.695855	0.792962
7.497397	1.301648	0.253568	-1.498609	-0.222069	-5.966839	-3.494134	-1.080268	0.838819	2.825702	1.166405
12.341900	0.590391	2.000888	1.744074	3.420918	2.112483	1.428751	0.451032	0.249846	0.298526	0.093369
3.458954	0.966207	2.580543	1.164199	2.952460	-9.422924	-5.877262	-7.356383	0.167178	0.446212	0.129188
4.133604	1.387263	0.309643	-0.563280	3.256139	-8.876390	-4.144061	-7.612167	0.806841	1.477625	0.104666
5.720529	0.892985	1.927153	-1.197183	3.332689	-6.094464	-3.525023	-6.252357	0.262948	2.292915	0.099257
11.225954	0.835302	2.615761	-1.539016	1.211287	1.687756	-0.729195	-0.314131	0.163146	2.905963	0.431883
8.602938	0.502235	-0.709902	0.053304	1.801170	-1.638713	-2.630924	-2.954981	1.635693	0.963727	0.286942
10.027568	0.648220	2.660224	2.099128	0.272902	0.117065	-1.708264	-1.359531	0.158195	0.233399	0.827653
9.645095	0.687076	1.279095	1.756208	0.389560	-0.489656	-2.642025	-0.966468	0.412054	0.296025	0.763362

delta delta Ct			2-delta delta Ct Average					
vanH			sigE		vanH			sigE
A	B	C	Average	SEM	AVERAGE	SEM		A
1.000000	1.000000	1.000000	1.000000	0.000000	1.000000	0.000000	J1929	0.000000
281.988654	47.248683	396.090867	1.174058	0.100652	241.776068	102.689672	J1929	0.100066
189.393552	19.639345	89.080245	1.259716	0.264561	99.371047	49.273212	J1929	0.016745
27.865940	8.057208	3.854919	1.578530	0.269442	13.259356	7.403356	J1929	0.260558
0.914870	1.223376	1.643731	1.177182	0.401817	1.260659	0.211228	DT3017	-0.239636
212.802847	4.029512	12.109566	1.165779	0.355329	76.313975	68.284286	DT3017	-0.233566
416.089581	3.359335	8.903739	0.821708	0.196287	142.784218	136.662054	DT3017	-0.130528
46.558840	1.279916	2.499719	0.836461	0.168774	16.779491	14.893837	DT3017	-0.219916
1.576646	0.610649	0.768909	1.067805	0.462050	0.985401	0.299132	pDT16	-0.309038
455.748932	26.323019	66.954241	1.030746	0.324026	183.008731	136.873588	pDT16	-0.232013
316.381966	1.893257	6.874907	1.395992	0.650496	108.383377	104.009237	pDT16	-0.155425
62.545729	11.267799	2.114429	1.610309	0.615010	25.309319	18.804775	pDT16	-0.076332
0.231249	0.371452	0.731519	0.213913	0.061889	0.444740	0.148992	DT2008	-0.602327
686.408707	58.780363	163.867167	0.247526	0.099947	303.018746	194.080487	DT2008	-0.776821
469.958795	17.680180	195.654890	0.796377	0.396374	227.764621	131.545002	DT2008	-0.093212
68.330779	11.511650	76.233726	0.885040	0.705522	52.025385	20.384930	DT2008	-0.580131
0.310409	1.657714	1.243263	1.166997	0.872937	1.070462	0.398415	pDT10	-0.787423
3.113879	6.194228	7.754216	0.962120	0.389352	5.687441	1.363306	pDT10	0.213702
0.922061	3.267675	2.566017	0.406416	0.211735	2.251918	0.695095	pDT10	-0.800807
1.404110	6.242070	1.954051	0.490481	0.140492	3.200077	1.529259	pDT10	-0.385046

Log fold change					Log fold change Average			
		vanH			sigE		vanH	
B	C	A	B	C	Average	SEM	AVERAGE	SEM
0.000000	0.000000	0.000000	0.000000	0.000000	0.000000	0.000000	0.000000	0.000000
-0.011654	0.110434	2.450232	1.674390	2.597795	0.066282	0.039083	2.240805	0.286394
0.252004	-0.020754	2.277365	1.293127	1.949781	0.082665	0.085359	1.840091	0.289370
0.272560	0.017223	1.445074	0.906185	0.586015	0.183447	0.083184	0.979091	0.250654
0.287709	0.006910	-0.038641	0.087560	0.215831	0.018328	0.152338	0.088250	0.073460
0.257712	0.042642	2.327977	0.605252	1.083129	0.022263	0.142185	1.338786	0.513474
0.077356	-0.275930	2.619187	0.526253	0.949572	-0.109701	0.102515	1.365004	0.638887
0.066034	-0.129308	1.668002	0.107181	0.397891	-0.094397	0.084372	0.724358	0.479227
0.296980	-0.136015	0.197734	-0.214209	-0.114125	-0.049358	0.180228	-0.043533	0.124045
0.220464	-0.073268	2.658726	1.420336	1.825778	-0.028272	0.132542	1.968280	0.364524
0.430697	-0.100747	2.500212	0.277210	0.837267	0.058175	0.186929	1.204896	0.667532
0.451126	0.066850	1.796198	1.051839	0.325193	0.147215	0.157477	1.057743	0.424653
-0.525018	-1.029799	-0.635921	-0.430097	-0.135774	-0.719048	0.156970	-0.400597	0.145131
-0.350459	-0.888779	2.836583	1.769232	2.214492	-0.672020	0.163997	2.273436	0.309524
0.169564	-0.980196	2.672060	1.247487	2.291491	-0.301281	0.347830	2.070346	0.425845
0.360388	-1.003239	1.834616	1.061138	1.882147	-0.407661	0.402980	1.592634	0.266102
0.463290	-0.364634	-0.508065	0.219510	0.094563	-0.229589	0.367309	-0.064664	0.224615
-0.016046	-0.542206	0.493302	0.791987	0.889538	-0.114850	0.223734	0.724942	0.119195
-0.631900	-0.082152	-0.035240	0.514239	0.409260	-0.504953	0.216951	0.296086	0.168412
-0.528671	-0.117269	0.147401	0.795329	0.290936	-0.343662	0.120551	0.411222	0.196472

Dataset S3: Gene for GO analysis

DT3017 : J1929						
Gene	log2 FC	p-value	GeneID	Symbol	Aliases	description
SCO3737	5.22732857	7.15E-47	1099173	SCO3737	SCO3737SCH22A.15c	lipoprotein, putative Sortase E
SCO3738	5.01876726	3.18E-14	1099174	SCO3738	SCO3738SCH22A.16c	hypothetical protein
SCO6183	4.04646883	0.03337329	1101624	SCO6183	SCO6183SC2G5.04 cwgE	transferase part of cwg operon sco6179-6190, GT1 heptosyl-transferase
SCO3736	3.75595274	2.06E-20	1099172	SCO3736	SCO3736SCH22A.14c	RNA polymerase ECF sigma factor
SCO5525	3.02459348	0.01739439	1100965	SCO5525	SCO5525 ureAB	bifunctional urease subunit gamma/beta
SCO5535	2.49833124	1.43E-05	1100975	SCO5535	SCO5535SC1C2.16 accB	carboxyl transferase
SCO4175	2.45797758	0.01910115	1099615	SCO4175	SCO4175SCD66.12c	hypothetical protein
SCO2414	2.34375333	0.01646835	1097848	SCO2414	SCO2414SC8A2.02c mce	hypothetical protein, possibly part of Mce protein complex
SCO7415	2.33829765	0.00423036	1102853	SCO7415	SCO7415SC6D11.11	racemase
SCO3706	2.24156167	6.43E-07	1099142	SCO3706	SCO3706SCH35.18c	ABC transporter ATP-binding protein
SCO2387	2.15966885	1.68E-06	1097821	SCO2387	SCO2387SC4A7.15, fabD	ACP S-malonyltransferase
SCO2472	2.07413879	0.0185831	1097906	SCO2472	SCO2472SC7A8.11	hypothetical protein secreted, SanA
SCO3707	2.0308984	2.37E-06	1099143	SCO3707	SCO3707SCH35.17	lipoprotein
SCO1815	1.91707253	2.30E-05	1097249	SCO1815	SCO1815SCI28.09c, fabG	3-oxacyl-ACP reductase
SCO1335	1.91485495	0.00349242	1096758	SCO1335	SCO13352SCG61.17c	oxidoreductase
SCO2026	1.90640417	0.01568253	1097460	SCO2026	SCO2026SC3A3.04c, gltB	glutamate synthase
SCO5526	1.89953742	0.00261889	1100966	ureC	SCO5526	urease subunit alpha
SCO1909	1.8639413	0.0012721	1097343	SCO1909	SCO1909SCI7.27c	hypothetical protein
SCO1814	1.83510828	7.85E-05	1097248	SCO1814	SCO1814SCI28.08c, fabI	enoyl-ACP reductase
SCO5950	1.81382462	0.0292013	1101392	SCO5950	SCO5950SC7H1.20c	export protein, drug resistance transporter EmrB/QacA subfamily
SCO5092	1.77342064	0.04872546	1100533	SCO5092	SCO5092SCBAC28G1.18, actVB	actinorhodin polyketide dimerase
SCO5527	1.76300958	0.00632636	1100967	SCO5527	SCO5527SC1C2.08	hypothetical protein, putative Peptidyl-arginine deiminase (PAD)
SCO5515	1.75904007	9.90E-06	1100955	SCO5515	SCO5515SC8D9.27, serA	D-3-phosphoglycerate dehydrogenase
SCO2025	1.74066765	0.00900683	1097459	gltD	SCO2025SC3A3.03c	glutamate synthase
SCO7036	1.69428699	5.97E-05	1102474	SCO7036	SCO7036SC4G1.02, argG	argininosuccinate synthase
SCO6999	1.68886923	0.04785862	1102437	SCO6999	SCO6999SC8F11.25c.	hypothetical protein, putative HutG, N-formylglutamate amidohydrolase
SCO1233	1.68478024	0.00332918	1096656	SCO1233	SCO12332SCG1.08c, ureF	urease accessroy protein UreF
SCO3656	1.68323618	0.00030916	1099092	SCO3656	SCO3656SCH10.34c	hypothetical protein
SCO2388	1.67143723	3.75E-05	1097822	SCO2388	SCO2388SC4A7.16, fabH	3-oxoacyl-ACP synthase
SCO1182	1.66368654	1.09E-07	1096605	SCO1182	SCO1182SCG11A.13	hypothetical protein
SCO2481	1.63093372	0.0487074	1097915	SCO2481	SCO2481SC7A8.20c	hypothetical protein, putative regulator
SCO3104	1.5777876	0.02384028	1098538	SCO3104	SCO3104SCE41.13c	hypothetical protein
SCO6564	1.56557775	0.0002604	1102003	SCO6564	SCO6564SC4B5.14, fabH2	3-oxoacyl-ACP synthase
SCO1342	1.54547041	0.00054352	1096765	SCO1342	SCO13422SCG61.24c	hypothetical protein
SCO3207	1.52575574	0.00203127	1098641	SCO3207	SCO3207SCE22.24c	TetR family transcriptional regulator
SCO4914	1.52406327	0.04451133	1100355	SCO4914	SCO4914SCK13.06c	deoxyribose-phosphate aldolase
SCO1577	1.52073619	0.01257825	1097008	argD	SCO1577SCL24.13c argD	acetylornithine aminotransferase
SCO5516	1.51468065	0.00013034	1100956	SCO5516	SCO5516SC8D9.28c	integral membrane efflux protein, EmrB/QacA family drug efflux
SCO7268	1.50978732	0.00888465	1102706	SCO7268	SCO7268SC5H1.24c, add	adenosine deaminase
SCO3127	1.44487769	0.00144788	1098561	SCO3127	SCO3127SCE66.06c, ppc	phosphoenolpyruvate carboxylase
SCO4913	1.43999556	0.02698643	1100354	SCO4913	SCO4913SCK13.05c	aldehyde dehydrogenase
SCO3771	1.43601259	0.03782396	1099207	SCO3771	SCO3771SCH63.18c	penicillin binding protein, FtsI like/ PBP2
SCO3379	1.42736306	0.03915888	1098816	SCO3379	SCO3379SCE94.30c	hypothetical protein
SCO1908	1.42242332	0.0022921	1097342	SCO1908	SCO1908SCI7.26	large hypothetical protein, putative extracellular nuclease
SCO18	1.41525103	0.03274651	1101187	rrnE	SCO18	5S ribosomal RNA

SCO5554	1.4041096	0.02526811	1100994	leuD	SCO5554	isopropylmalate isomerase small subunit
SCO4142	1.39513004	0.01836659	1099582	SCO4142	SCO4142SCD84.09c, pstS	phosphate-binding protein
SCO2391	1.39182774	0.0003971	1097825	SCO2391	SCO2391SC4A7.19c	hypothetical protein
SCO4912	1.39003632	0.02110597	1100353	SCO4912	SCO4912SCK13.04c	aldehyde dehydrogenase
SCO6172	1.36834937	0.002008	1101613	SCO6172	SCO6172SC6C5.08	oxidoreductase
SCO1580	1.36247597	0.00578432	1097011	argC	SCO1580	N-acetyl-gamma-glutamyl-phosphate reductase
SCO4239	1.35956269	0.04525137	1099679	SCO4239	SCO4239SCD8A.12c	small membrane protein
SCO1579	1.35398966	0.00398484	1097010	argJ	SCO1579SCL24.15c argJ	bifunctional ornithine acetyltransferase/N-acetylglutamate synthase
SCO6804	1.34946767	0.00096466	1102243	SCO6804	SCO6804SC1A2.13	hypothetical protein
SCO7724	1.34579418	0.04097975	1103162	SCO7724	SCO7724SC8D11.15c	hypothetical protein
SCO4049	1.33545477	0.02645228	1099485	SCO4049	SCO40492SCD60.15	antibiotic binding protein, Penicillin amidase or penicillin acylase
SCO7705	1.33398042	0.00974989	1103143	SCO7705	SCO7705SCBAC12C8.06	oxidoreductase
SCO1334	1.33242233	0.00769503	1096757	SCO1334	SCO13342SCG61.16	hypothetical protein
SCO6271	1.28937357	0.00138585	1101712	SCO6271	SCO6271SC2C4.01c, SCAH10.36c, acc	acyl-CoA carboxylase complex A subunit
SCO1570	1.28882089	0.00365482	1097001	SCO1570	SCO1570SCL24.06c, argH	argininosuccinate lyase
SCO4891	1.27425517	0.03088234	1100332	SCO4891	SCO48912SCK8.17c	hypothetical protein possibly secreted
SCO1244	1.26977039	0.0009418	1096667	SCO1244	SCO12442SCG1.19, bioB	biotin synthase
SCO2630	1.26129089	0.01042897	1098064	SCO2630	SCO2630SC8E4.05c	biotin synthase
SCO3206	1.2612665	0.0023635	1098640	SCO3206	SCO3206SCE22.23c	transmembrane efflux protein, EmrB/QacA subfamily
SCO2210	1.25974103	0.01352136	1097643	SCO2210	SCO2210SC10B7.05, glnII	glutamine synthetase
SCO1846	1.25526263	0.01628379	1097280	SCO1846	SCO1846SCI8.31	hypothetical protein
SCO5184	1.25323458	0.01451459	1100625	SCO5184	SCO51842SC3B6.08	ATP-dependent DNA helicase
SCO4369	1.23752475	0.0273341	1099809	SCO4369	SCO43692SCD52.01, SCD10.01	hypothetical protein
SCO6347	1.22874848	0.03018267	1101788	SCO6347	SCO6347SC3A7.15	beta-galactosidase
SCOt33	1.22595676	0.02414746	3240036	SCOt33	SCOt33	tRNA
SCO5584	1.22589266	0.04645387	1101025	SCO5584	SCO5584SC7A1.28, glnB	nitrogen regulatory protein P-II, GlnK
SCO0756	1.22576664	0.04168175	1096179	SCO0756	SCO0756SCF81.15	ABC transporter, part of a lantibiotic/bacteriocin export system
SCO1343	1.22540857	0.00163953	1096766	SCO1343	SCO13432SCG61.25c, ung	uracil-DNA glycosylase
SCO4921	1.2243441	5.85E-05	1100362	SCO4921	SCO4921SCK13.13c, accA2	acyl-CoA carboxylase complex A subunit
SCO3280	1.21950295	0.02431245	1098714	SCO3280	SCO3280SCE39.30	hypothetical protein
SCO4107	1.21897177	0.00029895	1099544	SCO4107	SCO4107SCD17.11	hypothetical protein, serine phosphatase SpoII E like
SCO5553	1.21710062	0.01090225	1100993	SCO5553	SCO5553leuC	isopropylmalate isomerase large subunit
SCO2014	1.21258777	1.55E-05	1097448	SCO2014	SCO2014SC7H2.28c, pyk1	pyruvate kinase
SCO5522	1.21184626	0.03700166	1100962	SCO5522	SCO5522leuB	3-isopropylmalate dehydrogenase
SCO2810	1.20592847	0.03404994	1098244	SCO2810	SCO28102SCC13.18, SCBAC17F8.01	hypothetical protein, putative helicase
SCO3383	1.20443628	0.00130087	1098820	panC	SCO3383SCE126.01c, SCE94.34c	pantoate--beta-alanine ligase
SCO2228	1.20391017	0.02180695	1097661	SCO2228	SCO2228SC10B7.23c, agIA	alpha-glucosidase
SCO1487	1.20013849	0.02369211	1096913	pyrB	SCO1487SC9C5.11c pyrB	aspartate carbamoyltransferase catalytic subunit
SCO5391	1.1955678	0.00884508	1100831	SCO5391	SCO53912SC6G5.35	ATP/GTP-binding protein
SCO5106	1.1770594	0.00533819	1100547	SCO5106	SCO5106SCBAC31E11.02c, shdB2	fumarate reductase iron-sulfur subunit
SCO4901	1.12828194	0.02954604	1100342	SCO4901	SCO49012SCK8.27	adenosine deaminase
SCO2230	1.12470606	0.04729329	1097663	SCO2230	SCO2230SC10B7.25c, malF	maltose permease
SCO5425	1.11431344	0.0062404	1100865	SCO5425	SCO5425SC6A11.01c, SC8F4.29c, pta	phosphate acetyltransferase
SCO6565	1.11076799	0.00126016	1102004	SCO6565	SCO6565SC4B5.15	transcriptional regulator
SCOt31	1.10861535	0.00228837	3240034	SCOt31	SCOt31	tRNA
SCO6173	1.10783534	0.00787534	1101614	SCO6173	SCO6173SC6C5.09	permease SC6C509, putative xanthin/uracil/vitC uptake
SCO5860	1.10288406	0.01083112	1101302	SCO5860	SCO5860SC9B10.27, suhB	SuhB protein, inositol monophosphatase
SCO1742	1.08977573	0.01638626	1097173	SCO1742	SCO1742SCI11.31	ABC transporter ATP-binding protein, part of a putative bacitracin resistance efflux system.

SCO1232	1.08518138	0.01057889	1096655	SCO1232	SCO12322SCG1.07c, ureG	urease accessory protein
SCO4637	1.08005808	0.01441786				FabA subunit 3-hydroxyacyl-ACP dehydratase
SCO3964	1.07969242	0.01713679	1099400	SCO3964	SCO3964SCBAC25E3.01c, SCD78.31c	hypothetical protein, putative copper export protein efflux
SCO1245	1.05843852	0.01101014	1096668	SCO1245	SCO12452SCG1.20, bioA	adenosylmethionine-8-amino-7-oxononanoate aminotransferase
SCO5797	1.05718402	0.00902066	1101239	SCO5797	SCO5797SC4H2.18c	hypothetical protein lipoprotein
SCO5423	1.05629964	0.03764574	1100863	SCO5423	SCO5423SC8F4.27c, pyk2	pyruvate kinase
SCO5609	1.05282785	0.00209643	1101050	SCO5609	SCO5609SC2E1.26c	hypothetical protein
SCO5467	1.05020555	0.00601183	1100907	SCO5467	SCO5467SC2A11.01, SC3D11.24	muramoyl-pentapeptide carboxypeptidase
SCO3345	1.047996	0.02035022	1098782	SCO3345	SCO3345SCE7.12c	dihydroxy-acid dehydratase
SCO3310	1.04736819	0.02343298	1098744	SCO3310	SCO3310SCE68.08	hypothetical protein
SCO4159	1.04450919	0.04076035	1099599	SCO4159	SCO4159SCD84.26c, glnR	transcriptional regulator GlnR
SCO0030	1.04322879	0.00725767	1095463	SCO0030	SCO0030SCJ4.11	hypothetical protein
SCO1243	1.04033225	0.01963125	1096666	SCO1243	SCO12432SCG1.18c, bioF	8-amino-7-oxononanoate synthase
SCO4445	1.03570115	0.01228103	1099885	SCO4445	SCO4445SCD6.23c	transcriptional regulator
SCO2961	1.03204411	0.00254762	1098394	SCO2961	SCO2961SCE59.20c	hypothetical protein, putative acyltransferase
SCO2232	1.02767584	0.00594784	1097665	SCO2232	SCO2232SC10B7.27, malR	maltose operon transcriptional repressor
SCO1486	1.0256003	0.03351964	1096912	pyrC	SCO1486SC9C5.10c	dihydroorotase
SCO2093	1.02062894	0.01268068	1097527	SCO2093	SCO2093SC4A10.26	hypothetical protein
SCO1662	1.02036049	0.01032877	1097093	SCO1662	SCO1662SCI52.04	hypothetical protein, proteasome assembly chaperone
SCO2048	1.01788602	0.0089681	1097482	SCO2048	SCO2048SC4G6.17c	imidazole glycerol phosphate synthase subunit HisF
SCO3058	1.0141049	0.03331063	1098491	SCO3058	SCO3058SCBAC19G2.13c	membrane dipeptidase
SCO3311	1.01250948	0.00625896	1098745	SCO3311	SCO3311SCE68.09c, hemB	delta-aminolevulinic acid dehydratase
SCO7020	1.00575796	0.0115876	1102458	SCO7020	SCO7020amlB	alpha-amylase, secreted
SCO1813	1.00534147	0.0131562	1097247	SCO1813	SCO1813SCI28.07	GntR family transcriptional regulator
SCO3756	1.00096581	0.02969241	1099192	SCO3756	SCO3756SCH63.03c	two component system response regulator
SCO5839	0.99455399	0.0498894	1101281	SCO5839	SCO5839SC9B10.06	hypothetical protein, putative metalloendopeptidase
SCO0870	0.99411984	0.01418603	1096293	SCO0870	SCO0870SCM1.03c	two-component system response regulator
SCO1578	0.99121965	0.01200289	1097009	SCO1578	SCO1578SCL24.14c, argB	acetylglutamate kinase
SCOt46	0.97294247	0.04112216	3240049	SCOt46	SCOt46	tRNA
SCO1922	0.96992786	0.0206485	1097356	SCO1922	SCO1922SCC22.04c	ABC transporter ATP-binding protein, part of SUF system; acts in Fe-S cluster formation in oxidative stress
SCO3450	0.95810869	0.03356476	1098887	SCO3450	SCO3450SCE46.07c	ECF subfamily RNA polymerase sigma factor
SCO4962	0.94620683	0.04195971	1100403	SCO4962	SCO49622SCK31.22	threonine dehydratase
SCO3309	0.93780531	0.02314469	1098743	SCO3309	SCO3309SCE68.07c	hypothetical protein, putative cell division protein ZipA
SCO1214	0.92591595	0.01497731	1096637	SCO1214	SCO12142SCG58.14, pfkA3	6-phosphofructokinase
SCO1490	0.92540503	0.04266022	1096916	nusB	SCO1490SC9C5.14c	transcription antitermination protein NusB
SCO4038	0.92218709	0.03334874	1099474	SCO4038	SCO40382SCD60.04c	putative cytosine/adenosine deaminase
SCO0280	0.92204628	0.03001684	1095704	SCO0280	SCO0280SCF85.08c	hypothetical protein, putative GDP-mannose pyrophosphatase NudK
SCO4636	0.91782728	0.0489006	1100077	SCO4636	SCO4636SCD82.07	Putative (3R)-hydroxyacyl-ACP dehydratase subunit HadA; FabA (Singh and Reynolds 2016)
SCO5289	0.8818767	0.03172312	1100730	SCO5289	SCO5289SC6G9.44c, SCCB12.13, cvnA	two component sensor kinase
SCO4464	0.87878623	0.01946299	1099904	SCO4464	SCO4464SCD65.07c	hydrolase
SCO7422	0.87566319	0.03686061	1102860	SCO7422	SCO7422SC6D11.18c, cvnA10	sensor histidine-kinase
SCOt62	0.87500337	0.03832349	3240065	SCOt62	SCOt62	tRNA
SCO5290	0.86676088	0.03748657	1100731	SCO5290	SCO5290SC6G9.43c, cvnB5	hypothetical protein
SCO2094	0.86673866	0.00403334	1097528	SCO2094	SCO2094SC4A10.27	regulatory protein
SCO1938	0.86111753	0.02722785	1097372	SCO1938	SCO1938SCC22.20	hypothetical protein, putative glucose-6-phosphate dehydrogenase assembly protein OpcA
SCO1483	0.86075683	0.03945893	1096909	carB	SCO1483SC9C5.07c, pyrA	carbamoyl phosphate synthase large subunit
SCO3059	0.85872702	0.03255055	1098492	SCO3059	SCO3059SCBAC19G2.14c, purE	phosphoribosylaminoimidazole carboxylase catalytic subunit PurE
SCOt37	0.85344638	0.02425942	3240040	SCOt37	SCOt37	tRNA

SCO5291	0.84747199	0.04778846	1100732	SCO5291	SCO5291SC6G9.42c, cvnC5	hypothetical protein
SCO2457	0.84069294	0.01390485	1097891	SCO2457	SCO2457SCC24.28c	lipoprotein
SCO5424	0.83296057	0.01745499	1100864	SCO5424	SCO5424SC8F4.28c, ackA	acetate kinase
SCO0871	0.83212333	0.0045943	1096294	SCO0871	SCO0871SCM1.04c	two-component sensor protein
SCO2390	0.83131564	0.02491241	1097824	SCO2390	SCO2390SC4A7.18, fabF	3-oxoacyl-ACP synthase, FabF/FabB
SCO5583	0.82348181	0.01692363	1101024	SCO5583	SCO5583SC7A1.27	ammonium transporter
SCO7219	0.82254635	0.0313864	1102657	SCO7219	SCO7219SC2H12.18c	phosphoglycerate mutase
SCO7465	0.82195193	0.00570404	1102903	SCO7465	SCO7465SCBAC14E8.05, cvnC13	hypothetical protein
SCO3382	0.81082749	0.01351651	1098819	SCO3382	SCO3382SCE94.33c, nadB	L-aspartate oxidase
SCO0872	0.8099131	0.02929893	1096295	SCO0872	SCO0872SCM1.05c	hypothetical protein, regulator putative serine phosphatase
SCO7466	0.80662976	0.03643229	1102904	SCO7466	SCO7466SCBAC14E8.06, cvnD13	ATP/GTP-binding protein
SCO7439	0.80537378	0.03456663	1102877	SCO7439	SCO7439SC6D11.35	hypothetical protein, putative Type 1 glutamine amidotransferase (GATase1)-like domain
SCO4510	0.80001471	0.01144239	1099950	SCO4510	SCO4510SCD35.17c	hypothetical protein
SCO0249	0.79006137	0.02272439	1095673	SCO0249	SCO0249SCJ9A.28c	hypothetical protein
SCO5732	0.78854428	0.01261973	1101171	SCO5732	SCO5732SC3C3.18c	hypothetical protein
SCO0461	0.77262507	0.0497584	1095884	SCO0461	SCO0461SCF51A.39, SCF76.01	hydrolase MhpC like
SCO1946	0.77134417	0.02375494	1097380	pgk	SCO1946SCC54.06c	phosphoglycerate kinase
SCO5220	0.76023795	0.01074036	1100661	SCO5220	SCO5220SC7E4.17	hypothetical protein
SCO5145	0.73991642	0.04089665	1100586	SCO5145	SCO5145SCP8.08	hypothetical protein
SCO5564	0.72522182	0.02820353	1101005	rpmB	SCO5564SC7A1.08c	50S ribosomal protein L28
SCO5719	0.70566034	0.04573059	1101158	SCO5719	SCO5719SC3C3.05c	hypothetical protein
SCO5731	0.70282232	0.02252611	1101170	SCO5731	SCO5731SC3C3.17c	serine protease
SCO2962	0.6833757	0.03620477	1098395	SCO2962	SCO2962SCE59.21c	bifunctional transferase/deacetylase membrane spanning
SCO3791	0.68302483	0.00967171	1099227	SCO3791	SCO3791SCH63.38	hypothetical protein
SCO3148	0.66795775	0.03892634	1098582	SCO3148	SCO3148SCE66.27c	4-diphosphocytidyl-2-C-methyl-D-erythritol kinase
SCO5734	0.65853344	0.03651915	1101173	SCO5734	SCO5734SC3C3.20c	ATP/GTP binding protein membrane protein
SCO4423	0.6542979	0.04577039	1099863	SCO4423	SCO4423SC6F11.21, SCD6.01, afsk	Ser/Thr protein kinase
SCO2051	0.64578243	0.04603788	1097485	hisH	SCO2051SC4G6.20c	imidazole glycerol phosphate synthase subunit HisH
SCO2303	0.63952223	0.01674217	1097737	SCO2303	SCO2303SCC30.11	hypothetical protein 55aa
SCO3767	0.63533862	0.01146803	1099203	SCO3767	SCO3767SCH63.14	hypothetical protein, TerB tellurium resistance
SCO3381	0.63398957	0.04223023	1098818	SCO3381	SCO3381SCE94.32c, nadC	nicotinate-nucleotide pyrophosphorylase
SCO5835	0.6213556	0.04275658	1101277	SCO5835	SCO5835SC9B10.02	ATP/GTP-binding protein
SCO2455	0.59068226	0.02904178	1097889	SCO2455	SCO2455SCC24.26c	spermidine synthase
SCO4039	0.57947617	0.04596553	1099475	SCO4039	SCO40392SCD60.05c	hypothetical protein, putative tRNA adenosine deaminase
SCO3343	0.57866166	0.04633327	1098780	SCO3343	SCO3343SCE7.10c	hypothetical protein
SCO5252	-0.5940067	0.04352194	1100693	SCO5252	SCO52522SC7G11.14	hypothetical protein
SCO2067	-0.6371408	0.02022089	1097501	SCO2067	SCO2067SC4G6.36	hypothetical protein
SCO0805	-0.6802069	0.02791649	1096228	SCO0805	SCO0805SCF43.16c	prolyl aminopeptidase
SCO2004	-0.6820355	0.01963905	1097438	SCO2004	SCO2004SC7H2.18	formate dehydrogenase
SCO4872	-0.6923778	0.04984318	1100313	SCO4872	SCO4872SCK20.13c	hypothetical protein
SCO4822	-0.7060296	0.02779588	1100263	SCO4822	SCO4822SC2A6.07c	hypothetical protein
SCO1024	-0.7096473	0.03665338	1096447	SCO1024	SCO1024SCG20A.04	hypothetical protein
SCO4259	-0.7398655	0.01735029	1099699	SCO4259	SCO4259SCD8A.32c	ATPase AAA
SCO1314	-0.7449593	0.048915	1096737	SCO1314	SCO1314SCBAC36F5.25c	sugar acetyltransferase
SCO0101	-0.7473248	0.0453803	1095526	SCO0101	SCO0101SCJ11.30c	hypothetical protein
SCO3484	-0.7481896	0.04314368	1098921	SCO3484	SCO3484SCE65.20c	sugar-binding protein
SCO3356	-0.7550618	0.0239024	1098793	SCO3356	SCO3356SCE94.07	ECF sigma factor, SigE
SCO6623	-0.7602652	0.0476237	1102062	SCO6623	SCO6623SC1F2.20	ATP/GTP binding protein

SCO4964	-0.7700103	0.01450179	1100405	SCO4964	SCO49642SCK31.24	integral membrane transport protein
SCO3975	-0.7733291	0.01371516	1099411	SCO3975	SCO3975SCBAC25E3.12c	regulator
SCO6008	-0.7901769	0.0374392	1101450	SCO6008	SCO6008SC7B7.05	transcriptional repressor protein
SCO0087	-0.7922533	0.01880639	1095515	SCO0087	SCO0087SCJ11.16c	hypothetical protein
SCO2318	-0.7996268	0.01396731	1097752	SCO2318	SCO2318SCC53.09c	glycosyl transferase
SCO6065	-0.8065341	0.04414436	1101506	SCO6065	SCO6065SC9B1.12	substrate-binding protein
SCO5214	-0.8084335	0.04385642	1100655	SCO5214	SCO5214SC7E4.11	hypothetical protein
SCO6789	-0.8148398	0.02012818	1102228	SCO6789	SCO6789SC6A5.38	fatty oxidation protein
SCO1989	-0.818492	0.049638	1097423	SCO1989	SCO1989SC7H2.03c	aminopeptidase
SCO2954	-0.8218257	0.04433948	1098387	SCO2954	SCO2954SCE59.13c	RNA polymerase sigma factor SigU; PMID: 18065550 elevates extracellular proteases
SCO3203	-0.8218867	0.02858457	1098637	SCO3203	SCO3203SCE22.20, bar	phosphinothricin acetyltransferase
SCO1755	-0.8225538	0.04504712	1097186	SCO1755	SCO17552SCI34.08c	hypothetical protein
SCO4813	-0.8258495	0.02229004	1100254	purN	SCO4813SCD63A.24	phosphoribosylglycinamide formyltransferase
SCO6178	-0.8348784	0.02091978	1101619	SCO6178	SCO6178SC6C5.14c	deacetylase, secreted possible PG deacetylase
SCO1511	-0.8364716	0.04011516	1096937	SCO1511	SCO1511SC9C5.35, SCL2.01	hypothetical protein
SCO4994	-0.8446655	0.03071142	1100435	SCO4994	SCO49942SCK36.17	hypothetical protein
SCO7236	-0.8456504	0.03761518	1102674	SCO7236	SCO7236qcrB3	ubiquinol-cytochrome C reductase cytochrome subunit B
SCO1443	-0.8515811	0.00244105	1096869	SCO1443	SCO1443SC6D7A.06c	riboflavin synthase subunit alpha
SCO5385	-0.8588378	0.02393705	1100825	SCO5385	SCO53852SC6G5.29	3-hydroxybutyryl-CoA dehydrogenase
SCO4869	-0.8623426	0.01576042	1100310	SCO4869	SCO4869SCK20.10, mutA2	methylmalonyl CoA mutase
SCO4441	-0.8719573	0.04498402	1099881	SCO4441	SCO4441SCD6.19	DNA-binding protein
SCO4514	-0.8785804	0.02885008	1099954	SCO4514	SCO4514SCD35.21c	hypothetical protein
SCO6428	-0.8805981	0.01562531	1101867	SCO6428	SCO6428SC1A6.17c	hypothetical protein
SCO4777	-0.8899836	0.01019354	1100218	SCO4777	SCO4777SCD63.09, pkaD	protein Ser/Thr kinase
SCO5194	-0.8992806	0.03228327	1100635	SCO5194	SCO51942SC3B6.18	hypothetical protein
SCO1430	-0.8995075	0.04334774	1096856	SCO1430	SCO1430SC6D7.09	TetR family transcriptional regulator
SCO6053	-0.9112592	0.02251604	1101494	SCO6053	SCO6053SC1B5.13c	hypothetical protein
SCO0735	-0.9120643	0.0406046	1096158	SCO0735	SCO07353SC5B7.13	oxidoreductase
SCO5189	-0.9121279	0.03121788	1100630	SCO5189	SCO51892SC3B6.13	hypothetical protein CL35 Strakova et al
SCO4447	-0.9167142	0.01917631	1099887	SCO4447	SCO4447SCD6.25	hypothetical protein
SCO1444	-0.9178788	0.02589119	1096870	SCO1444	SCO1444SCL6.01	chitinase
SCO1982	-0.9294227	0.01603753	1097416	SCO1982	SCO1982SC3C9.17c	hypothetical protein
SCO7824	-0.9412907	0.02948357	1103262	SCO7824	SCO7824SC8E7.21c	TetR family transcriptional regulator
SCO5850	-0.9423436	0.04083458	1101292	SCO5850	SCO5850SC9B10.17	hypothetical protein
SCO5660	-0.9458206	0.0383107	1101099	SCO5660	SCO5660SC6A9.07	AmpC beta-lactamase distantly related to pfam00905 and PF00768 D-alanyl-D-alanine carboxypeptidase.
SCO2626	-0.959086	0.03701158	1098060	SCO2626	SCO2626SCC80.11c	DNA repair hydrolase (fragment)
SCO6004	-0.9663489	0.01526711	1101446	SCO6004	SCO6004SC7B7.01c, SCBAC1C11.07c	ATP/GTP binding protein
SCO0236	-0.9692137	0.02582976	1095660	SCO0236	SCO0236SCJ9A.15c	DNA-binding protein
SCO0105	-0.9719724	0.03671155	1095530	SCO0105	SCO0105SCJ11.34c, xlnC	endo-1,4-beta-xylanase
SCO4258	-0.9746007	0.04326187	1099698	SCO4258	SCO4258SCD8A.31	hydrolytic protein carbohydrate binding
SCO4598	-0.9760018	0.04345377	1100038	SCO4598	SCO4598SCD20.16c	two-component system sensor kinase
SCO5043	-0.9948104	0.01407193	1100484	SCO5043	SCO5043SCK7.16c	hydrolase membrane protein
SCO7823	-1.0032944	0.04731835	1103261	SCO7823	SCO7823SC8E7.20c	hypothetical protein
SCO2383	-1.0044901	0.04910985	1097817	SCO2383	SCO2383SC4A7.11	hypothetical protein
SCO5045	-1.0056495	0.01096671	1100486	SCO5045	SCO5045SCK7.18	hypothetical protein
SCO5044	-1.0075861	0.02148664	1100485	SCO5044	SCO5044SCK7.17c, fumB	fumarate hydratase class I
SCO0535	-1.0143617	0.01769636	1095958	SCO0535	SCO0535SCF11.15	hydrolase MhpC like
SCO2953	-1.0144104	0.04179123	1098386	SCO2953	SCO2953SCE59.12c	hypothetical protein

SCO7095	-1.0150053	0.03613319	1102533	SCO7095	SCO7095SC3A4.21c	hydrolase
SCO6388	-1.0174551	0.01903839	1101829	SCO6388	SCO6388SC3C8.07c	hypothetical protein
SCO1887	-1.0177796	0.03493298	1097321	SCO1887	SCO1887SCI7.05c	integral membrane transport protein
SCO1895	-1.0187911	0.03939762	1097329	SCO1895	SCO1895SCI7.13c	5-dehydro-4-deoxyglucarate dehydratase
SCO4079	-1.0247206	0.00102117	1099516	SCO4079	SCO4079SCD25.15, purL	phosphoribosylformylglycinamide synthase II
SCO3009	-1.0258731	0.01741134	1098442	SCO3009	SCO3009SCE33.11c	hypothetical protein
SCO5783	-1.0278388	0.00975505	1101225	SCO5783	SCO5783SC4H2.04c	hypothetical protein
SCO5399	-1.0292836	0.02462097	1100839	SCO5399	SCO5399SC8F4.03	acetyl-CoA acetyltransferase
SCO2561	-1.0348763	0.00039975	1097995	SCO2561	SCO2561SCC77.28c	long-chain fatty-acid CoA ligase
SCO5028	-1.0410003	0.0041875	1100469	SCO5028	SCO5028SCK7.01	ATP-binding protein
SCO4759	-1.0503524	0.0200821	1100200	SCO4759	SCO4759SC6G4.37	hypothetical protein
SCO4055	-1.0507445	0.01739508	1099491	SCO4055	SCO40552SCD60.21c	alcohol dehydrogenase
SCO4078	-1.0512646	0.00106214	1099515	SCO4078	SCO4078SCD25.14, purQ	phosphoribosylformylglycinamide synthase I
SCO2469	-1.0514186	0.0171081	1097903	SCO2469	SCO2469SC7A8.08c	reductase
SCO6732	-1.052917	0.00200693	1102171	SCO6732	SCO6732SC5F2A.15	fatty acid oxidative multifunctional enzyme
SCO1396	-1.0549897	0.02383087	1096822	SCO1396	SCO1396SC1A8A.16c	D-alanyl-D-alanine dipeptidase
SCO0346	-1.0560937	0.03628197	1095769	SCO0346	SCO0346SCF41.05	2-hydroxyhepta-2,4-diene-1,7-dioate isomerase
SCO1528	-1.0595903	0.03660664	1096954	SCO1528	SCO1528fusA	elongation factor G
SCO4352	-1.064125	0.01892397	1099792	SCO4352	SCO4352SCD19.07	oxidoreductase
SCO1224	-1.0648446	0.04231456	1096647	SCO1224	SCO12242SCG58.24c	sugar-phosphate isomerase
SCO7611	-1.0702186	0.03149459	1103049	SCO7611	SCO7611SC2H2.09	hypothetical protein
SCO0079	-1.0703477	0.02171802	1095508	SCO0079	SCO0079SCJ11.08c	integral membrane transport protein
SCO0766	-1.073018	0.02951067	1096189	SCO0766	SCO0766SCF81.25c	beta-galactosidase
SCO1533	-1.0864658	0.02593568	1096959	SCO1533	SCO1533SCL2.23c	hypothetical protein
SCO7012	-1.0947742	0.03087336	1102450	SCO7012	SCO7012SC1H10.01c, SC8F11.38c	binding protein dependent transport protein
SCO6952	-1.100734	0.02483597	1102390	SCO6952	SCO6952SC6F7.05c	hypothetical protein
SCO2018	-1.1019587	0.03172033	1097452	SCO2018	SCO2018SC7H2.32c	aminopeptidase pepN
SCO5026	-1.1025966	0.0339411	1100467	SCO5026	SCO5026SCK15.28	hypothetical protein
SCO3563	-1.1038638	0.02627836	1098999	SCO3563	SCO3563SCH5.26, acsA	acetyl-CoA synthetase
SCO0439	-1.1074638	0.01211983	1095862	SCO0439	SCO0439SCF51A.17c	hypothetical protein
SCO5657	-1.1108087	0.03763986	1101096	SCO5657	SCO5657SC6A9.10c	aldehyde dehydrogenase
SCO2800	-1.1120818	0.03056538	1098234	SCO2800	SCO28002SCC13.08c	two component system histidine kinase
SCO4077	-1.1151632	0.00385661	1099514	SCO4077	SCO4077SCD25.13	phosphoribosylformylglycinamide synthase subunit PurS
SCO3164	-1.1225888	0.01811912	1098598	SCO3164	SCO3164SCE87.15c	hypothetical protein
SCO5025	-1.1237068	0.01203305	1100466	SCO5025	SCO5025SCK15.27	transcriptional regulator
SCO4005	-1.1246788	0.03083396	1099441	SCO4005	SCO40052SC10A7.09	RNA polymerase sigma factor; PMID: 17683547 Induced by ppGpp
SCO6814	-1.1248084	0.0492456	1102253	SCO6814	SCO6814SC1A2.23c	ABC transporter ATP-binding protein
SCO5299	-1.1254025	0.0497461	1100739	SCO5299	SCO5299SC6G9.34	hypothetical protein
SCO7710	-1.1356304	0.03537994	1103148	SCO7710	SCO7710SC8D11.01, SCBAC12C8.11	phosphotransferase
SCO6384	-1.1416249	0.00261905	1101825	SCO6384	SCO6384SC3C8.03c	integral membrane lysyl-tRNA synthetase
SCO0783	-1.1431431	0.01181955	1096206	SCO0783	SCO07833SCF60.15, tetM	tetracycline resistance protein
SCO6399	-1.1546158	0.01041136	1101838	SCO6399	SCO6399SC3C8.18c	hypothetical protein
SCO5398	-1.1549266	0.03979902	1100838	SCO5398	SCO5398SC8F4.02c	hypothetical protein, putative methylmalonyl-CoA epimerase.
SCO7013	-1.1577663	0.02666938	1102451	SCO7013	SCO7013SC1H10.02c	sugar-binding lipoprotein
SCO4071	-1.1583569	0.0117192	1099508	hemH	SCO4071SCD25.07, purC	phosphoribosylaminoimidazole-succinocarboxamide synthase
SCO4440	-1.1593685	0.04985673	1099880	SCO4440	SCO4440SCD6.18	hypothetical protein
SCO6027	-1.1600757	0.04632064	1101468	SCO6027	SCO6027SC1C3.15c	acetyl-CoA acetyltransferase
SCO5035	-1.1642095	0.04903448	1100476	SCO5035	SCO5035SCK7.08c	ABC transporter ATP-binding protein

SCO1440	-1.1668322	0.00635516	1096866	ribH	SCO1440SC6D7A.03c	6,7-dimethyl-8-ribityllumazine synthase
SCO6373	-1.1678056	0.04497161	1101814	SCO6373	SCO6373SC4A2.09	hypothetical protein
SCO7555	-1.1678075	0.0498048	1102993	SCO7555	SCO7555SC5F1.09	solute binding lipoprotein
SCO1441	-1.1684141	0.00281166	1096867	SCO1441	SCO1441SC6D7A.04c, ribAB	bifunctional 3,4-dihydroxy-2-butanone 4-phosphate synthase/GTP cyclohydrolase II protein
SCO5148	-1.1710116	0.04570437	1100589	SCO5148	SCO5148SCP8.11	hypothetical protein
SCO1240	-1.188578	0.04799388	1096663	SCO1240	SCO12402SCG1.15	hypothetical protein CL35 Strakova et al
SCO5782	-1.1938642	0.02696515	1101224	SCO5782	SCO5782SC4H2.03c	transmembrane transport protein
SCO0021	-1.1993581	0.00441403	1095456	SCO0021	SCO0021SCJ4.02	hypothetical protein
SCO5258	-1.2014174	0.04519989	1100699	SCO5258	SCO52582SC7G11.20c, atrC	ATP-binding protein
SCO0322	-1.2027997	0.01226895	1095746	SCO0322	SCO0322SC5G9.31c, SCF12.01c	ABC transport ATP-binding subunit
SCO7544	-1.2072474	0.0431692	1102982	SCO7544	SCO7544SC8G12.20	ABC transporter membrane protein
SCO0309	-1.212534	0.03364248	1095733	SCO0309	SCO0309SC5G9.18c	amide hydrolase
SCO0600	-1.2169915	0.01965013	1096023	SCO0600	SCO0600SC5F5.24, sig8	RNA polymerase sigma factor sig8/sigB
SCO2729	-1.2195013	0.02878267	1098163	SCO2729	SCO2729SCC46.14	acetyltransferase
SCO2698	-1.221986	0.02201606	1098132	SCO2698	SCO2698SCC61A.19	small hydrophilic protein
SCO6730	-1.2250856	0.02620335	1102169	SCO6730	SCO6730SC5F2A.13	racemase
SCO4564	-1.2284437	0.02100994	1100004	SCO4564	SCO4564SCD16A.19c, nuoC	NADH dehydrogenase subunit C
SCO7410	-1.2303826	0.01798887	1102848	SCO7410	SCO7410SC6D11.06c	binding-protein dependent transport protein
SCO7197	-1.2305069	0.01913662	1102635	SCO7197	SCO7197SC8A11.25c	amino acid ABC transporter permease
SCO7265	-1.2319619	0.02199026	1102703	SCO7265	SCO7265SC5H1.27	hypothetical protein
SCO6332	-1.2339692	0.04536992	1101773	SCO6332	SCO6332SC10H5.08c	hypothetical protein
SCO0137	-1.2374128	0.01701312	1095561	SCO0137	SCO0137SCJ21.18c, SCJ33.01c	sugar-transport protein
SCO3010	-1.2375496	0.01237786	1098443	SCO3010	SCO3010SCE33.12c	hypothetical protein
SCO1218	-1.2390603	0.03868886	1096641	SCO1218	SCO12182SCG58.18c	transmembrane transport protein
SCO0815	-1.2408014	0.03540589	1096238	SCO0815	SCO0815SCF43A.05	hypothetical protein
SCO4256	-1.2517025	0.00725892	1099696	SCO4256	SCO4256SCD8A.29	hydrolytic protein carbohydrate binding
SCO1366	-1.2517451	0.04440305	1096789	SCO1366	SCO1366SC10A9.08c	hypothetical protein
SCO5259	-1.2577006	0.0321283	1100700	SCO5259	SCO52592SC7G11.21c, atrB	permease
SCO5017	-1.2578031	0.04475442	1100458	SCO5017	SCO5017SCK15.19	AraC family transcription regulator
SCO1729	-1.261507	0.04290643	1097160	SCO1729	SCO1729SC111.18	hypothetical protein
SCO1988	-1.2627759	0.00476581	1097422	SCO1988	SCO1988SC7H2.02	hypothetical protein
SCO4783	-1.2705064	0.03836347	1100224	SCO4783	SCO4783SCD63.15	hypothetical protein
SCO1147	-1.2715908	0.00116743	1096570	SCO1147	SCO11472SCG38.40, SCG8A.01	ABC transporter transmembrane subunit CL35 Strakova et al
SCO6731	-1.2756499	0.00054097	1102170	SCO6731	SCO6731SC5F2A.14	acetyl-CoA acetyltransferase
SCO3815	-1.2959344	0.02615942	1099251	SCO3815	SCO3815SCGD3.16c, bkdC1	branched-chain alpha-keto acid dehydrogenase E2
SCO5415	-1.2985974	0.02764478	1100855	SCO5415	SCO5415SC8F4.19, icmA	isobutyryl-CoA mutase A
SCO2827	-1.2993047	0.03393689	1098261	SCO2827	SCO2827SCBAC17F8.18c	hypothetical protein
SCO6719	-1.3019551	0.02322505	1102158	SCO6719	SCO6719SC5F2A.02c	UvrA-like ABC transporter
SCO4257	-1.3041952	0.00119154	1099697	SCO4257	SCO4257SCD8A.30	hydrolytic protein carbohydrate binding
SCO1442	-1.3149347	0.00215866	1096868	SCO1442	SCO1442SC6D7A.05c	hypothetical protein
SCO3667	-1.319192	0.03204494	1099103	SCO3667	SCO3667SCH44.07c	solute-binding protein
SCO0409	-1.3258528	0.04350296	1095832	SCO0409	SCO0409SCF51.08c, sapA	spore-associated protein
SCO5785	-1.325935	0.00822481	1101227	SCO5785	SCO5785SC4H2.06	two-component regulator
SCO0725	-1.331583	0.00628857	1096148	SCO0725	SCO07253SC5B7.03	hypothetical protein
SCO5380	-1.3330979	0.03992505	1100820	SCO5380	SCO53802SC6G5.24	hypothetical protein
SCO0939	-1.3341378	0.0480469	1096362	SCO0939	SCO0939SCM10.27c	hydrolase MhpC like
SCO0533	-1.3351314	0.04425517	1095956	SCO0533	SCO0533SCF11.13	sugar transporter membrane protein
SCO3816	-1.3426793	0.03257553	1099252	SCO3816	SCO3816SCGD3.17c, bkdB1	branched-chain alpha-keto acid dehydrogenase E1 subunit beta CL35 Strakova et al

SCO1640	-1.3439945	0.04030802	1097071	SCO1640	SCO1640SCI41.23c	hypothetical protein
SCO2587	-1.3453967	2.04E-05	1098021	SCO2587	SCO2587proB	gamma-glutamyl kinase
SCO1082	-1.3478495	4.91E-05	1096505	SCO1082	SCO1082SCG22.28c	electron transfer flavoprotein subunit beta
SCO5973	-1.3483439	0.02510209	1101415	SCO5973	SCO5973StBAC16H6.08	phosphatase
SCO5429	-1.3487441	0.02978033	1100869	SCO5429	SCO5429SC6A11.05c	integral membrane transport protein
SCO7277	-1.3674692	0.00197996	1102715	SCO7277	SCO7277SC5H1.15c	regulator protein
SCO1354	-1.3681399	0.03479062	1096777	SCO1354	SCO13542SCG61.36c	hypothetical protein
SCO0260	-1.3738624	0.02544004	1095684	SCO0260	SCO0260SCF1.02	hypothetical protein
SCO6784	-1.3774459	0.0109934	1102223	SCO6784	SCO6784SC6A5.33c	regulatory protein
SCO2673	-1.3846957	0.03016795	1098107	SCO2673	SCO2673SC6D10.16	hypothetical protein
SCO6721	-1.3855864	0.00090274	1102160	SCO6721	SCO6721SC5F2A.04	hypothetical protein
SCO1732	-1.3877999	0.01331755	1097163	SCO1732	SCO1732SCI11.21	hypothetical protein
SCO6228	-1.3887744	0.02487651	1101669	SCO6228	SCO6228SC2H4.10	hypothetical protein
SCO7028	-1.3955846	0.01850385	1102466	SCO7028	SCO7028SC1H10.17	sugar-binding lipoprotein
SCO4262	-1.4022549	0.00101382	1099702	SCO4262	SCO4262SCD49.03	hypothetical protein
SCO0203	-1.4034202	0.01489267	1095627	SCO0203	SCO0203SCJ12.15c	two-component sensor
SCO5884	-1.4050464	0.03746746	1101326	SCO5884	SCO5884SC3F7.04c	hypothetical protein
SCO1669	-1.4066087	0.0027955	1097100	SCO1669	SCO1669SCI52.11c	ATP/GTP-binding protein
SCO3113	-1.4072659	0.03319066	1098547	SCO3113	SCO3113SCE41.22	SCO3113 transposase remnant
SCO6738	-1.4109534	0.01799603	1102177	SCO6738	SCO6738SC5F2A.21	carboxypeptidase
SCO4597	-1.4173771	0.02562279	1100037	SCO4597	SCO4597SCD20.15c	two-component system sensor kinase
SCO0952	-1.4236577	0.00326967	1096375	SCO0952	SCO0952SCM11.07c	solute-binding protein
SCO1914	-1.4269417	0.02597813	1097348	SCO1914	SCO1914SCI7.32	hypothetical protein
SCO6011	-1.431962	4.81E-05	1101453	SCO6011	SCO6011SC7B7.08	ABC transporter
SCO0974	-1.4402864	0.03534966	1096397	SCO0974	SCO0974SCBAC19F3.01c, SCM11.29c	hypothetical protein
SCO4681	-1.4438688	0.00668191	1100122	SCO4681	SCO4681SCD31.06	short chain dehydrogenase
SCO3957	-1.4453186	0.04694573	1099393	SCO3957	SCO3957SCD78.24	hypothetical protein CL35 Strakova et al
SCO2493	-1.4633095	0.00241752	1097927	SCO2493	SCO2493SC7A8.32c	hypothetical protein
SCO1839	-1.4660987	0.04727474	1097273	SCO1839	SCO1839SCI8.24c	transcriptional regulator
SCO5260	-1.4737187	0.03445479	1100701	SCO5260	SCO52602SC7G11.22c, atrA	hypothetical protein
SCO5229	-1.4737989	0.02312831	1100670	SCO5229	SCO5229SC7E4.26c	permease
SCO3958	-1.4739248	0.03536152	1099394	SCO3958	SCO3958SCD78.25	ABC transporter ATP-binding protein
SCO6010	-1.4793502	3.57E-05	1101452	SCO6010	SCO6010SC7B7.07	ABC transporter ATP-binding protein
SCO6989	-1.4920113	0.0316697	1102427	SCO6989	SCO6989SC8F11.15c	hypothetical protein
SCO1056	-1.4933751	0.02832881	1096479	SCO1056	SCO1056SCG22.02	sugar transport sugar binding protein
SCO0591	-1.5009327	0.02864391	1096014	SCO0591	SCO0591SCF55.15	endo-N-acetylmuramidases
SCO1340	-1.5083141	0.00412099	1096763	SCO1340	SCO13402SCG61.22	hypothetical protein
SCO6718	-1.5121362	0.03719433	1102157	SCO6718	SCO6718SC5F2A.01c, ddah	dimethylarginine dimethylaminohydrolase
SCO2925	-1.5136013	0.01115333	1098358	SCO2925	SCO2925SCE19A.25c	oxidoreductase subunit
SCO6968	-1.5190717	0.01563016	1102406	SCO6968	SCO6968SC6F7.21	long-chain-fatty-acid-CoA ligase
SCO0178	-1.5248701	0.0288573	1095602	SCO0178	SCO0178SCJ1.27	hypothetical protein
SCO0255	-1.5264789	0.00996091	1095679	SCO0255	SCO0255SCF20.01c, SCJ9A.34c	sigma factor
SCO5230	-1.5281394	0.015086	1100671	SCO5230	SCO5230SC7E4.27c	hypothetical protein
SCO4254	-1.5326734	0.01373842	1099694	SCO4254	SCO4254SCD8A.27	hypothetical protein
SCO0544	-1.5402096	0.02949671	1095967	SCO0544	SCO0544SCF11.24	hypothetical protein
SCO5889	-1.5469515	0.04596249	1101331	SCO5889	SCO5889SC3F7.09, redO	hypothetical protein
SCO2999	-1.5472914	0.00442127	1098432	SCO2999	SCO2999SCE33.01c, SCE99.06c	Bacterial NAD-glutamate dehydrogenase.
SCO1112	-1.5553157	0.00840536	1096535	SCO1112	SCO11122SCG38.05	oxidoreductase

SCO0698	-1.5567765	0.00788208	1096121	SCO0698	SCO0698SCF42.08c	hypothetical protein
SCO2895	-1.5659291	0.03439587	1098328	SCO2895	SCO2895SCE6.32c	integral membrane transport protein
SCO5324	-1.5674382	0.00252939	1100764	SCO5324	SCO5324SC6G9.09c	oxidoreductase
SCO2247	-1.5709454	0.03633818	1097680	SCO2247	SCO2247SC1G2.09c	hypothetical protein
SCO1081	-1.5725544	9.34E-05	1096504	SCO1081	SCO1081SCG22.27c	electron transfer flavoprotein subunit alpha
SCO0540	-1.5736178	0.02723296	1095963	SCO0540	SCO0540SCF11.20	sugar transport membrane protein
SCO0876	-1.5859918	0.04100203	1096299	SCO0876	SCO0876SCM1.09c	hypothetical protein
SCO6702	-1.6056288	0.00962701	1102141	SCO6702	SCO6702SC4C6.12c, pcaJ	3-oxoadipate CoA-transferase subunit B
SCO1585	-1.6090088	0.01702944	1097016	SCO1585	SCO1585SCI35.07c	hypothetical protein
SCO6009	-1.6099713	1.18E-05	1101451	SCO6009	SCO6009SC7B7.06	solute-binding protein, possible xylose binding
SCO0009	-1.6102124	0.02088183	1095441	SCO0009	SCO0009SCJ30.04c	hypothetical protein
SCO2746	-1.6125097	0.03043273	1098180	SCO2746	SCO2746SCC57A.17	ABC transporter ATP-binding protein
SCO4222	-1.6198737	0.00140301	1099662	SCO4222	SCO4222SCD46.36	hypothetical protein
SCO7221	-1.6234576	0.04543529	1102659	SCO7221	SCO7221SC2H12.20c	polyketide synthase
SCO2829	-1.6272084	0.01469204	1098263	SCO2829	SCO2829SCE20.03	amino acid ABC transporter transmembrane protein
SCO4828	-1.6282017	0.03599873	1100269	SCO4828	SCO4828SC2A6.13, gbsA	betaine aldehyde dehydrogenase
SCO4255	-1.6372744	0.00033718	1099695	SCO4255	SCO4255SCD8A.28	hypothetical protein CL35 Strakova et al
SCO0427	-1.6384131	0.00220241	1095850	SCO0427	SCO0427SCF51A.05	hydrolase MhpC like
SCO5656	-1.6386654	0.01930151	1101095	SCO5656	SCO5656SC6A9.11	transcriptional regulator
SCO0410	-1.640241	0.00927831	1095833	SCO0410	SCO0410SCF51.09c	hypothetical protein
SCO2379	-1.6424981	0.01374332	1097813	SCO2379	SCO2379SC4A7.07	acetyltransferase
SCO6744	-1.64427	0.00580727	1102183	SCO6744	SCO6744SC5F2A.27	hypothetical protein
SCO1196	-1.6458162	0.00851179	1096619	SCO1196	SCO1196SCG11A.27c	hypothetical protein
SCO6500	-1.647057	0.01839677	1101939	SCO6500	SCO6500gvpA	gas vesicle synthesis-like protein
SCO2831	-1.6531334	0.00634472	1098265	SCO2831	SCO2831SCE20.05	amino acid ABC transporter ATP-binding protein
SCO5655	-1.6614101	0.00694098	1101094	SCO5655	SCO5655SC6A9.12	hypothetical protein
SCO7175	-1.6638867	0.03859212	1102613	SCO7175	SCO7175SC8A11.03	regulator CL35 Strakova et al
SCO1346	-1.6683049	1.70E-06	1096769	SCO1346	SCO13462SCG61.28c, fabG3	3-oxoacyl-ACP reductase
SCO2830	-1.6766753	0.00459166	1098264	SCO2830	SCO2830SCE20.04	amino acid ABC transporter transmembrane protein
SCO7806	-1.6768261	0.00201268	1103244	SCO7806	SCO7806SC8E7.03c	DNA-binding protein
SCO0592	-1.688755	0.04393063	1096015	SCO0592	SCO0592SCF55.16c	hypothetical protein
SCO7063	-1.6892506	0.01408007	1102501	SCO7063	SCO7063SC4G1.29c	hypothetical protein
SCO6745	-1.6952238	0.0009285	1102184	SCO6745	SCO6745SC5F2A.28c	hypothetical protein
SCO4006	-1.7141558	0.00198959	1099442	SCO4006	SCO40062SC10A7.10	long-chain-fatty-acid--CoA ligase
SCO0616	-1.7174517	0.01027731	1096039	SCO0616	SCO0616SCF55.40c	hypothetical protein
SCO6544	-1.7174754	0.04932425	1101983	SCO6544	SCO6544SC5C7.29	hypothetical protein
SCO7329	-1.7188796	0.04711807	1102767	SCO7329	SCO7329SC4G10.08c	long-chain-fatty-acid-CoA ligase
SCO6499	-1.7201011	0.00108622	1101938	SCO6499	SCO6499gvpO	gas vesicle synthesis protein
SCO2828	-1.7208402	0.00298018	1098262	SCO2828	SCO2828SCE20.02	amino acid ABC transporter substrate-binding protein
SCO3928	-1.7218374	0.03277359	1099364	SCO3928	SCO3928SCQ11.11, thiC	thiamine biosynthesis protein ThiC
SCO6987	-1.7297005	0.02949153	1102425	SCO6987	SCO6987SC8F11.13	hypothetical protein
SCO6433	-1.7558408	0.00347704	1101872	SCO6433	SCO6433SC1A6.22	hypothetical protein
SCO0111	-1.7574439	0.02698317	1095536	SCO0111	SCO0111SCJ11.40	oxidoreductase
SCO3710	-1.7677601	0.01811382	1099146	SCO3710	SCO3710SCH35.14c	large integral membrane protein
SCO6504	-1.7729228	0.00985469	1101943	SCO6504	SCO6504SC1E6.13	hypothetical protein
SCO1824	-1.7815857	0.00935306	1097258	SCO1824	SCO1824ssp	subtilisin-like protease
SCO7606	-1.7816208	0.01054566	1103044	SCO7606	SCO7606SC2H2.04	amino acid binding protein
SCO7608	-1.7922566	0.02636609	1103046	SCO7608	SCO7608SC2H2.06	hypothetical protein

SCO2007	-1.8016251	0.0163183	1097441	SCO2007	SCO2007SC7H2.21	hypothetical protein
SCO3079	-1.8074593	4.25E-06	1098512	SCO3079	SCO3079SCE25.20	acetyl-CoA acetyltransferase
SCO1683	-1.8139783	0.00106767	1097114	SCO1683	SCO1683SCI30A.04c	amino acid permease
SCO1317	-1.8149255	0.00252191	1096740	SCO1317	SCO1317SCBAC36F5.28c	hypothetical protein
SCO1453	-1.8278918	0.00020913	1096879	SCO1453	SCO1453SCL6.10	hypothetical protein
SCO1225	-1.8353608	0.00033228	1096648	SCO1225	SCO12252SCG58.25	osmoprotectant transporter
SCO6765	-1.8372297	0.01354668	1102204	SCO6765	SCO6765SC6A5.14	lipoprotein
SCO3247	-1.8432387	0.03439402	1098681	SCO3247	SCO3247SCE29.16c	acyl CoA oxidase
SCO7747	-1.8437846	0.00200927	1103185	SCO7747	SCO7747SC8D11.38	hypothetical protein
SCO2978	-1.8456453	0.01011318	1098411	SCO2978	SCO2978SCE50.06	hypothetical protein
SCO0543	-1.8492501	8.91E-05	1095966	SCO0543	SCO0543SCF11.23	Murein DD-endopeptidase MepM and murein hydrolase activator NlpD, contain LysM domain
SCO7311	-1.8507136	0.03265893	1102749	SCO7311	SCO7311SC5F8.21c	amino acid decarboxylase
SCO0408	-1.8541555	0.0035851	1095831	SCO0408	SCO0408SCF51.07	methyltransferase
SCO3711	-1.855714	0.00155208	1099147	SCO3711	SCO3711SCH35.13c	small membrane protein
SCO0273	-1.8621277	0.01916741	1095697	SCO0273	SCO0273SCF1.15, SCF85.01	substrate binding protein
SCO6503	-1.8629766	0.00416809	1101942	SCO6503	SCO6503SC1E6.12	hypothetical protein
SCO1838	-1.8653484	0.00722646	1097272	SCO1838	SCO1838SCI8.23c	enoyl-CoA hydratase/isomerase
SCO0435	-1.8656458	0.01537345	1095858	SCO0435	SCO0435malY	aminotransferase
SCO0618	-1.866493	0.01869663	1096041	SCO0618	SCO0618SCF56.02	hypothetical protein
SCO3055	-1.8724747	0.001664	1098488	SCO3055	SCO3055SCBAC19G2.10	hypothetical protein CL35 Strakova et al
SCO2248	-1.8763558	0.02242751	1097681	SCO2248	SCO2248SC1G2.10	hypothetical protein
SCO3051	-1.8826185	6.97E-09	1098484	SCO3051	SCO3051SCBAC19G2.06c, fadE	acyl-CoA dehydrogenase
SCO2980	-1.8906462	0.02505335	1098413	SCO2980	SCO2980SCE50.08	integral membrane transport protein
SCO1345	-1.8925424	7.29E-06	1096768	fabG	SCO13452SCG61.27c, fabG2	3-ketoacyl-ACP reductase
SCO0458	-1.9212826	0.04442668	1095881	SCO0458	SCO0458SCF51A.36	Beta-glucosidase
SCO7210	-1.9217412	0.00194741	1102648	SCO7210	SCO7210SC2H12.09	hypothetical protein
SCO2727	-1.9218336	0.04248327	1098161	SCO2727	SCO2727SCC46.12c	hypothetical protein
SCO1563	-1.9265657	0.00454179	1096994	SCO1563	SCO1563SCL11.19c	acetyltransferase
SCO3090	-1.9277931	0.02030102	1098524	SCO3090	SCO3090SCE25.31	ABC transporter
SCO3362	-1.9347792	0.03096271	1098799	SCO3362	SCO3362SCE94.13	hypothetical protein
SCO7596	-1.9419372	0.00503083	1103034	SCO7596	SCO7596SC7H9.08c	integral membrane transport protein
SCO5911	-1.9424452	0.01533385	1101353	SCO5911	SCO5911SC10A5.16c	oligopeptide binding protein
SCO2912	-1.9444554	0.02690586	1098345	SCO2912	SCO2912SCE19A.12c	hypothetical protein
SCO1307	-1.9490462	0.00288363	1096730	SCO1307	SCO1307SCBAC36F5.18c	hypothetical protein
SCO7721	-1.9559289	0.0447063	1103159	SCO7721	SCO7721SC8D11.12	hypothetical protein
SCO6362	-1.9743461	0.00515902	1101803	SCO6362	SCO6362SC3A7.30	two-component sensor
SCO2861	-1.9801648	0.00104837	1098295	SCO2861	SCO2861SCE20.35.	hypothetical protein
SCO1692	-1.9919414	0.0140943	1097123	SCO1692	SCO1692SCI30A.13c	oxidoreductase
SCO0992	-1.9933745	0.02638156	1096415	SCO0992	SCO09922SCG2.05	cysteine synthase
SCO5430	-1.9986602	0.00190696	1100870	SCO5430	SCO5430SC6A11.06c	extracellular solute-binding lipoprotein
SCO2417	-2.0057761	0.00808366	1097851	SCO2417	SCO2417SC8A2.05c mce	hypothetical protein, possibly part of Mce protein complex
SCO4980	-2.013444	1.19E-05	1100421	SCO4980	SCO49802SCK36.03c	hypothetical protein
SCO4930	-2.0147131	0.01007507	1100371	SCO4930	SCO4930SCK13.22	enoyl-CoA hydratase
SCO0596	-2.0161697	0.00065766	1096019	SCO0596	SCO0596SCF55.20	DNA-binding protein
SCO5915	-2.0169579	0.02003694	1101357	SCO5915	SCO5915SC10A5.20	hypothetical protein
SCO3607	-2.0193936	0.0002716	1099043	SCO3607	SCO3607SC66T3.18c	hypothetical protein
SCO4207	-2.0205335	0.00545021	1099647	SCO4207	SCO42072SCD46.21	hypothetical protein CL35 Strakova et al
SCO6700	-2.024708	0.0228484	1102139	SCO6700	SCO6700SC4C6.10c, pcaH	protocatechuate 3,4-dioxygenase subunit beta

SCO2401	-2.0352812	0.00081296	1097835	SCO2401	SCO2401SC4A7.29	dehydratase
SCO4562	-2.0574858	0.00263565	1100002	SCO4562	SCO4562SCD16A.21c, nuoA	NADH dehydrogenase subunit A
SCO0257	-2.0580139	0.018112	1095681	SCO0257	SCO0257SCF20.03	hypothetical protein
SCO2749	-2.063794	0.00078669	1098183	SCO2749	SCO2749SCC57A.20	D-ribose pyranase
SCO2774	-2.0670871	2.15E-09	1098208	SCO2774	SCO2774SCC105.05c, acdH2	acyl-CoA dehydrogenase
SCO2466	-2.0813891	0.00766622	1097900	SCO2466	SCO2466SC7A8.05	hypothetical protein
SCO6986	-2.0879227	0.04448497	1102424	SCO6986	SCO6986SC8F11.12	DNA-binding protein
SCO5916	-2.0968425	0.01802199	1101358	SCO5916	SCO5916SC10A5.21	hypothetical protein
SCO2213	-2.099307	0.0191776	1097646	SCO2213	SCO2213SC10B7.08	regulatory protein
SCO3945	-2.1005832	0.00285678	1099381	SCO3945	SCO3945SCD78.12, cydA	cytochrome oxidase subunit I
SCO7040	-2.1078393	0.00076517	1102478	SCO7040	SCO7040SC4G1.06c, gap2	glyceraldehyde-3-phosphate dehydrogenase
SCO2625	-2.1165534	0.00384573	1098059	SCO2625	SCO2625SCC80.10	hypothetical protein
SCO4477	-2.1400828	0.00961205	1099917	SCO4477	SCO4477SCD65.20c	MerR family transcriptional regulator
SCO1230	-2.1437321	0.01162163	1096653	SCO1230	SCO12302SCG1.05c	tripeptidylaminopeptidase
SCO6506	-2.1450096	0.00787908	1101945	SCO6506	SCO6506gvpL	gas vesicle protein
SCO6516	-2.1493833	0.00124771	1101955	SCO6516	SCO6516SC1E6.25c, SC5C7.01c	hypothetical protein
SCO1457	-2.1642324	0.00052255	1096883	SCO1457	SCO1457SCL6.14c	transporter
SCO6475	-2.1729374	0.01552382	1101914	SCO6475	SCO6475SC9C7.11c	oxidoreductase
SCO0107	-2.1747363	5.06E-06	1095532	SCO0107	SCO0107SCJ11.36c	aminoglycoside nucleotidyltransferase
SCO4054	-2.1774137	0.00129533	1099490	SCO4054	SCO40542SCD60.20	hypothetical protein
SCO4563	-2.197312	0.00288274	1100003	SCO4563	SCO4563SCD16A.20c, nuoB	NADH dehydrogenase subunit B
SCO6511	-2.2095224	0.00464603	1101950	SCO6511	SCO6511SC1E6.20c	hypothetical protein
SCO2009	-2.2236138	0.0037835	1097443	SCO2009	SCO2009SC7H2.23	branched-chain amino acid ABC transporter permease
SCO3946	-2.2292424	0.00454854	1099382	SCO3946	SCO3946SCD78.13, cydB	cytochrome oxidase subunit II
SCO0930	-2.2332106	0.02251018	1096353	SCO0930	SCO0930SCM10.18c	lipoprotein
SCO5910	-2.2369145	0.02596678	1101352	SCO5910	SCO5910SC10A5.15	hypothetical protein
SCO2773	-2.2591878	2.09E-05	1098207	SCO2773	SCO2773SCC105.04c, tesB2	acyl CoA thioesterase II
SCO0209	-2.2686921	0.04521813	1095633	SCO0209	SCO0209SCJ12.21	hypothetical protein
SCO5676	-2.2848884	0.00011135	1101115	SCO5676	SCO5676gabT	4-aminobutyrate aminotransferase
SCO1455	-2.3130886	0.00045559	1096881	SCO1455	SCO1455SCL6.12c	hydrolase
SCO1140	-2.3251669	0.00196413	1096563	SCO1140	SCO11402SCG38.33	hypothetical protein
SCO0172	-2.3579051	0.00645518	1095596	SCO0172	SCO0172SCJ1.21	hypothetical protein
SCO6200	-2.3584895	0.02295048	1101641	SCO6200	SCO6200SC2G5.21c	hypothetical protein
SCO6198	-2.3798725	0.01452349	1101639	SCO6198	SCO6198SC2G5.19	hypothetical protein
SCO3285	-2.3838474	0.00094967	1098719	SCO3285	SCO3285SCE15.02c	large glycine/alanine rich protein
SCO7005	-2.3970192	0.00736406	1102443	SCO7005	SCO7005SC8F11.31	oxidoreductase
SCO4931	-2.4196458	0.00603599	1100372	SCO4931	SCO4931SCK13.23	hypothetical protein
SCO0221	-2.4203766	0.00909934	1095645	SCO0221	SCO0221SCJ12.33c	pseudo
SCO2920	-2.424557	0.00926131	1098353	SCO2920	SCO2920SCE19A.20c	protease
SCO5531	-2.438489	0.03588651	1100971	SCO5531	SCO5531SC1C2.12c	hypothetical protein
SCO1426	-2.4477108	0.00357054	1096852	SCO1426	SCO1426SC6D7.13c	hypothetical protein
SCO5667	-2.457523	0.00321084	1101106	SCO5667	SCO5667SC8B7.11c	ABC transporter substrate-binding protein
SCO0335	-2.5212643	9.28E-05	1095758	SCO0335	SCO0335SCF12.14	hypothetical protein
SCO5671	-2.5377301	0.00122644	1101110	SCO5671	SCO5671SC8B7.07c	oxidoreductase CL35 Strakova et al
SCO7205	-2.5545345	0.00151073	1102643	SCO7205	SCO7205SC2H12.04	hydrolase
SCO0426	-2.5681194	0.00053011	1095849	SCO0426	SCO0426SCF51A.04	hypothetical protein
SCO3287	-2.5854135	0.00067478	1098721	SCO3287	SCO3287SCE15.04	serine/arginine rich protein
SCO5666	-2.5889309	0.00543364	1101105	SCO5666	SCO5666SC6A9.01c, SC8B7.12c	gamma-aminobutyraldehyde dehydrogenase

SCO6007	-2.5899495	0.004395	1101449	SCO6007	SCO6007SC7b7.04	transmembrane transport protein
SCO0256	-2.6018131	0.00702507	1095680	SCO0256	SCO0256SCF20.02	short chain oxidoreductase
SCO1454	-2.6137139	2.22E-06	1096880	SCO1454	SCO1454SCL6.11c	amino oxidase
SCO6196	-2.6207195	0.00342721	1101637	SCO6196	SCO6196SC2G5.17	AMP-binding domain-containing protein
SCO3286	-2.6207248	0.00033637	1098720	SCO3286	SCO3286SCE15.03c	hypothetical protein
SCO0177	-2.6338865	0.00384842	1095601	SCO0177	SCO0177SCJ1.26	hypothetical protein
SCO0198	-2.6708248	0.00286179	1095622	SCO0198	SCO0198SCJ12.10c	hypothetical protein
SCO0208	-2.6836314	0.001454	1095632	SCO0208	SCO0208SCJ12.20	pyruvate phosphate dikinase
SCO7204	-2.7186897	0.0011227	1102642	SCO7204	SCO7204SC2H12.03c	hypothetical protein
SCO0165	-2.7236501	3.26E-05	1095589	SCO0165	SCO0165SCJ1.14c	hypothetical protein
SCO6502	-2.7357936	0.00025518	1101941	SCO6502	SCO6502gvpG	gas vesicle synthesis protein
SCO7447	-2.7476314	0.00069955	1102885	SCO7447	SCO7447SC5C11.04c	acetyltransferase
SCO7473	-2.7563449	0.03747439	1102911	SCO7473	SCO7473SCBAC17A6.06, paaC	phenylacetic acid degradation protein PaaC
SCO6197	-2.7753295	0.00547881	1101638	SCO6197	SCO6197SC2G5.18c	hypothetical protein
SCO5669	-2.8319512	0.00115794	1101108	SCO5669	SCO5669SC8B7.09c	polyamine ABC-transporter integral membrane protein
SCO2474	-2.848668	0.02367058	1097908	SCO2474	SCO2474SC7A8.13	metalloproteinase probably secreted
SCO0166	-2.8578221	0.00024295	1095590	SCO0166	SCO0166SCJ1.15	regulator
SCO4689	-2.8596219	0.03752547	1100130	SCO4689	SCO4689SCD31.14	hypothetical protein
SCO2453	-2.8709398	0.04036891	1097887	SCO2453	SCO2453SCC24.24	hypothetical protein
SCO0179	-2.8791703	0.00226599	1095603	SCO0179	SCO0179SCJ1.28c	zinc-containing dehydrogenase
SCO5786	-2.8970565	0.0223686	1101228	SCO5786	SCO5786SC4H2.07c	hydrolase
SCO0274	-2.9504152	0.02510314	1095698	SCO0274	SCO0274SCF85.02	alpha-galactosidase
SCO1137	-2.9576077	7.88E-05	1096560	SCO1137	SCO11372SCG38.30c	two component system histidine kinase
SCO2011	-2.9688662	0.00142617	1097445	SCO2011	SCO2011SC7H2.25	branched-chain amino acid ABC transporter ATP-binding protein
SCO7255	-2.9954394	0.02974349	1102693	SCO7255	SCO7255SC5H1.37	hypothetical protein
SCO1459	-3.0104249	1.63E-05	1096885	SCO1459	SCO1459SCL6.16c	amino acid transporter
SCO2008	-3.019596	0.00199129	1097442	SCO2008	SCO2008SC7H2.22	branched-chain amino acid ABC transporter substrate-binding protein
SCO7242	-3.0306136	0.03338414	1102680	SCO7242	SCO7242SC7A12.09	hypothetical protein
SCO7446	-3.0638414	2.49E-05	1102884	SCO7446	SCO7446SC5C11.03	regulator
SCO1222	-3.0665127	0.00050732	1096645	SCO1222	SCO12222SCG58.22	hypothetical protein
SCO4621	-3.0774142	0.0336443	1100061	SCO4621	SCO4621SCD39.21c, traA1	sporulation-like protein
SCO5441	-3.0962338	0.03133934	1100881	SCO5441	SCO5441SC6A11.17c, pep2A	hypothetical protein
SCO2779	-3.2523475	1.54E-05	1098213	SCO2779	SCO2779SCC105.10, acdH	acyl-CoA dehydrogenase
SCO0167	-3.2872483	7.17E-05	1095591	SCO0167	SCO0167SCJ1.16c	hypothetical protein CL35 Strakova et al
SCO4690	-3.4117588	8.71E-05	1100131	SCO4690	SCO4690SCD31.15	hypothetical protein
SCO0205	-3.4621291	0.00255928	1095629	SCO0205	SCO0205SCJ12.17c	pseudo
SCO7469	-3.4697893	0.00046468	1102907	SCO7469	SCO7469SCBAC17A6.02c, paaK	phenylacetate-CoA ligase
SCO2402	-3.5939142	0.01327689	1097836	SCO2402	SCO2402SC4A7.30	dehydrogenase
SCO0168	-3.5952134	0.00027506	1095592	SCO0168	SCO0168SCJ1.17	regulator protein CL35 Strakova et al
SCO0923	-3.6880393	4.77E-05	1096346	sdhA	SCO0923SCM10.11c	succinate dehydrogenase flavoprotein subunit
SCO0181	-3.7000628	0.00021901	1095605	SCO0181	SCO0181SCJ1.30c	hypothetical protein
SCO2776	-3.835056	1.49E-06	1098210	SCO2776	SCO2776SCC105.07, accD1	acetyl/propionyl CoA carboxylase subunit beta
SCO4938	-3.8870903	0.02420272	1100379	SCO4938	SCO4938SCK13.30	ECF-sigma factor
SCO0211	-4.0072317	0.00032479	1095635	SCO0211	SCO0211SCJ12.23	hypothetical protein
SCO2492	-4.0254929	0.00038101	1097926	SCO2492	SCO2492SC7A8.31	hypothetical protein
SCO0174	-4.108257	1.93E-05	1095598	SCO0174	SCO0174SCJ1.23c	DNA-binding protein
SCO6560	-4.1102196	0.01983053	1101999	SCO6560	SCO6560SC4B5.10c	respiratory chain oxidoreductase
SCO1175	-4.1127909	0.00121496	1096598	SCO1175	SCO1175SCG11A.06c	hypothetical protein

SCO0215	-4.169633	1.84E-05	1095639	SCO0215	SCO0215SCJ12.27c	hypothetical protein
---------	-----------	----------	---------	---------	------------------	----------------------

GO:0044710	biological_process	single-organism metabolic process	2	57	1557	7910	175	SC05525 // SC05535 // SC02387 // SC01815 // SC01335 // SC02026 // SC05526 // SC01814 // SC02025 // SC05515 // SC02025 // SC07036 // SC02388 // SC02481 // SC03104 // SC06564 // SC04914 // SC01577 // SC02768 // SC03127 // SC06172 // SC01580 // SC01579 // SC07705 // SC06271 // SC01570 // SC01244 // SC02210 // SC04921 // SC05553 // SC05522 // SC03383 // SC04487 // SC05106 // SC04921 // SC03880 // SC01245 // SC03345 // SC01243 // SC01486 // SC02048 // SC03058 // SC03311 // SC01578 // SC04962 // SC04464 // SC01483 // SC03059 // SC05424 // SC02390 // SC03382 // SC02025 // SC03148 // SC02051 // SC03381	GO:0005737	0.726587653	0.00773984
GO:0044238	biological_process	primary metabolic process	2	73	2273	7910	175	SC05535 // SC07415 // SC02387 // SC01815 // SC02026 // SC01814 // SC05515 // SC02025 // SC07036 // SC02388 // SC02481 // SC03104 // SC06564 // SC04914 // SC01577 // SC02768 // SC03127 // SC05554 // SC04912 // SC06172 // SC01580 // SC01579 // SC02232 // SC01486 // SC02048 // SC03058 // SC02026 // SC01813 // SC03756 // SC01578 // SC04450 // SC04962 // SC01214 // SC01490 // SC04038 // SC04464 // SC01483 // SC03059 // SC00871 // SC02390 // SC07219 // SC03382 // SC07439 // SC01946 // SC05564 // SC05731 // SC03148 // SC04423 // SC02051 // SC03381	GO:0000166	0.537693458	0.02884059
GO:0006807	biological_process	nitrogen compound metabolic process	2	55	1567	7910	175	SC05525 // SC02026 // SC05526 // SC05515 // SC02025 // SC07036 // SC01233 // SC02481 // SC03104 // SC04914 // SC01577 // SC07268 // SC03771 // SC05554 // SC06172 // SC01580 // SC01579 // SC01570 // SC01244 // SC02210 // SC01584 // SC05584 // SC01343 // SC05513 // SC05122 // SC03383 // SC0487 // SC04901 // SC05655 // SC01232 // SC01245 // SC03345 // SC04159 // SC01243 // SC02232 // SC01486 // SC02048 // SC03058 // SC03311 // SC01813 // SC03756 // SC05839 // SC01578 // SC03450 // SC04962 // SC01490 // SC04038 // SC04464 // SC01483 // SC03059 // SC03382 // SC02051 // SC03381 // SC02455	GO:0005737	0.665821117	0.02985799
GO:0044281	biological_process	small molecule metabolic process	3	48	842	7910	175	SC05525 // SC02026 // SC05526 // SC05515 // SC02025 // SC07036 // SC01233 // SC02481 // SC03104 // SC04914 // SC01577 // SC07268 // SC03771 // SC05554 // SC06172 // SC01580 // SC01579 // SC01570 // SC01244 // SC02210 // SC01584 // SC05584 // SC01343 // SC05513 // SC05122 // SC03383 // SC0487 // SC04901 // SC05655 // SC01232 // SC01245 // SC03345 // SC04159 // SC01243 // SC02232 // SC01486 // SC02048 // SC03058 // SC03311 // SC01813 // SC03756 // SC05839 // SC01578 // SC04962 // SC04464 // SC01483 // SC03059 // SC03382 // SC02051 // SC03381	GO:0005737	1.365536045	4.53E-07
GO:0044711	biological_process	single-organism biosynthetic process	3	31	400	7910	175	SC05535 // SC02387 // SC01815 // SC02026 // SC01814 // SC05515 // SC02025 // SC07036 // SC02388 // SC06564 // SC04914 // SC01577 // SC02768 // SC03127 // SC01244 // SC02210 // SC04921 // SC05553 // SC05522 // SC03383 // SC01244 // SC02210 // SC04921 // SC05553 // SC05522 // SC03383 // SC01487 // SC04901 // SC05860 // SC01245 // SC03345 // SC01243 // SC01486 // SC02048 // SC03058 // SC03311 // SC01813 // SC03756 // SC01578 // SC04962 // SC04464 // SC01483 // SC03059 // SC03382 // SC02051 // SC03381	GO:0000166	1.808590988	6.81E-07
GO:1901564	biological_process	organonitrogen compound metabolic p	3	40	646	7910	175	SC05525 // SC02026 // SC05526 // SC05515 // SC02025 // SC07036 // SC01233 // SC02481 // SC03104 // SC04914 // SC01577 // SC07268 // SC03771 // SC05554 // SC06172 // SC01580 // SC01579 // SC01570 // SC01244 // SC02210 // SC01584 // SC05584 // SC01343 // SC05513 // SC05122 // SC03383 // SC0487 // SC04901 // SC05655 // SC01232 // SC01245 // SC03345 // SC04159 // SC01243 // SC02232 // SC01486 // SC02048 // SC03058 // SC03311 // SC01813 // SC03756 // SC05839 // SC01578 // SC04962 // SC04464 // SC01483 // SC03059 // SC03382 // SC02051 // SC03381 // SC02455	GO:0005737	1.48478608	1.05E-06
GO:0044249	biological_process	cellular biosynthetic process	3	61	1539	7910	175	SC05535 // SC02387 // SC01815 // SC02026 // SC01814 // SC05515 // SC02025 // SC07036 // SC02388 // SC06564 // SC04914 // SC01577 // SC02768 // SC03127 // SC01244 // SC02210 // SC04921 // SC05553 // SC05522 // SC03383 // SC01244 // SC02210 // SC04921 // SC05553 // SC05522 // SC03383 // SC01487 // SC04901 // SC05860 // SC01245 // SC03345 // SC01243 // SC01486 // SC02048 // SC03058 // SC03311 // SC01813 // SC03756 // SC01578 // SC04962 // SC04464 // SC01483 // SC03059 // SC03382 // SC02051 // SC03381 // SC02455	GO:0000166	0.841210689	0.00035896
GO:1901576	biological_process	organic substance biosynthetic process	3	57	1498	7910	175	SC05525 // SC02026 // SC05526 // SC05515 // SC02025 // SC07036 // SC01233 // SC02481 // SC03104 // SC04914 // SC01577 // SC07268 // SC03771 // SC05554 // SC06172 // SC01580 // SC01579 // SC01570 // SC01244 // SC02210 // SC01584 // SC05584 // SC01343 // SC05513 // SC05122 // SC03383 // SC0487 // SC04901 // SC05655 // SC01232 // SC01245 // SC03345 // SC04159 // SC01243 // SC02232 // SC01486 // SC02048 // SC03058 // SC03311 // SC01813 // SC03756 // SC01578 // SC04962 // SC04464 // SC01483 // SC03059 // SC03382 // SC02051 // SC03381 // SC02455	GO:0000166	0.782318973	0.00289885
GO:0005622	cellular_component	intracellular	3	42	1086	7910	175	SC05525 // SC02026 // SC05526 // SC05515 // SC02025 // SC07036 // SC01233 // SC02481 // SC03104 // SC04914 // SC01577 // SC07268 // SC03771 // SC05554 // SC06172 // SC01580 // SC01579 // SC01570 // SC01244 // SC02210 // SC01584 // SC05584 // SC01343 // SC05513 // SC05122 // SC03383 // SC0487 // SC04901 // SC05655 // SC01232 // SC01245 // SC03345 // SC04159 // SC01243 // SC02232 // SC01486 // SC02048 // SC03058 // SC03311 // SC01813 // SC03756 // SC01578 // SC04962 // SC04464 // SC01483 // SC03059 // SC03382 // SC02051 // SC03381 // SC02455	GO:0005737	0.805759903	0.02985799
GO:0016810	molecular_function	hydrolase activity, acting on carbon-nit	3	9	95	7910	175	SC01486 // SC04038 // SC04464	GO:0005737	2.098320261	0.04061661
GO:0043168	molecular_function	anion binding	3	38	979	7910	175	SC05535 // SC0706 // SC05092 // SC05515 // SC02025 // SC07036 // SC01233 // SC02481 // SC03104 // SC04914 // SC01577 // SC07268 // SC03771 // SC05554 // SC06172 // SC01580 // SC01579 // SC01570 // SC01244 // SC02210 // SC01584 // SC05584 // SC01343 // SC05513 // SC05122 // SC03383 // SC0487 // SC04901 // SC05655 // SC01232 // SC01245 // SC03345 // SC04159 // SC01243 // SC02232 // SC01486 // SC02048 // SC03058 // SC03311 // SC01813 // SC03756 // SC01578 // SC04962 // SC04464 // SC01483 // SC03059 // SC03382 // SC02051 // SC03381 // SC02455	GO:0000166	0.810113331	0.0526016
GO:0043169	molecular_function	cation binding	3	34	868	7910	175	SC05535 // SC0706 // SC05092 // SC05515 // SC02025 // SC07036 // SC01233 // SC02481 // SC03104 // SC04914 // SC01577 // SC07268 // SC03771 // SC05554 // SC06172 // SC01580 // SC01579 // SC01570 // SC01244 // SC02210 // SC01584 // SC05584 // SC01343 // SC05513 // SC05122 // SC03383 // SC0487 // SC04901 // SC05655 // SC01232 // SC01245 // SC03345 // SC04159 // SC01243 // SC02232 // SC01486 // SC02048 // SC03058 // SC03311 // SC01813 // SC03756 // SC01578 // SC04962 // SC04464 // SC01483 // SC03059 // SC03382 // SC02051 // SC03381 // SC02455	GO:0005737	0.824162476	0.07429049
GO:0044283	biological_process	small molecule biosynthetic process	4	31	363	7910	175	SC05535 // SC02387 // SC01815 // SC02026 // SC01814 // SC05515 // SC02025 // SC07036 // SC02388 // SC06564 // SC04914 // SC01577 // SC02768 // SC03127 // SC01244 // SC02210 // SC04921 // SC05553 // SC05522 // SC03383 // SC01244 // SC02210 // SC04921 // SC05553 // SC05522 // SC03383 // SC01487 // SC04901 // SC05860 // SC01245 // SC03345 // SC01243 // SC01486 // SC02048 // SC03058 // SC03311 // SC01813 // SC03756 // SC01578 // SC04962 // SC04464 // SC01483 // SC03059 // SC03382 // SC02051 // SC03381	GO:0000166	1.94862144	1.37E-07
GO:1901566	biological_process	organonitrogen compound biosyntheti	4	34	439	7910	175	SC05535 // SC02387 // SC01815 // SC02026 // SC01814 // SC05515 // SC02025 // SC07036 // SC02388 // SC06564 // SC04914 // SC01577 // SC02768 // SC03127 // SC01244 // SC02210 // SC04921 // SC05553 // SC05522 // SC03383 // SC01244 // SC02210 // SC04921 // SC05553 // SC05522 // SC03383 // SC01487 // SC04901 // SC05860 // SC01245 // SC03345 // SC01243 // SC01486 // SC02048 // SC03058 // SC03311 // SC01813 // SC03756 // SC01578 // SC04962 // SC04464 // SC01483 // SC03059 // SC03382 // SC02051 // SC03381 // SC02455	GO:0003824	1.80736579	1.55E-07
GO:0006082	biological_process	organic acid metabolic process	4	36	531	7910	175	SC05525 // SC02026 // SC05526 // SC05515 // SC02025 // SC07036 // SC01233 // SC02481 // SC03104 // SC04914 // SC01577 // SC07268 // SC03771 // SC05554 // SC06172 // SC01580 // SC01579 // SC01570 // SC01244 // SC02210 // SC01584 // SC05584 // SC01343 // SC05513 // SC05122 // SC03383 // SC0487 // SC04901 // SC05655 // SC01232 // SC01245 // SC03345 // SC04159 // SC01243 // SC02232 // SC01486 // SC02048 // SC03058 // SC03311 // SC01813 // SC03756 // SC01578 // SC04962 // SC04464 // SC01483 // SC03059 // SC03382 // SC02051 // SC03381 // SC02455	GO:0000166	1.615607818	8.31E-07
GO:0044424	cellular_component	intracellular part	4	42	1025	7910	175	SC05525 // SC02026 // SC05526 // SC05515 // SC02025 // SC07036 // SC01233 // SC02481 // SC03104 // SC04914 // SC01577 // SC07268 // SC03771 // SC05554 // SC06172 // SC01580 // SC01579 // SC01570 // SC01244 // SC02210 // SC01584 // SC05584 // SC01343 // SC05513 // SC05122 // SC03383 // SC0487 // SC04901 // SC05655 // SC01232 // SC01245 // SC03345 // SC04159 // SC01243 // SC02232 // SC01486 // SC02048 // SC03058 // SC03311 // SC01813 // SC03756 // SC01578 // SC04962 // SC04464 // SC01483 // SC03059 // SC03382 // SC02051 // SC03381 // SC02455	GO:0005737	0.889160096	0.00955875

GO:0044712	biological_process	single-organism catabolic process	3	19	151	7910	398	SCO6789 // SCO4869 // SCO1895 // SCO2469 // SCO6732 // SCO6027 // SCO6730 // SCO6968 // SCO2999 // SCO3247 // SCO1838 // SCO2401 // SCO2774 // SCO2773 // SCO5676 // SCO2556 // SCO7473 // SCO7469 // SCO2776	GO:0003824	1.322360133	0.06922117
GO:0071702	biological_process	organic substance transport	4	31	261	7910	398	SCO1887 // SCO5035 // SCO7555 // SCO5258 // SCO7410 // SCO7197 // SCO0137 // SCO1147 // SCO3667 // SCO0952 // SCO6011 // SCO5260 // SCO5229 // SCO6010 // SCO0540 // SCO6609 // SCO2746 // SCO2829 // SCO2831 // SCO2830 // SCO2828 // SCO1225 // SCO2978 // SCO2980 // SCO5911 // SCO5430 // SCO2009 // SCO5667 // SCO2011 // SCO1459 // SCO2008	GO:0005886	1.239127673	0.00751505
GO:0016042	biological_process	lipid catabolic process	4	11	48	7910	398	SCO6789 // SCO4869 // SCO2469 // SCO6732 // SCO6027 // SCO6730 // SCO6968 // SCO3247 // SCO1838 // SCO2774 // SCO2773 // SCO6789 // SCO4869 // SCO1895 // SCO2469 // SCO6732 // SCO6027 // SCO6730 // SCO6968 // SCO2999 // SCO3247 // SCO1838 // SCO2401 // SCO2774 // SCO2773 // SCO5676 // SCO2556 // SCO7473 // SCO7469 // SCO2776	GO:0003824	2.187306477	0.01627492
GO:0044282	biological_process	small molecule catabolic process	4	19	151	7910	398	SCO6789 // SCO4869 // SCO2469 // SCO6732 // SCO6027 // SCO6730 // SCO6968 // SCO3247 // SCO1838 // SCO2774 // SCO2773 // SCO6789 // SCO4869 // SCO1895 // SCO2469 // SCO6732 // SCO6027 // SCO6730 // SCO6968 // SCO2999 // SCO3247 // SCO1838 // SCO2401 // SCO2774 // SCO2773 // SCO5676 // SCO2556 // SCO7473 // SCO7469 // SCO2776	GO:0003824	1.322360133	0.06922117
GO:0044242	biological_process	cellular lipid catabolic process	5	11	34	7910	398	SCO6789 // SCO4869 // SCO2469 // SCO6732 // SCO6027 // SCO6730 // SCO6968 // SCO3247 // SCO1838 // SCO2774 // SCO2773 // SCO6789 // SCO4869 // SCO1895 // SCO2469 // SCO6732 // SCO6027 // SCO6730 // SCO6968 // SCO2999 // SCO3247 // SCO1838 // SCO2401 // SCO2774 // SCO2773 // SCO5676 // SCO2556 // SCO7473 // SCO7469 // SCO2776	GO:0003824	2.684806136	0.0018004
GO:0030258	biological_process	lipid modification	5	9	33	7910	398	SCO5258 // SCO7197 // SCO5260 // SCO5229 // SCO2829 // SCO2831 // SCO2830 // SCO2828 // SCO1225 // SCO2009 // SCO2011 // SCO1459 // SCO2008	GO:0003824	2.438368241	0.0178864
GO:0015849	biological_process	organic acid transport	5	13	69	7910	398	SCO1459 // SCO2008	GO:0000166	1.90475262	0.02006722
GO:0016054	biological_process	organic acid catabolic process	5	17	121	7910	398	SCO6789 // SCO4869 // SCO1895 // SCO6732 // SCO6027 // SCO6730 // SCO6968 // SCO3247 // SCO1838 // SCO2774 // SCO2773 // SCO6789 // SCO4869 // SCO1895 // SCO2469 // SCO6732 // SCO6027 // SCO6730 // SCO6968 // SCO2999 // SCO3247 // SCO1838 // SCO2401 // SCO2774 // SCO2773 // SCO5676 // SCO2556 // SCO7473 // SCO7469 // SCO2776	GO:0003824	1.481436963	0.05432081
GO:0008643	biological_process	carbohydrate transport	5	13	80	7910	398	SCO1887 // SCO7555 // SCO7410 // SCO0137 // SCO3667 // SCO6011 // SCO6010 // SCO0540 // SCO6609 // SCO2746 // SCO2978 // SCO2980 // SCO5430	GO:0005886	1.691348982	0.06177801
GO:0034440	biological_process	lipid oxidation	6	9	24	7910	398	SCO6789 // SCO4869 // SCO6732 // SCO6027 // SCO6730 // SCO6968 // SCO3247 // SCO1838 // SCO2774	GO:0003824	2.89779986	0.00196951
GO:0006820	biological_process	anion transport	6	16	97	7910	398	SCO6814 // SCO5258 // SCO7197 // SCO0952 // SCO5360 // SCO5229 // SCO2829 // SCO2831 // SCO2830 // SCO2828 // SCO1225 // SCO7596 // SCO2009 // SCO2011 // SCO1459 // SCO2008	GO:0000166	1.712924517	0.0178864
GO:0015711	biological_process	organic anion transport	7	14	72	7910	398	SCO5258 // SCO7197 // SCO0952 // SCO5260 // SCO5229 // SCO2829 // SCO2831 // SCO2830 // SCO2828 // SCO1225 // SCO2009 // SCO2011 // SCO1459 // SCO2008	GO:0000166	1.950267279	0.0102471
GO:0046395	biological_process	carboxylic acid catabolic process	7	17	121	7910	398	SCO6789 // SCO4869 // SCO1895 // SCO6732 // SCO6027 // SCO6730 // SCO6968 // SCO2999 // SCO3247 // SCO1838 // SCO2401 // SCO2774 // SCO2773 // SCO5676 // SCO2556 // SCO7473 // SCO7469 // SCO2776	GO:0003824	1.481436963	0.05432081
GO:0032787	biological_process	monocarboxylic acid metabolic process	7	23	199	7910	398	SCO6789 // SCO4869 // SCO1895 // SCO6732 // SCO6027 // SCO6730 // SCO6968 // SCO3247 // SCO1838 // SCO2774 // SCO2773 // SCO5676 // SCO2556 // SCO7473 // SCO7469 // SCO2776	GO:0003824	1.199774694	0.06177801
GO:0072329	biological_process	monocarboxylic acid catabolic process	8	14	63	7910	398	SCO5258 // SCO7197 // SCO5260 // SCO5229 // SCO2829 // SCO2831 // SCO2830 // SCO2828 // SCO1225 // SCO2009 // SCO2011 // SCO1459 // SCO2008	GO:0003824	2.142912357	0.00277394
GO:0046942	biological_process	carboxylic acid transport	8	13	69	7910	398	SCO2980 // SCO5430	GO:0000166	1.90475262	0.02006722
GO:0006631	biological_process	fatty acid metabolic process	8	16	108	7910	398	SCO6789 // SCO5385 // SCO4869 // SCO2561 // SCO6732 // SCO6027 // SCO6730 // SCO6968 // SCO1345 // SCO4006 // SCO7329 // SCO3247 // SCO1838 // SCO2774 // SCO6475 // SCO2773	GO:0003824	1.557949857	0.05257308
GO:0009062	biological_process	fatty acid catabolic process	9	10	27	7910	398	SCO6789 // SCO4869 // SCO6732 // SCO6027 // SCO6730 // SCO6968 // SCO3247 // SCO1838 // SCO2774 // SCO2773	GO:0003824	2.879877952	0.0018004
GO:0019395	biological_process	fatty acid oxidation	9	9	24	7910	398	SCO6789 // SCO4869 // SCO6732 // SCO6027 // SCO6730 // SCO6968 // SCO3247 // SCO1838 // SCO2774	GO:0003824	2.89779986	0.00196951
GO:0006865	biological_process	amino acid transport	9	13	61	7910	398	SCO5258 // SCO7197 // SCO5260 // SCO5229 // SCO2829 // SCO2831 // SCO2830 // SCO2828 // SCO1225 // SCO2009 // SCO2011 // SCO1459 // SCO2008	GO:0000166	2.082539730	0.00820408
GO:0006635	biological_process	fatty acid beta-oxidation	10	9	24	7910	398	SCO6789 // SCO4869 // SCO6732 // SCO6027 // SCO6730 // SCO6968 // SCO3247 // SCO1838 // SCO2774	GO:0003824	2.89779986	0.00196951

Term	Definition
GOID	Gene Ontology identifier
Ontology	Category of GO identifier
Term	GOID term identification
Level	The level of the GO term, defined by the longest path connecting back to the root of the GO hierarchical tree
q	Count of genes associated with the listed GOID in the dataset
k	total number of probes in the dataset
m	count of genes associated with the listed GOID in the full gene list
t	number of genes in the full gene list
probes	genes associated with the GOID
log_odds_ratio	Log2 of the odds ratio for the enrichment of the GOID.
p	P-value of the significance for the enrichment in your dataset of the listed GOID